Modelling, mathematical analysis and numerical simulation to value derivatives related to renewable energy certificates

Author: María de los Ángeles Baamonde Seoane

Doctoral Thesis UDC / Year 2021

Supervisors: María del Carmen Calvo Garrido

Carlos Vázquez Cendón

Doctoral Programme in Mathematical Modelling and Numerical Simulation in Engineering and Applied Science

UNIVERSIDADE DA CORUÑA

UNIVERSIDADE DA CORUÑA

PhD. Thesis

Modelling, mathematical analysis and numerical simulation to value derivatives related to renewable energy certificates

AUTORA:

María de los Ángeles Baamonde Seoane

DIRECTORES:

María del Carmen Calvo Garrido

Carlos Vázquez Cendón

TESE PRESENTADA PARA A OBTENCIÓN DO TÍTULO DE DOUTOR NA UNIVERSIDADE DA CORUÑA

DEPARTAMENTO DE MATEMÁTICAS

FACULTADE DE INFORMÁTICA, A CORUÑA (SPAIN)

2021

UNIVERSIDADE DA CORUÑA

Los abajo firmantes hacen constar que son directores de la Tesis Doctoral titulada **"Modelling, mathematical analysis and numerical simulation to value derivatives related to renewable energy certificates"** desarrollada por María de los Ángeles Baamonde Seoane, cuya firma también se incluye, dentro del programa de doctorado **"Métodos Matemáticos y Simulación Numérica en Ingeniería y Ciencias Aplicadas"** en el Departamento de Matemáticas (Universidade da Coruña), dando su consentimiento para su presentación y posterior defensa.

The undersigned hereby certify that they are supervisors of the Thesis entitled **"Modelling, mathematical analysis and numerical simulation to value derivatives related to renewable energy certificates"** developed by María de los Ángeles Baamonde Seoane, whose signature is also included, inside the Ph.D Program **"Mathematical Methods and Numerical Simulation in Applied Sciences and Engineering"** at the Department of Mathematics (University of A Coruña), consenting to its presentation and posterior defense.

6 de Octubre, 2021

Directores:

CALVO GARRIDO MARIA DEL CARMEN - Firmado digitalmente por CALVO GARRIDO MARIA DEL CARMEN - Fecha: 2021.10.06 18:38:13 +02'00'

María del Carmen Calvo Garrido

VAZQUEZ CENDON CARLOS - Firmado digitalmente por VAZQUEZ CENDON CARLOS - Fecha: 2021.10.06 18:46:27 +02'00'

Carlos Vázquez Cendón

Doctoranda:

BAAMONDE SEOANE MARIA DE LOS ANGELES - Firmado digitalmente por BAAMONDE SEOANE MARIA DE LOS ANGELES - Fecha: 2021.10.06 18:34:36 +02'00'

María de los Ángeles Baamonde Seoane

Funding

This research has been partially funded by the following projects:

- Project PID2019-108584RB-I00 from Ministerio de Ciencia e Innovavión.
- Project MTM2016-76497-R from Ministerio de Economía y Competitividad.
- Project ED431C 2018/033 from Xunta de Galicia.
- Project ED431G 2019/01 from Xunta de Galicia.

All previous projects include FEDER funding.

A mis padres

Agradecimientos

Al finalizar un trabajo tan arduo y lleno de dificultades como es una tesis doctoral, quiero mostrar mi agradecimiento a todas aquellas personas que han ayudado de una manera u otra a que este trabajo llegase a su término. Por ello, debo agradecer de manera especial y sincera a mis directores de tesis los profesores Carlos Vázquez Cendón y María del Carmen Calvo Garrido su ayuda y apoyo, fundamentales para la realización de esta tesis.

El primero de ellos, me ha transmitido a lo largo de los años, primero siendo mi profesor y tutor en el trabajo de fin de máster y a continuación en esta etapa de doctorado, su entusiasmo y dedicación en todo lo que hace y, en particular, el gusto por la investigación y la Matemática Aplicada. Sus conocimientos, ideas y consejos a lo largo de la realización de esta tesis han sido fundamentales, convirtiéndose así en un referente para mi. Además, quiero agradecerle el apoyo y confianza que siempre ha depositado en mi así como todo el ánimo y energía que en todo momento me ha transmitido. Por todo ello, muchas gracias Carlos.

Al segundo de ellos, quiero agradecer sus consejos y orientaciones, algo que ha sido la clave del buen trabajo que hemos realizado, el cuál no se puede concebir sin su participación. Debo destacar su paciencia y total disponibilidad para poder aclarar mis dudas además de escucharme y aconsejarme en todo momento, algo fundamental en numerosas ocasiones. Su forma de trabajar y dedicación son también un ejemplo. No concibo esta tesis sin su incalculable ayuda. Muchas gracias, Carmen.

Debo agradecer también al profesor Michael Coulon, su colaboración en esta tesis.

Durante este curso he tenido la suerte de impartir docencia en el Campus

de Esteiro de Ferrol de las asignaturas de Matemáticas II y Álgebra en la Escuela Universitaria de Diseño Industrial y en la Escuela Politécnica Superior, respectivamente. Por ello, les doy las gracias a los profesores José A. Antón, Jesús Cardenal, Álvaro Deibe y Ana Díaz, por toda su ayuda. Me siento afortunada por poder trabajar y, sobre todo, aprender de y con ellos. Muchas gracias.

No puedo olvidarme del Departamento de Matemáticas y sus profesores así como de mis compañeros del grupo de investigación M2NICA. En especial, debo nombrar al profesor Íñigo Arregui por su interés y apoyo durante esta etapa, así como a los profesores José Antonio Rodríguez y Ana María Ferreiro que fueron mis profesores durante el máster y a los cuales aprecio.

Gracias también a Luis Rodríguez por estar siempre disponible para ayudarme con cualquier problema informático.

Son varios los compañeros que han pasado por el Laboratorio 2.1. Sin embargo, debo destacar a Bea, Dani y Jonatan con los que he compartido la mayoría de este tiempo experiencias y pensamientos. Con ellos y con Jesús, Mónica, David, Yerai, Daniel, Mark, Elmurod y Micha, he compartido muchos cafés, risas, alguna que otra comida y, sobre todo, conversaciones de todo tipo a lo largo de estos años que han hecho más fácil esta etapa.

A lo largo de mi época de estudiante, me he encontrado con profesores con los que he establecido una relación especial a lo largo de los años. Uno de ellos es el profesor Francisco Tugores, al que debo agradecer su interés por mi trabajo, aún desde la distancia, dándome ánimos y compartiendo experiencias conmigo.

No puedo olvidar el apoyo incondicional de mis amigos y mi familia, pero en especial quiero agradecérselo a Cristina y Rocío. Siempre que lo he necesitado han estado ahí, interesándose por mi trabajo y escuchándome. Aunque hubo periodos en los que no teníamos mucho tiempo o no podíamos vernos, siempre han encontrado de una manera u otra un momento para mi.

Por último, si hay alguien al que debo la realización de esta tesis es a Santi. Desde el primer momento me animó con este proyecto, ha sido mi gran apoyo y ha soportado

mis ausencias pero, sobre todo, me ha transmitido esa tranquilidad que le caracteriza y de la cual en muchas ocasiones carezco. Muchas gracias.

Estas últimas palabras de agradecimiento son para las personas más importantes de mi vida: mis padres. Debo agradecerles todo su apoyo y cariño incondicional, pero sobre todo agradecerles que me hayan enseñando desde pequeña con su ejemplo estas tres palabras: trabajo, constancia y esfuerzo. Gracias a ellos, no me cabe duda alguna, he podido alcanzar mis metas y esta es una más. Muchas gracias.

A Coruña, 2021.

Table of Contents

List of Tables

List of Figures

Abstract

The main objective of this thesis concerns to the modelling, mathematical analysis and numerical solution of partial differential equations (PDEs) models for pricing renewable energy certificates (RECs) and associated derivatives products.

In the modelling, the price of the REC plays a relevant role. A non-linear PDE model with two stochastic factors is proposed. The stochastic factors are the accumulated green certificates and the renewable electricity generation rate. One novelty of this thesis comes from the numerical treatment of the non-linear convective term in the PDE. In order to solve the obtained linearized problem, semi-Lagrangian schemes in time combined with finite differences discretizations, or alternative Lagrange-Galerkin methods are proposed.

An equivalent methodology has been used for the valuation of the REC derivatives to obtain a linear PDE model once the REC price is known. Existence of solution is obtained in this setting. The application to the pricing of European options and futures on RECs is addressed.

Finally, we show illustrative results of the performance of the models and numerical methods that have been implemented.

Resumen

El objetivo principal de esta tesis se centra en el modelado, análisis matemático y resolución numérica de problemas de ecuaciones en derivadas parciales (EDPs) para la fijación de precios de certificados de energía renovable (RECs, por sus siglas en inglés) y productos derivados asociados.

En el modelado, el precio del REC juega un papel relevante. Se propone un modelo de EDP no lineal con dos factores estocásticos. Los factores estocásticos son los certificados verdes acumulados y la tasa de generación de energía renovable. Una novedad de esta tesis es el tratamiento numérico del término convectivo no lineal en la EDP. Para resolver el problema linealizado obtenido, se proponen esquemas de semi-Lagrange en tiempo combinados con diferencias finitas, o métodos alternativos de Lagrange-Galerkin.

Se ha utilizado una metodología equivalente para la valoración de los derivados de REC para obtener un modelo de EDP lineal una vez conocido el precio del REC. La existencia de solución se obtiene en este escenario. Se aborda la fijación de precios de opciones europeas y futuros sobre RECs.

Finalmente, se muestran resultados del comportamiento de los modelos y de los métodos numéricos implementados.

Resumo

O obxectivo principal desta tese céntrase na modelaxe, análise matemática e resolución numérica de problemas de ecuacións en derivadas parciais (EDPs) para a fixación de prezos de certificados de enerxía renovable (RECs, polas súas siglas en inglés) e produtos derivados asociados.

Na modelaxe, o prezo do REC xoga un papel importante. Proponse un modelo de EDP non lineal con dous factores estocásticos. Os factores estocásticos son os certificados verdes acumulados e a taxa de xeración de enerxía renovable. Unha novidade desta tese é o tratamento numérico do término convectivo non lineal na EDP. Para resolver o problema linealizado obtido, propóñense esquemas de semi-Lagrange en tempo conxugados con diferenzas finitas, ou métodos alternativos de Lagrange-Galerkin.

Utilizouse unha metodoloxía semellante para a valoración dos derivados de REC para obter un modelo de EDP lineal unha vez coñecido o prezo do REC. A existencia de solución obtense neste escenario. Abórdase a fixación de prezos de opcións europeas e futuros sobre RECs.

Finalmente, móstranse os resultados do comportamento dos modelos e dos métodos numéricos implementados.

Introduction

The trading in financial derivatives has increased tremendously in recent years. A financial derivative is a contract whose value depends on one or more assets, called underlying assets. Typically, the underlying asset is a stock (or equity), a currency exchange rate, the market price of a commodity (such us oil or wheat), a credit/bond (interest rate), an index or another variable. A derivative is traded between two parties (buyer and seller), who are referred to as the counterparties. These counterparties are subject to a pre-agreed set of terms and conditions that determine their rights and obligations. The price of the derivative is the premium that the buyer of the derivative has to pay at the initial time to get the guaranteed rights by the contract or the price the buyer has to pay in the market to get the derivative. The main two reasons for using financial derivatives are hedging risks and speculation purposes.

There exist several kinds of derivatives depending on the type of contract payment flows between the counterparties. The most common types of derivatives are options, futures/forwards and swaps. In particular, an option is a contract that gives the right (but not the obligation) to its holder to buy (*call option*) or sell (*put option*) some amount of the underlying asset at a future date (*maturity date*), for an agreed price (*strike price*). Depending on the time when the right to buy or sell can be exercised, options are classified as European or American options: only at maturity or at any time before maturity, respectively. Those options in which the final payment (*payoff*) only depends on the price of the underlying at maturity or at the exercise date are referred as plain vanilla options.

Financial derivatives are efficient instruments for risk management purposes and allow market participants to hedge against the various types of common financial risks (for example currency, credit or interest rate risks, among others), as well as those risks now emerging as a result of climate change. Global warming and environmental problems represent a challenge for policy makers. Derivatives markets can play an essential role in facilitating the transition to a sustainable economy. Different policies to reduce greenhouse gas emissions and promote renewable energy generation are of increasing importance. The most well known of these policies are cap-and-trade markets.

Emissions trading, which can also be referred to as cap and trade, emissions trading schemes or allowance trading, is a market-based approach to reduce pollution. It is designed to set a geographic limit on the amount of (primarily) carbon dioxide that can be emitted into the atmosphere by specific sectors of the economy. Emissions trading includes two key components: a limit (or cap) on pollution and tradable allowances that authorize allowance holders to emit a specific quantity (e.g., one ton) of the pollutant. The limit declines on an annual basis, with the intention of reducing the overall amount of emissions.

Market participants can trade emission allowances (including offset credits) and derivatives based on emission allowances (primarily futures and options). Emission allowances can be purchased through centrally organized auctions or from other companies that have more than they need for compliance. Secondary trading can be executed on exchanges or in over-the-counter (OTC) markets as spot, forwards, futures and options contracts. The behavior of prices in emission trading schemes has already attracted considerable interest in the literature (see [37], [58] and [61]).

Markets for tradable *Renewable Energy Certificates* (RECs) represent an interesting and closely related alternative. They can be used to encourage the growth of a particular type of renewable energy, as in the case of Solar Renewable Energy Certificates (SRECs) (see [26] and [57]). A renewable energy certificate (or green certificate) is a financial instrument traded in the marketplace, which guaranties that

an amount of electricity has been produced by means of renewable energy sources such as solar or wind plants, for example. One certificate is issued to the renewable power generator for each MWh or higher units of energy produced. Thus tradable green certificates are designed to promote electricity generation from renewable energy sources.

On one hand, this kind of contracts are used by companies (buyers) to cover their requirements of supplying "clean" electricity by purchasing green certificates instead of making a huge investment in technologies to produce renewable energy themselves. In [27], the optimal percentage requirement of the total electricity production that must be obtained from renewable sources is analyzed. On the other hand, sellers can fund the cost of renewable energy installations by selling these green certificates.

There are similarities between REC markets and carbon cap-and-trade ones. However, there are also some differences. The main important difference is the uncertainty in the market. In the former market, this uncertainty comes from the supply of certificates (driven by some generation process), while in the latter, it is related to the demand for allowances (driven by an emission process). Furthermore, the regulator now fixes demand (requirement) instead of supply (cap), and borrowing and withdrawal are not present.

In the last years, due to the necessity of fighting against climate change, the production of electricity from energy renewable sources has increased and consequently the demand of this kind of certificates has grown. RECs markets can provide opportunities for investing, although the risk due to their volatile price behaviour is relevant. Therefore, the study of these markets and their characteristics have begun to gain traction.

There are several references discussing tradable green certificates in different world regions. In [63], the tradable green certificates system in some regions of Belgium is studied in detail and they analysed, in particular, the system established in the Flemish region. More recently, the effects of the new Chinese government policy in green certificate pricing and transaction decisions are evaluated in [29] and [65].

In the literature, the valuation problem of green certificates has been tackled with different models and techniques. For example, in [6], for the particular case of the Swedish-Norwegian market, the valuation problem is modelled as a control problem for which the authors derive a closed formula. In [32], the authors describe three models based on a game theory approach for the implementation of the tradable green certificates system. Additionally, in the reference [26], which is devoted to the valuation of solar renewable energy certificates in the New Jersey market, the price of the certificate is obtained by using a dynamic programming algorithm. Moreover, the renewable energy production rate is modelled by means of a geometric Brownian motion process instead of the Ornstein-Uhlenbeck (OU) process considered in the present thesis.

From the mathematical point of view, the valuation problem of green certificates can also be modelled as a PDE problem associated with a non-linear operator. In previous works existing in the literature, non-linear PDEs also appear in the valuation of financial instruments in emission markets with the possibility of multiple periods for which an obligation is set. For example, in [37], the authors describe the asymptotic behaviour of the solution close to the end of a compliance period.

In this thesis we study some mathematical models for pricing RECs and specific financial derivatives on them. More precisely, we address the mathematical modelling, the analysis and numerical simulation of derivatives related to renewable energy certificates (RECs).

In the present work, assuming that the price of the REC depends on two stochastic factors, which are the accumulated green certificates and the renewable energy production rate, we present the PDE model that governs the valuation of such financial instruments and we propose appropriate numerical methods for its numerical resolution. Note that the same stochastic factors are considered in [6]. However, the formulation of the problem and the numerical techniques to solve it are different.

Concerning the numerical solution of the PDE problem, first, in order to deal with the non-linear convective term, we apply the Bermúdez-Moreno algorithm proposed

in [8]. This duality method is based on the approximation of a non-linear maximal monotone operator by means of its Yosida regularization. Next, the resulting linear problem is discretized by using two methods. Firstly, we use a characteristics scheme to discretize the material derivative operator in one of the spatial directions combined with the use of a second order implicit finite differences scheme in the other spatial direction. Secondly, we use a Lagrange-Galerkin method which mainly consists of Crank-Nicolson characteristics scheme for time discretization combined with finite elements for the discretization in the accumulated green certificates and the natural logarithm of the renewable generation rate directions. These numerical techniques, which result very efficient for convection dominated problems as the one treated in this work, were developed in [11] for Asian option pricing problems. Moreover, in [9], the authors address the numerical analysis of the Crank-Nicolson time discretization proposed here for a general convection-difussion reaction equation. Additionally, the fully discretized problem which is obtained by combining Crank-Nicolson characteristics with Lagrange finite elements is studied in [10].

The outline of this thesis is as follows.

In Chapter 1, an introduction to energy markets is given, mainly describing their characteristics.

In Chapter 2, the mathematical modelling corresponding to the price of REC is posed. At the beginning of the chapter, the two stochastic factors corresponding to the model are presented. Then, the PDE model governing the valuation of the REC is derived by using Itô lemma.

In Chapter 3, we describe the numerical methods, including the treatment of the non-linear convective term, the analysis of boundary conditions and the full discretization of the PDE. Moreover, we show some numerical examples.

In Chapter 4, we state the mathematical model that governs the valuation of derivatives whose underlying is a REC, in particular we study European options and futures contracts. Thus, we derive the PDE model to price these derivatives,

study the existence of solution and we propose how to solve the models by using numerical techniques. Finally, we present some of the obtained results to illustrate the performance of the methods and the model.

Chapter 1

Basic ideas about energy markets

1.1 Energy markets

Over the last decades, worldwide energy consumption has been growing and everything seems to indicate that this trend will continue (see Figure 1.1). Besides future economic growth, an important driver of global energy demand is policy commitments, such as renewable energy or energy efficiency targets.

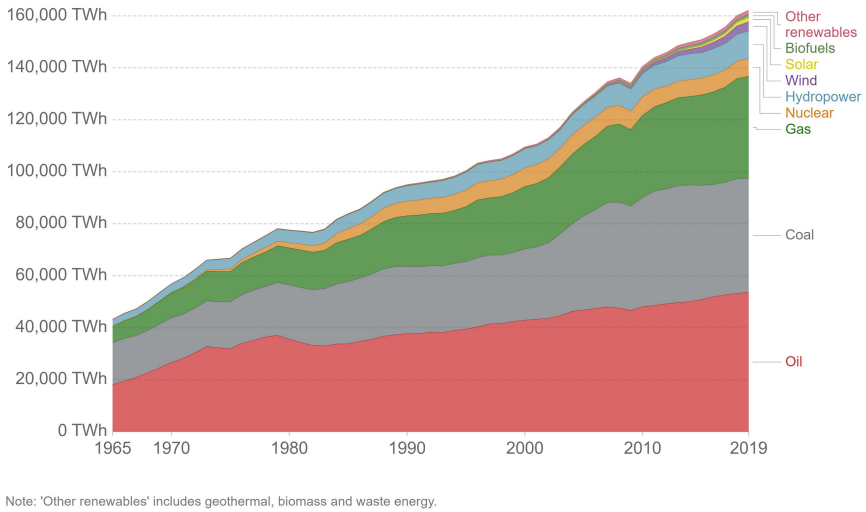

Figure 1.1: World energy consumption by source.

(*Source*: BP Statistical Review of World Energy (2020)).

The main primary energy source worldwide is oil, covering more than 30% of worldwide energy consumption (see Figure 1.2). In the second and third position of this ranking are coal and natural gas, with a share around 30% and 20%, respectively. Nuclear energy (around 6%) and renewables (around 13%) have a much smaller share. In order to meet the worldwide growing demand for energy, an increase in energy supply from all primary energy sources will be mandatory.

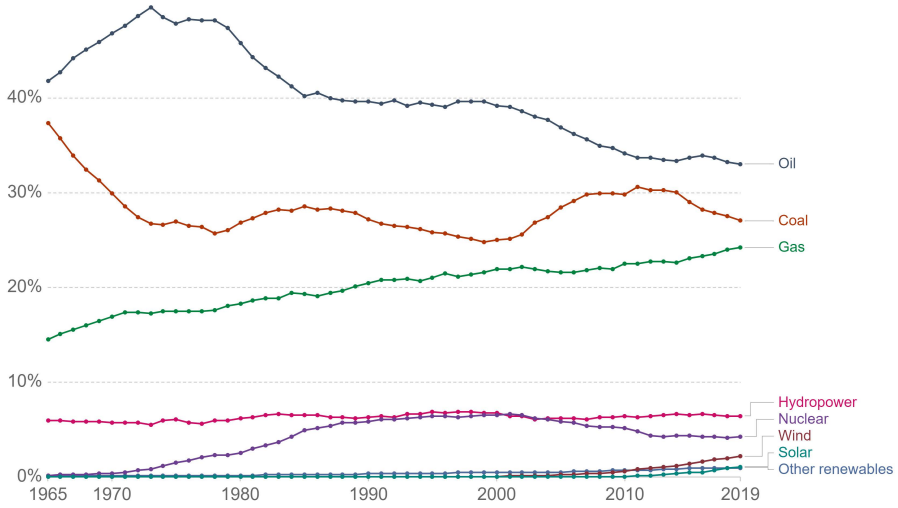

Figure 1.2: World share of energy consumption by source.

(*Source*: BP Statistical Review of World Energy (2020)).

The average annual growth rate in energy demand is estimated to grow in the next years. The strength and composition of energy growth over the next 30 years depends importantly on how that energy is used across the main sectors of the economy: industry, transport and buildings. In *Energy Outlook: 2020 edition* (see [66]), BP indicates that the industrial sector consumed around 45% of global energy in 2018, with the non-combusted use of fuels accounting for a additional 5% or so; and the remainder was used within residential and commercial buildings (29%) and transport (21%).

The Covid-19 pandemic has caused more disruption to the energy sector than any other event in recent history (see Figure 1.3), leaving impacts that will be felt

for years to come, in particular how it affects the prospects for rapid clean energy transitions. Uncertainty over the duration of the pandemic, its economic and social impacts, and the policy responses open up a wide range of possible energy futures.

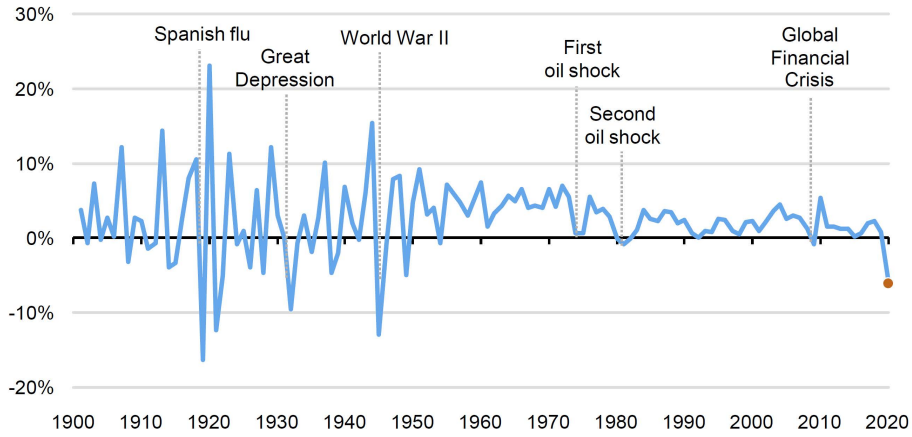

Figure 1.3: Rate of change in global primary energy demand, 1900-2020.

(*Source*: International Energy Agency (IEA), 2020).

1.2 The electricity market

Around 70% of global emissions today come from countries with a government pledge to achieve net-zero emissions. The Covid-19 pandemic delivered a major shock to the world economy, with an unprecedented 5.8% decline in CO_2 emissions in 2020. But nowadays, the data shows that global energy-related CO_2 emissions started to climb again. By considering different assumptions, in *World Energy Outlook 2020* (see [68]), the International Energy Agency (IEA) examined what would be needed over the period until 2030 to put the world on a path towards net-zero emissions by 2050 in the context of the pandemic-related economic recovery.

The Net-Zero Emissions (NZE) by 2050 Scenario is designed to achieve two objectives:

- Net-zero energy-related and industrial process CO_2 emissions by 2050.

- To minimise methane emissions from the energy sector which was responsible for around three-quarters of global greenhouse gas (GHG) emissions.

There are many possible paths to achieve net-zero CO_2 emissions by 2050 that depends on innovation in new and emerging technologies, the behaviour of the citizens or international coalitions between the countries, for example. The momentum towards emissions-neutral energy systems affects the electricity sector which is placed at the centre of the net zero pathway, requiring rapid and deep decarbonisation even as electricity demand grows more than 2.5 times, partly due to massive electrification of end-uses now served by fossil fuels. Huge growth of renewables generation is at the core of this decarbonisation. Solar and wind power are expected to play the largest role, together growing by 20 times from 2020 to 2050 (see Figure 1.4), raising the share of renewables in total generation from 29% in 2020 to nearly 90% in 2050, complemented by nuclear, hydrogen and carbon capture, utilisation and storage (CCUS).

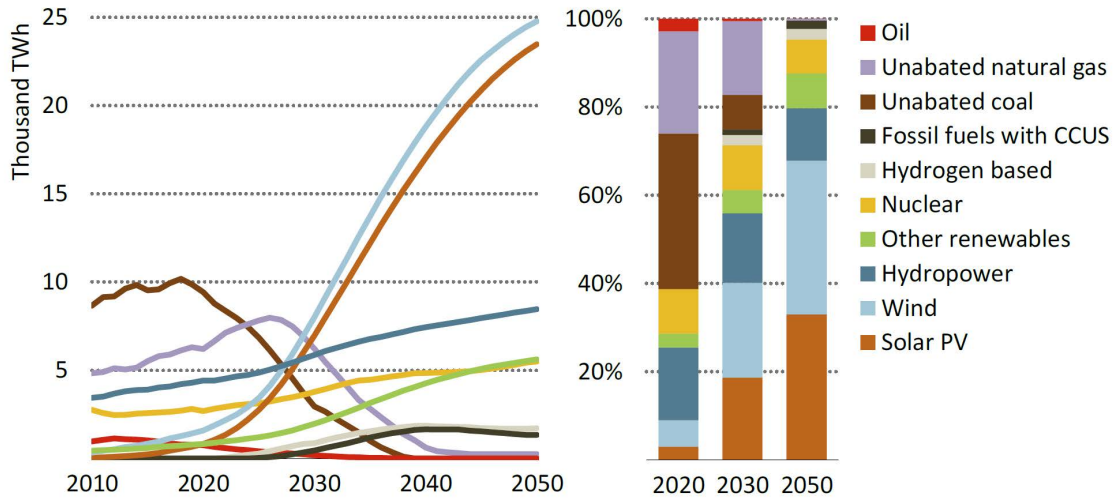

Figure 1.4: Global electricity generation by source.

(*Source*: International Energy Agency (IEA), 2021).

1.2.1 Price setting mechanism

This change of the electricity system to use low-carbon technologies requires overcoming challenges such as incentives for market participants due to the use of renewables and thus safeguarding security of supply.

The deregulation of many electricity markets has produced that power generators and suppliers need to understand and model the often unusual behaviour of electricity prices. As we said previously, the most important production method remains the burning of fossil fuels and their conversion to electricity. Moreover, renewables, such as wind, solar, nuclear and hydropower, are involved in the electricity generation process. Due to high dependence on the fuel prices, global electricity markets have huge jumps in prices and very high volatility.

The number of financial institutions interested in trading energy and power derivatives is growing and it has sparked a drive in both industry and academia to find suitable mathematical models. For this reason, new pricing and hedging techniques are being developed. However, these new models may take into account the "price spikes" which appear in electricity markets. This volatile behaviour is the main object of study in this kind of financial markets.

The use of stochastic processes to describe the spot and forward prices is suggested, although there exist several obstacles to overcome such as the unusual electricity prices or the limited historical data. These problems are present in the construction, calibration and testing of the mathematical models. In order to model the price of electricity, its characteristics are very important. One of them is its *unstorable* nature because it is produced immediately before being consumed. The total supply and demand for electricity must be in balance all the time. In fact, prices follow economic equilibrium arguments where the market price is determined by finding the intersection point between both. Nonetheless, prices in consecutive time periods are clearly linked by the autocorrelations of underlying factors, such as weather conditions (driving demand) and fuel prices (driving supply).

1.2.2 Electricity market factors: demand and supply

Electricity markets have their own intrinsic complexities. In order to understand the importance of the roles of supply and demand on the electricity price, we may identify the primary causes of its behaviour and also how to incorporate them appropriately into a modelling framework.

Seasonality is one of the most typical characteristics of energy prices, so that any realistic model must incorporate this characteristic. On the perspective of the demand, electricity price depends on regional weather conditions, specially on the temperature. For instance, some electricity markets exhibit a discernible pattern between winter and summer months: cold and hot weather produce more use of heating and air-conditioning, respectively. Furthermore, the demand of electricity also depends on the day of the week and the hour. Actually, higher levels of demand arise during business hours. On the side of the supply, seasonal patterns are also present, through the total available capacity of the market (as a percentage of maximum capacity), for example. Finally, fuel prices can exhibit this seasonality characteristic, as well as natural gas prices. This pattern is modelled in different ways. For example, with a deterministic or seasonal function which distinguish between weekdays and a monthly seasonal component or a combination of trigonometric functions (see [44]). Other alternatives include a constant piece-wise function (see [42]), a sinusoidal function (see [54]) or a Fourier series of order 5, while wavelet decomposition can also be applied (see [21]).

Many markets exhibit very high rates of volatility with large and frequent price spikes, particularly during times of high demand. The intraday movement is extremely volatile during high demand hours and, over night, when demand is at a low level, prices revert to nearly normal levels. These spikes can occur only during a few hours so that they become very significant when looking at real-time prices. They can be related to weather conditions, transmission failures or spikes in fuel prices. The use of jump-diffusion processes is the most common approach to incorporate spikes and a deterministic function is used by various authors in the case of volatility (see

[15], [21], [34]). As it is advocated in [25], using a supply and demand approach, it is possible to induce some spikes in the price process simply as a result of the shape of the supply curve, particularly for high demand (the higher the demand, the higher the volatility).

Other typical feature of the electricity price dynamics is the mean-reversion property. In the context of electricity prices, Geometric Brownian Motion results to be an unsuitable model for many reasons, primarily because it is not be able to emulate the intraday behaviour in a fully satisfactory way, especially when spikes occur. Temperature, and hence demand, is strongly mean-reverting to its seasonal level over few days. Regardless of the variety of the models proposed in the literature, Ornstein-Uhlenbeck (OU) process is quite often used. The most basic model is the exponential of an OU process (see [16], [44], for example).

Finally, non-stationarity behaviour is present in some markets. This behaviour could be seen as capturing stochastic changes, such as in fuel prices or demand. Global and technological changes in power generation and market participants are other factors to take into account. By including an additional factor which follows an arithmetic Brownian Motion, it is possible to incorporate this characteristic into the model. This approach is used in [16], [44] and [55].

For further details on the impact of supply and demand related factors, see [14] and [30], for example.

1.3 The emissions market

There exists a relationship between the financial market in which electricity and emissions are traded and real economy. The electricity sector involves the generation, transmission, and distribution of electricity. CO_2 makes up the vast majority of green gas emissions from the sector, jointly with methane (CH_4) and nitrous oxide (N_2O). These gases are released during the combustion of fossil fuels, such as coal, oil and natural gas, to produce electricity.

Global warming caused by the greenhouse effect is one of the key environmental challenges of the 21st century. Increased concentrations of greenhouse gases in the atmosphere are responsible for the anthropogenic greenhouse effect, with an increase in the average air surface temperature. This change has several impacts on the environment, such as the appearance of extreme weather events. In the Paris Agreement (see [69]), countries agreed to *"achieve a balance between anthropogenic emissions by sources and removals by sinks of greenhouse gases in the second-half of the century"*. A broad range of energy policies and accompanying measures are introduced across all regions to reduce emissions: renewable fuel mandates, efficiency standars, market reforms, research, development, deployment and, in some cases, direct emissions reduction regulations, such as in the transport sector to reduce sales of internal combustion engine vehicles.

The fastest and largest reductions in global emissions in the NZE correspond to the electricity sector (see Figure 1.5). Nowadays, electricity generation was the largest source of emissions.

1.3.1 Kyoto protocol: market-based mechanisms

The Kyoto Protocol sets binding emission reduction targets for 37 industrialized countries and economies in transition and the European Union (see [67]). It was adopted at the 3rd Conference of the Parties (COP) in Kyoto in December 1997, Japan and entered into force in 2005. Due to the USA and Canada withdraw from it in December 2012, it was not ratified.

In order to lower the overall costs of achieving its emissions targets, three "flexible market mechanisms" are defined: Joint Implementation (JI), Clean Development Mechanism (CDM) and International Emissions Trading (IET). These mechanisms are based on the trade of emissions permits and stimulate green investment in developing countries. Not only CO_2, but all greenhouse gases (GHG) under the Kyoto Protocol are considered for JI and CDM projects.

JI and CDM are project-based mechanisms. They involve developing and

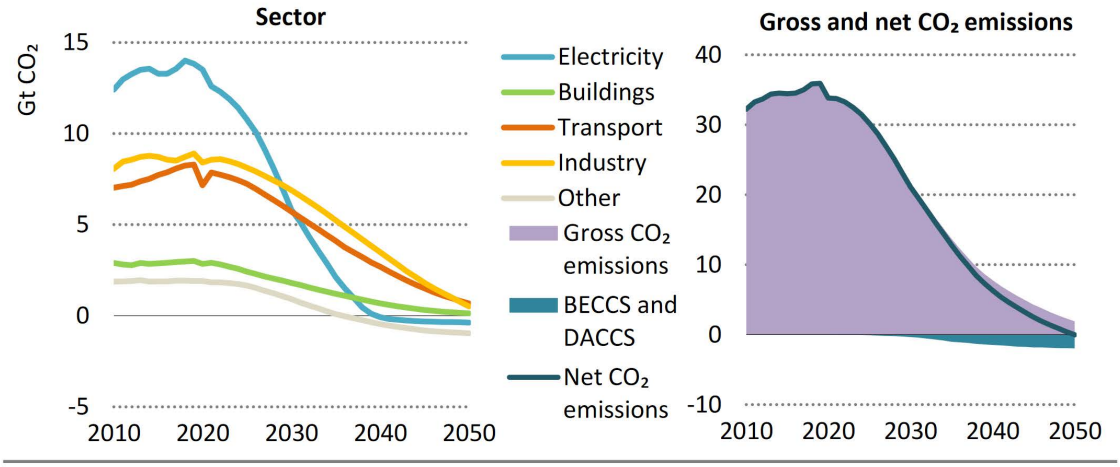

Notes: Other = agriculture, fuel production, transformation and related process emissions, and direct air capture. BECCS = bioenergy with carbon capture and storage; DACCS = direct air capture with carbon capture and storage. BECCS and DACCS includes CO_2 emissions captured and permanently stored.

Figure 1.5: Global net-CO_2 emissions by sector, and gross and net-CO_2 emissions in the NZE.

(*Source*: International Energy Agency (IEA), 2021).

implementing measures that reduce greenhouse gas emissions in another country to generate emission credits. JI projects are carried out in industrialised countries with existing emission targets. CDM projects are carried out in developing countries without targets. JI projects generate Emission Reduction Units (ERUs) and CDM projects generate Certified Emission Reductions (CERs). The unit of ERUs and CERs is tonne of CO_2 equivalents. Sometimes these credits are also called Kyoto offsets.

JI is defined in Article 6 of the Kyoto Protocol and allows countries to earn ERUs from an emission-reduction or emission removal project in other Kyoto countries, each equivalent to one tonne of CO_2, which can be counted towards meeting its Kyoto target. JI projects have to be approved by the country in which they are implemented with the incentives created by JI. Therefore, measures covered by a company emissions trading scheme like the European Union Trading Schemes (EU ETS) are not eligible as JI projects.

CDM is defined in Article 12 of the Kyoto Protocol and allows a country with an emission-reduction or emission-limitation commitment under the Kyoto Protocol to implement an emission-reduction project in developing countries. Such projects can earn saleable CER credits, each equivalent to one tonne of CO_2, which can be counted towards meeting Kyoto targets. A key requirement for CDM projects is additionality: emissions reductions will only be recognised if the reduction of greenhouse gas emissions is in addition to any reduction that would have occured without the certified project activity. The mechanism could be considered innovative because it is the first global, environmental investment and credit scheme of its kind, providing a standardized emissions offset instrument, CERs.

IET of Assigned Amount Units (AAUs) is defined in Article 17 of the Kyoto Protocol and allows industrialised countries with emission targets to exchange emission allowances to meet their national Kyoto targets. They can also use CERs and ERUs for meeting these targets. Thus, a new commodity was created in the form of emission reductions or removals. Carbon is traded like any other commodity and this is known as the "carbon market".

The Linking Directive (Directive 2009/27/EC), adopted by the EU Parliament in 2009, allows emission reduction units generated by project-based flexible mechanisms (JI and CDM) to be utilised for compliance by companies under the EU ETS, in which the use of all ERUs or CERs is allowed. The EU ETS is a "cap-and-trade" system.

1.3.2 Cap-and-trade factors: demand and supply

In cap-and-trade markets, the market is subject to an Emissions Trading Scheme (ETS) in which regulators impose a limit of carbon emissions (cap) during one compliance period. Each registered firm receives an initial allocation of allowances in the amount of this limit, each allowing for a unit of CO_2 emission, usually one tonne. These allowances can be used to offset its cumulative emissions at the end of the compliance period. If a firm produces a higher level of emissions than its permits

allow must pay a penalty per extra tonne of CO_2 emitted. Throughout a compliance period, allowances are traded actively and this leads to the formation of a price, which represents the cost of carbon. This is the trade part of a cap-and-trade scheme. The behavior of prices in ETS has already attracted considerable interest in the literature (see [37], [58], [61]).

In practice, an ETS has multiple compliance periods, each with its own distinct cap and penalty. Between these periods, an ETS can provide some flexibility for firms to reduce emissions. There are three main mechanisms to provide more temporal flexibility: borrowing, banking and withdrawal. Borrowing and banking provide firms with flexibility in determining their compliance strategy because they can use next period's certificates for compliance at the end of the current trading period, when allowances might be scarce and prices high. Both help avoid price spikes. Borrowing can make it harder to meet short-term targets and regulators might find it difficult to monitor the creditworthiness of the borrowers. For this reason, most markets allow banking but not borrowing. Finally, the withdrawal mechanism prescribes that, in addition to the monetary penalty payment, one allowance certificate from next period's allocation is withdrawn for each unit of excess emissions at the end of the current period.

Due to the relationship between electricity generation and emissions, the allowance price factors are demand and supply in this kind of markets, particularly demand for electricity and the cost of the emission or electricity supplied. The actions of consumers in the market result in demand for electricity and firms respond by generating electricity. The academic treatment of emissions markets has been widely studied with two different points of view. Firstly, full equilibrium models that derive the price process of allowances and goods (the production of which causes pollution) from the preferences of individual firms and additional sources of uncertainty (see [17] and [18]). Secondly, reduced-form models that specify the allowance price evolution directly in the form of a process and the parameters are calibrated to market data. Within this class of models, there are models that ignore the feedback from the

allowance price to the rate at which firms emit (see [19], [24]) and others that take this feedback into account through an exogenously specified abatement function (see [20]). In [37], the feedback from the cost of the emission to the market emission rate in a realistic setting is included.

1.4 The renewable energy market

Renewables are considered by many policy-makers to contribute to improving energy security and protecting the environment. On an average cost basis, some renewables in the best locations are competitive with conventional energy sources, however, in many cases renewables are still not competitive. Supportive policies are still needed to encourage the further development and deployment especially of "new" renewables in energy markets.

Wind power, biomass technologies, solar photovoltaic (PV) and concentrating solar power are some examples of emerging technologies. The renewables industry includes decentralised manufacturers and systems companies, electric utilities, independent power producers and retail equipment suppliers.

In 2019, according to IEA, the 13.8% of world total primary energy supply (TES) was produced from renewable energy sources, which includes hydro, biofuels, renewable municipal waste, solar PV, solar thermal, wind, geothermal and tidal. The share of renewables was a record high, up from 13.5% in 2018 (see Figure 1.6). Moreover, solid biofuels/charcoal is by far the largest renewable energy source (58.1%), followed by hydro (18.2%). Wind (6.2%), liquid biofuels (5.1%), and geothermal (5.0%) follow and, with shares lower than 3%, biogases, renewable municipal waste, solar PV, solar thermal and tidal.

Since 1990, global renewable energy sources have grown at an average annual rate of 2.1%, which is slightly higher than the 1.8% growth rate of world TES. Solar PV and wind power have experimented a significant growth (see Figure 1.7), with average annual rates of 36.0% and 22.6%, respectively. Biogases had the third highest growth

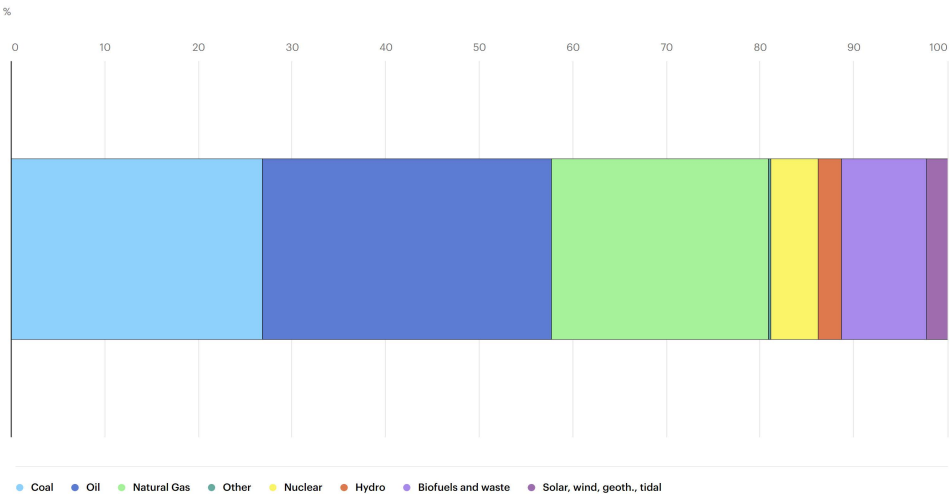

Figure 1.6: Fuel shares in world Total Energy Supply (TES), 2019.

(*Source*: International Energy Agency (IEA), 2021).

rate at 11.3%, followed by solar thermal (10.5%) and liquid biofuels (9.6%). Hydro, which is one of the largest sources, had one of the lowest growth rates, just 2.4%. On the other hand, solid biofuel, the world's most commonly used renewable energy source, grew just 1.1% a year.

Policy-makers need to consider them all. Therefore, three groups of policies are necessary to deploy new energy techologies into the marketplace:

- *Research and Innovation Policies* that support the development of new technologies through basic and applied research.

- *Market Deployment Policies* that underwrite the cost of introducing technologies into the market to improve and encourage development of the industry.

- *Market-Based Energy Policies* that provide a competitive market framework.

In recent years, several governments have encouraged environmental policies for promoting renewable energy sources and have established targets for renewable energy

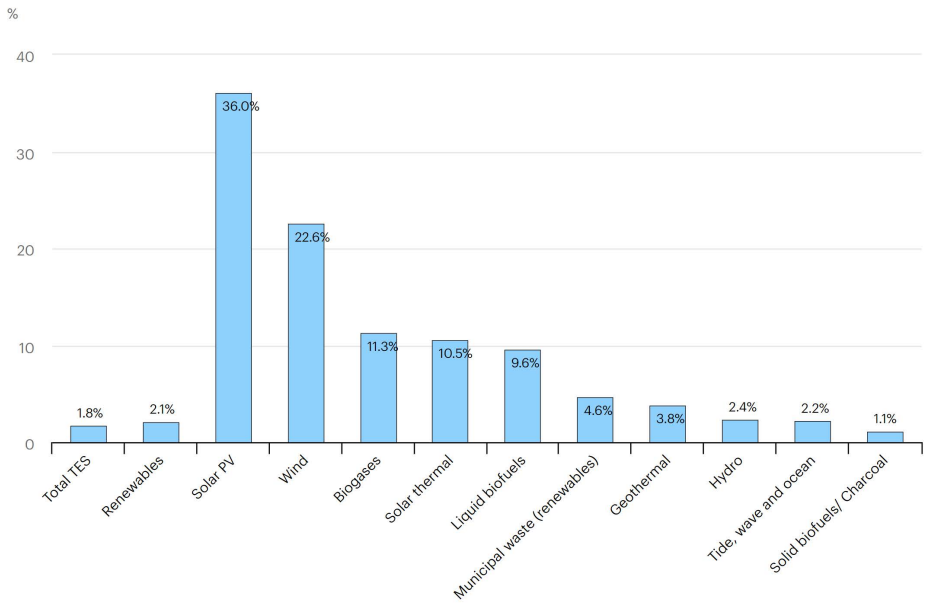

Figure 1.7: Average annual growth rates of world renewables supply, 1990-2020. (*Source*: International Energy Agency (IEA), 2021).

growth. Many countries or states have adopted Renewable Portfolio Standards (RPSs) and trading of RECs. Through these schemes, electric utility quote obligations are supported and a certain percentage of the electricity from renewable energy sources is required. This required percentage is generally increased annually by a regulator to meet longer-term political-targets.

Nevertheless, renewable energy technologies often require a large investment, hence alternative market tools are required to achieve these targets. One tool to implement these policies and to incentivize investing in renewables is the use of renewable energy certificates or RECs (often called green certificates or GCs in Europe). When renewable energy generators meet certain criteria, they receive one certificate for a specific unit, typically 1 MWh of renewable electricity produced. This REC can be sold to a Load Serving Entity (LSE) that is subject to the annual requirement of some percentage of electricity procured from renewables. If this quota obligation is not met by the LSE, a non-compliance penalty applies. This penalty is

called the Alternative Compliance Payment (ACP).

In principle, a quote obligation scheme treats all renewable energy equally. These instruments can also be linked to the generation of a particular type of energy, as is the case of the New Jersey (NJ) market for SRECs (solar renewable energy certificates) presented in [26]. Similar markets exist around the world (eg, Italy, UK, Sweden, Norway, US or Australia) and are considered an important alternative to implementing other environmental policies such as taxes or regulatory limits, thus helping to address climate change, especially in countries with an absence of carbon emissions markets, such as the US.

These electric utility quota obligations have some advantages, such as to create efficient incentives to generate renewable energy at the lowest possible cost and no excessive costs of customers if renewable energy targets are exceeded. In contrast, there exist high market risks for investors and they suppose a high entrance barrier for small generators.

The academic treatment of RECs markets is more recent than the study of cap-and-trade schemes for carbon emissions (see [18], [23], [35], [37], [49], [59], [60]). Although related, there are several differences between carbon and REC markets: supply and demand in opposite roles, different inter-temporal connecting mechanisms (such as withdrawal or unlimited banking) or external and underlying factors (such as fuel prices, power demand or renewable energy generation). Nonetheless, related approaches exist for the mathematical modelling of the valuation problem of green certificates. Some models of RECs markets are obtained by using a stochastic dynamic setting, thus replicating the price volatility (see [41] and [38]).

Chapter 2

A mathematical model for RECs pricing

2.1 Introduction

In this chapter of the thesis, we address the mathematical modelling for the valuation of green certificates (RECs) as the solution to a coupled system of forward-backward stochastic differential equations (FBSDE). This type of equations have been used for the pricing of financial instruments in emission markets in [20] and [37]. More precisely, we consider a *forward* stochastic differential equation (FSDE) for the renewable generation rate and another one for the accumulated green certificates, jointly with a *backward* stochastic differential equation (BSDE) for the green certificate price. This backward component of the FBSDE can be formulated in terms of a semilinear partial differential equation (PDE). As the analytical expression of a solution for the PDE is not available, in the present thesis we propose a set of numerical techniques, which are described in Chapter 3, to solve this non-linear equation.

2.2 Statement of the mathematical model

In this section we introduce the mathematical modelling when considering two stochastic factors. In order to model the price of a REC we assume that it is given by a stochastic process, which is denoted at time t by P_t and depends on two stochastic factors. More precisely, these factors are the renewable generation rate and the number of accumulated green certificates, which are denoted by G_t and B_t, respectively. We assume that the values of these two factors are known at the initial time $t = t_0$.

Specifically, for $t \in [t_0, T]$, the generation rate G_t is most influenced by weather patterns and by the construction of new renewable capacity. It is therefore natural to assume that the dynamics of G_t is given by

$$G_t = \mu_b(t, \widetilde{G}_t), \tag{2.1}$$

where $\mu_b(t, \widetilde{G}) = \exp(\widetilde{G})$ and $\widetilde{G}_t$ is a Ornstein-Uhlenbeck (OU) process which satisfies the following forward stochastic differential equations written in integral form:

$$\widetilde{G}_t = g_0 + \int_{t_0}^{t} \mu_g(s, \widetilde{G}_s, P_s)\, ds + \int_{t_0}^{t} \sigma_g\, dW_s^0, \qquad \text{for } \ t \in [t_0, T], \tag{2.2}$$

where $\mu_g(t, \widetilde{G}_t, P_t)$ and σ_g are the drift and the volatility, respectively. Moreover, W_t^0 is a standard $\mathcal{F}_t$-adapted $\mathbb{Q}$-Brownian motion, where $\mathbb{Q}$ denotes the risk neutral probability measure. In particular, we assume that the drift is linear with respect to P and given by the expression

$$\mu_g(t, \widetilde{G}, P) = \alpha_g \left(f(t) + \frac{\beta_g}{\alpha_g} P - \widetilde{G} \right), \tag{2.3}$$

where α_g is the mean reversion speed of the process and β_g is the parameter which controls the level of feedback from the price of the certificate. This feedback parameter captures the elasticity of supply to price, meaning the tendency of new renewable generation to be installed at times when certificate prices are high. Moreover, the seasonality is represented by the deterministic function f, which depends on time

t. Moreover, we assume that this function f is a combination of cosine and sine functions to represent the influence of weather on prices. For this purpose, there are more options to represent these seasonal patterns, such as the time series used in the particular case of Swedish-Norwegian market (see [6]).

Similarly to some methodologies used in the pricing of Asian options, the number of accumulated green certificates at time t, B_t, satisfies the following equation in the integral form:

$$B_t = \int_{t_0}^{t} G_s \, ds, \qquad \text{for } \; t \in [t_0, T]. \tag{2.4}$$

Moreover, as accumulation is measured from the beginning of the compliance period, t_0, we assume that $B_{t_0} = 0$. Note that since the process B_t represents an accumulated quantity, it turns out to be positive and non-decreasing.

The main objective of the model is to characterize the price of the renewable energy certificate, P_t, at time t. In our formulation in terms of a PDE problem, we assume the existence of a function P, such that $P_t = P(t, B_t, G_t)$. Once the function P is obtained as the solution of the PDE problem, we can compute the value P_t of the REC for given values of t, G_t and B_t.

2.2.1 Single compliance period

Assuming risk-neutral market participants, we consider a finite time horizon $[T-\gamma, T]$, where T is the maturity of the certificate and γ is the number of life years of the certificate (i.e. the number years since issuance for which the REC is valid to submit for compliance). We initialize the life of the certificate at $t_0 = T - \gamma$. So, in the single period case, we assume one year with no intermediary compliance before T and we take $\gamma = 1$. The value of the REC at time $t = t_0$ is unknown. However, its value at maturity, P_T, is given by the terminal condition:

$$P_T = \psi(B_T), \tag{2.5}$$

where $\psi : \mathbb{R}^+ \longrightarrow \mathbb{R}^+$ is a bounded measurable and decreasing function. More precisely, it is given by $\psi(\cdot) := \pi_T \mathbb{1}_{[0,R_T)}(\cdot)$, where π_T is the penalty amount at time

T and R_T is the requirement at time T.

Since the discounted price of the REC is a martingale under $\mathbb{Q}$ (a 'no arbitrage' condition), the price of the certificate at time t is equal to the discounted value of the conditional expectation of its terminal value, i.e.

$$P_t = e^{-r(T-t))}\mathbb{E}^{\mathbb{Q}}\left[\psi(B_T)|\mathcal{F}_t\right], \quad \text{for } t \in [T-\gamma, T], \tag{2.6}$$

where r is the constant risk free interest rate. The previous expression implies that the process P_t is bounded, taking values in $[0, \pi_T]$. Moreover, since the filtration $\mathcal{F}_t$ is generated by the Brownian motion W_t^0, the price of the renewable energy certificate can be represented as an Itô Integral with respect to W_t^0 as follows

$$P_t = \pi_T \mathbb{1}_{[0,R_T)}(B_T) - r\int_t^T P_s\, ds - \int_t^T e^{rs} Z_s^0\, dW_s^0, \quad \text{for } t \in [T-\gamma, T], \tag{2.7}$$

for some $\mathcal{F}_t$-adapted square integrable process Z_t^0.

Combining (2.2), (2.4) and (2.7) and applying Itô's Lemma, we find that the pricing problem is summarised by the following FBSDE for $t \in [t_0, T]$,

$$\begin{cases} \widetilde{G}_t = g_0 + \displaystyle\int_{t_0}^t \mu_g(s, \widetilde{G}_s, P_s)\, ds + \int_{t_0}^t \sigma_g\, dW_s^0, \\ B_t = \displaystyle\int_{t_0}^t \mu_b(s, \widetilde{G}_s)\, ds, \\ P_t = \pi_T \mathbb{1}_{[0,R_T)}(B_T) - r\displaystyle\int_t^T P_s\, ds - \int_t^T e^{rs} Z_s^0\, dW_s^0. \end{cases} \tag{2.8}$$

Equation (2.8) can be rewritten in differential form as

$$\begin{cases} d\widetilde{G}_t = \mu_g(t, \widetilde{G}_t, P_t)\, dt + \sigma_g\, dW_t^0, & \widetilde{G}_{t_0} = g_0, \\ dB_t = G_t\, dt, & B_{t_0} = 0, \\ dP_t = rP_t\, dt + Z_t^0\, dW_t^0, & P_T = \psi(B_T). \end{cases} \tag{2.9}$$

Note that there are two kinds of stochastic differential equations in (2.9) depending on the direction of time: the first two equations are forward ones while the last is a backward equation. Analogous equations have been considered for carbon emission prices in [37].

Assuming the existence of a solution for (2.9) and that $P_t = P(t, B_t, \widetilde{G}_t)$, where P_t is a traded asset with a drift equal to risk neutral rate under the risk neutral measure (as indicated in the third equation of (2.8)), we can use Itô's formula for a process depending on the two Itô processes B_t and $\widetilde{G}_t$ (see [39], for example) to obtain:

$$dP_t = \left(\frac{\partial P}{\partial t} + \frac{\sigma_g^2}{2} \frac{\partial^2 P}{\partial \widetilde{G}^2} + \mu_g(t, \widetilde{G}, P) \frac{\partial P}{\partial \widetilde{G}} + \exp(\widetilde{G}) \frac{\partial P}{\partial B} \right) (t, B_t, \widetilde{G}_t)\, dt + \sigma_g \frac{\partial P}{\partial \widetilde{G}} (t, B_t, \widetilde{G}_t)\, dW_t^0.$$

Therefore, identifying the drift coefficient of the previous expression and the corresponding one of the third equation in (2.9), the function $P = P(t, B, \widetilde{G})$ satisfies the following non-linear PDE:

$$\mathcal{L}_1[P] = \frac{\partial P}{\partial t} + \frac{1}{2}\sigma_g^2 \frac{\partial^2 P}{\partial \widetilde{G}^2} + \mu_g(t, \widetilde{G}, P) \frac{\partial P}{\partial \widetilde{G}} + \exp(\widetilde{G}) \frac{\partial P}{\partial B} - rP = 0. \tag{2.10}$$

Moreover, by taking into account that the value of the REC at maturity is given by (2.5), then PDE (2.10) jointly with the final condition

$$P(T, B, \widetilde{G}) = \psi(B) \tag{2.11}$$

defines the final value problem associated to the single period case.

2.2.2 Multiple compliance periods

The previously presented arguments for the single period case can be extended to an arbitrary number of compliance periods. In the multiple period case, the price of the certificate at maturity T is equal to the payoff (2.5), while a jump condition must be applied at each compliance date T^i, $i = 1, \ldots, \gamma - 1$. More precisely, the value of the certificate at the compliance date T^i is given by

$$P(T^i, B, \widetilde{G}) = \max\left(\psi(B), P\left(T_+^i, \max(0, B - R_i), \widetilde{G} \right) \right), \quad i = 1, \ldots, \gamma - 1, \tag{2.12}$$

where $\psi(\cdot) = \pi_i \mathbb{1}_{[0, R_i)}(\cdot)$ and R_i is the requirement at time T^i. In this case, a sequence of linked final value problems is defined by equations (2.10) and (2.12) for $i = \gamma - 1, \ldots, 1$.

The existence and uniqueness of solution for the final value non-linear PDE problem (2.10)-(2.11) remains as an open problem. We note that the FBSDE (2.8) is non-standard and exhibits some similarities to the one appearing in emission markets in [37], the existence and uniqueness of solution of which is rigorously analyzed in [56]. However, the ideas in [56] cannot be used to address existence and uniqueness of solution of (2.8). The main reason is that in [56], the FBSDE appearing in emission markets contains a first forward SDE which is uncoupled with the other two, so that the existence and uniqueness for this first equation can be obtained in a first step. Then, the two remaining equations are understood as SDEs with stochastic drift terms and the methodologies developed in [45], [46] and [47] can be used.

However, in the case of the FBSDE (2.8), the three equations are coupled each other. This is the reason why the existence and uniqueness of solution for FBSDE (2.8) remains as an open problem, as well as the same results for the PDE problem (2.10)-(2.11).

Chapter 3

Numerical methods for the REC pricing model

3.1 Introduction

Once the final value problems associated to the single period and multiple period cases have been posed in the previous Chapter 2, since there are no analytical expression for their respective solutions, we propose a set of numerical methods to approximate them.

For this purpose, first note that the PDE (2.10) is initially posed in a spatial unbounded domain, so that a truncation of the domain to a bounded one is required for the numerical solution. This domain truncation is very common in option pricing problems, for example, and requires an appropriate selection of the truncation boundaries and the corresponding boundary conditions to obtain a proper approximation of the solution in the region of actual financial interest [40].

Secondly, as the drift term (2.3) depends linearly on the unknown P, the corresponding first order (convective) term introduces a non-linear aspect that needs to be solved. More precisely, the governing PDE is semilinear. A possible approach could be to treat this nonlinear term in a semi-explict way in the time discretization, by considering the drift coefficient evaluated at the previous time step, which linearizes

the problem to be solved at each time step. However, implicit methods are usually preferred to explicit or semi-explicit ones. In the present work we will take advantage of the fact that the non-linear term can be written in terms of a maximal monotone operator to apply a duality method.

A third aspect is related to the lack of second order derivative with respect to variable B, which makes the second order PDE degenerate. In order to overcome the difficulties associated to this last aspect, we propose two methods: a semi-Lagrangian numerical scheme to jointly discretize the terms of time derivative and the first order derivative with respect to B, and a Lagrange-Galerkin method, which mainly consists of Crank-Nicolson characteristics for time discretization combined with finite elements for the discretization in the accumulated green certificates and the natural logarithm of the renewable generation rate directions. Note that semi-Lagrangian schemes and Lagrange-Galerkin methods are specially suitable for convection dominated problems, where the convection term related to first order derivatives in space dominate diffusion terms associated to second order derivatives in space in some regions of the spatial domain where the PDE problem is posed. In this respect, we point out the degenerate PDE problem we are considering for pricing RECs can be understood as a limit case of convection dominated problem.

Clearly, in view of these important specific characteristics of the PDE (2.10) suitable and efficient numerical techniques need to be applied.

3.1.1 Treatment of the non-linear convective term

As previously pointed out, the PDE problem (2.10) includes a non-linear convective term. One possibility to deal with this non-linearity is based on the Bermúdez-Moreno algorithm, which involves the Yosida regularization of non-linear maximal monotone operators (see [8], for further details).

In [2], the here proposed techniques to deal with this nonlinear term have been previously applied to a one-dimensional problem with a non-linear diffusion term instead of the non-linear convection one. Furthermore, in [1] the convergence of the

method in the non-linear diffusion setting has been analysed. On the other hand, in [3] the methodology has been extended from one to two spatial dimensions.

Thus, following the idea used in [2], let us first introduce the maximal monotone operator m, defined by

$$m(P) = \begin{cases} 0, & \text{if } P < 0 \\ P^2, & \text{if } P \geq 0, \end{cases} \tag{3.1}$$

so that

$$P\frac{\partial P}{\partial \widetilde{G}} = \frac{1}{2}\frac{\partial m(P)}{\partial \widetilde{G}}. \tag{3.2}$$

Therefore, equation (2.10) can be written in terms of the maximal monotone operator m in the equivalent form:

$$\frac{\partial P}{\partial t} + \frac{\sigma_g^2}{2}\frac{\partial^2 P}{\partial \widetilde{G}^2} + \alpha_g\left(f(t) - \widetilde{G}\right)\frac{\partial P}{\partial \widetilde{G}} + \frac{\beta_g}{2}\frac{\partial m(P)}{\partial \widetilde{G}} + \exp(\widetilde{G})\frac{\partial P}{\partial B} - rP = 0. \tag{3.3}$$

Following the duality technique developed by Bermúdez and Moreno in [8], for the constant parameter $\omega > 0$, we introduce the new additional unknown

$$\theta = (m - \omega I)(P), \tag{3.4}$$

where I denotes the identity operator. So, we have

$$\frac{1}{2}\frac{\partial m(P)}{\partial \widetilde{G}} = \frac{1}{2}\frac{\partial \theta}{\partial \widetilde{G}} + \frac{\omega}{2}\frac{\partial P}{\partial \widetilde{G}}. \tag{3.5}$$

Next, by using the Bermúdez-Moreno lemma from [8], also applied in [3], for $\lambda\omega < 1$, we can obtain the equivalence

$$\theta = m(P) - \omega P \Leftrightarrow \theta = m_\lambda^\omega(P + \lambda\theta), \tag{3.6}$$

where m_λ^ω denotes the Yosida approximation of the operator $m_\omega = m - \omega I$ with parameter λ.

The Yosida approximation is given by

$$m_\lambda^\omega = (I - J_\lambda^\omega)/\lambda,$$

where

$$J_\lambda^\omega = (I + \lambda_\omega)^{-1}$$

is the resolvent operator of m_ω with parameter λ, which is defined for $\lambda\omega < 1$ and it is a monotone Lipschitz function with constant $(1-\lambda\omega)^{-1}$.

It is easy to prove the equivalence (3.6). For this purpose, starting from the right hand side of (3.6) and using the definition of m_λ^ω, we get:

$$\theta = m_\lambda^\omega(P+\lambda\theta) = \frac{1}{\lambda}(I - J_\lambda^\omega)(P+\lambda\theta) = \frac{P}{\lambda} + \theta - \frac{1}{\lambda}J_\lambda^\omega(P+\lambda\theta),$$

which is equivalent to

$$P = J_\lambda^\omega(P+\lambda\theta).$$

Next, using the definition of the resolvent operator J_λ^ω, we get

$$P = (I+\lambda m_\omega)^{-1}(P+\lambda\theta),$$

or equivalently:

$$(I+\lambda m_\omega)(P) = P+\lambda\theta,$$

From this identity, we easily get

$$\theta = m(P) - \omega P,$$

last identity being the left hand side of (3.6).

For details about Yosida approximation of maximal monotone operators, we address the reader to [13].

In [1], the convergence of the method for a model with the same nonlinear term in the diffusion part of an elliptic operator in one dimension has been analyzed, obtaining that the optimal choice for convergence comes from condition $2\lambda\omega = 1$.

Although we have not addressed this theoretical analysis for the here treated problem, we consider also this relation between both parameters. Also this choice is theoretically obtained in [8] for some elliptic variational inequalities formulated in terms of a multivalued subdifferential operator.

Under this choice $2\lambda\omega = 1$, the expression of Yosida approximation can be

computed and is given by [2]:

$$m_\lambda^\omega\left(P+\frac{\theta}{2\omega}\right)=\begin{cases}-\theta-2\omega P, & \text{if } P+\dfrac{\theta}{2\omega}\leq 0,\\[2ex] \theta+2\omega P+\omega^2-\omega\sqrt{4\theta+8\omega P+\omega^2}, & \text{if } P+\dfrac{\theta}{2\omega}\geq 0.\end{cases}$$

Next, if we introduce the linear differential operator

$$\mathcal{L}_2[P]=\frac{\partial P}{\partial t}+\frac{\sigma_g^2}{2}\frac{\partial^2 P}{\partial \widetilde{G}^2}+\alpha_g\left(f(t)-\widetilde{G}\right)\frac{\partial P}{\partial \widetilde{G}}+\frac{\beta_g\omega}{2}\frac{\partial P}{\partial \widetilde{G}}+\exp(\widetilde{G})\frac{\partial P}{\partial B}-rP. \tag{3.7}$$

and take into account the expressions (3.4) and (3.5), then equation (3.3) can be rewritten in the equivalent form:

$$\mathcal{L}_2[P]=-\frac{\beta_g}{2}\frac{\partial \theta}{\partial \widetilde{G}}. \tag{3.8}$$

Moreover, from the equivalence stated in (3.6), equation (3.8) is coupled with the following non-linear equation:

$$\theta=m_\lambda^\omega(P+\lambda\theta). \tag{3.9}$$

In order to solve the non-linear system given by (3.8)-(3.9), we propose a fixed point iteration which mainly starts with an initial value of θ to solve the linear PDE (3.8). Then, we replace the obtained P and the last computed value of θ in the right hand side of (3.9) to update the value of θ and start solving again the PDE (3.8) in the next step. This fixed point algorithm will be explicitly written in a forthcoming section once the discretized problem has been introduced.

3.1.2 Localization and analysis of boundary conditions

In order to apply the numerical discretization using finite differences or finite elements to the PDE problem (3.8), it is necessary to consider a bounded computational domain. Thus, for a given value of θ we approximate the linear PDE problem (3.8) through a localization procedure, which consists in truncating the initial

unbounded domain to a bounded one and introducing the appropriate conditions at the boundaries of the bounded domain.

Let $\bar{\Omega}^* = (T-\gamma, T) \times (0, +\infty) \times \mathbb{R}$ be the initial unbounded domain. Moreover, let $\bar{\Omega} = (T-\gamma, T) \times (0, \hat{b}) \times (-\bar{g}, \bar{g})$ be the truncated bounded domain where $\hat{b}$ and $\bar{g}$ are large enough real numbers, which are influenced by the requirement of the payoff function and the jump conditions at compliance dates. Now, we introduce the changes of variables:

$$\hat{B} = \frac{B}{\hat{b}}, \qquad \hat{G} = \frac{\widetilde{G} + \bar{g}}{\hat{g}},$$

with $\hat{g} = 2\bar{g}$, so that the truncated domain $\Omega^* = (T-\gamma, T) \times (0,1) \times (0,1)$ in the new variables $(t, \hat{B}, \hat{G})$ is considered.

In order to establish the boundaries of the truncated domain which require boundary conditions to be imposed, we follow the results in [51] and introduce the following notation

$$y_0 = t, \quad y_1 = \hat{B}, \quad y_2 = \hat{G}, \tag{3.10}$$

so that equation (3.7) can be equivalently written as

$$\sum_{i,j=0}^{2} a_{ij} \frac{\partial^2 P}{\partial y_i y_j} + \sum_{j=0}^{2} a_j \frac{\partial P}{\partial y_j} + b_0 P = 0, \quad \text{in } \Omega^*, \tag{3.11}$$

where

$$\begin{aligned} A = (a_{ij}) &= \begin{pmatrix} 0 & 0 & 0 \\ 0 & 0 & 0 \\ 0 & 0 & \dfrac{\hat{g}^2 \sigma_g^2}{2} \end{pmatrix}, \\ \vec{a} = (a_j) &= \begin{pmatrix} 1 \\ \hat{b} \exp(y_2 \hat{g} - \bar{g}) \\ \hat{g}\alpha_g \left(f(y_0) - (y_2 \hat{g} - \bar{g}) + \dfrac{\beta_g \omega}{2\alpha_g} \right) \end{pmatrix}, \quad b_0 = -r, \end{aligned} \tag{3.12}$$

and we use the notation

$$\Omega^* = \prod_{i=0}^{2} \left(\underline{y}_i, \overline{y}_i \right), \quad \Gamma^* = \partial\Omega^*,$$
$$\Gamma_i^{*,-} = \left\{ y \in \Gamma^* / y_i = \underline{y}_i \right\}, \quad \Gamma_i^{*,+} = \left\{ y \in \Gamma^* / y_i = \overline{y}_i \right\}, \quad i = 0, 1, 2.$$

Next, we denote by $\vec{n} = (n_0, n_1, n_2)$ the normal vector to Γ^* pointing inwards Ω^*. Let us define the following subsets of Γ^*:

$$\Sigma^0 = \left\{ y \in \Gamma^* / \sum_{i,j=0}^{2} a_{ij} n_i n_j = 0 \right\}, \quad \Sigma^1 = \Gamma^* - \Sigma^0,$$
$$\Sigma^2 = \left\{ y \in \Sigma^0 / \sum_{i=0}^{2} \left(a_i - \sum_{j=0}^{2} \frac{\partial a_{ij}}{\partial y_j} \right) n_i < 0 \right\}.$$

Following [51], we need to impose boundary conditions at $\Sigma^1 \cup \Sigma^2$. Thus, for (3.10), we conclude:

$$\Sigma^0 = \Gamma_0^{*,-} \cup \Gamma_0^{*,+} \cup \Gamma_1^{*,-} \cup \Gamma_1^{*,+}, \quad \Sigma^1 = \Gamma_2^{*,-} \cup \Gamma_2^{*,+}, \quad \Sigma^2 = \Gamma_0^{*,+} \cup \Gamma_1^{*,+},$$

so that

$$\Sigma^1 \cup \Sigma^2 = \Gamma_0^{*,+} \cup \Gamma_1^{*,+} \cup \Gamma_2^{*,-} \cup \Gamma_2^{*,+}.$$

Hence, we impose the following homogeneous Neumann boundary conditions at the spatial boundaries:

$$\begin{aligned} &\frac{\partial P}{\partial y_1} = 0, \text{ on } \Gamma_1^{*,+}, \\ &\frac{\partial P}{\partial y_2} = 0, \text{ on } \Gamma_2^{*,-} \cup \Gamma_2^{*,+}, \end{aligned} \tag{3.13}$$

jointly with the final condition at the boundary $y_0 = T$ in the single period case.

In addition, in the multiple period case the condition (2.12) is applied at the boundaries $y_0 = T^i$, which represent each compliance date for each linked PDE problem with final condition at $t = T^i$.

3.1.3 First numerical method

In this first method, as we previously indicated, we use a characteristics scheme to discretize the material derivative operator in one of the spatial directions combined with the use of a second order implicit finite differences scheme in the other spatial direction.

The development of this numerical method, jointly with the statement of the mathematical model for pricing RECs has been already published in [4].

3.1.3.1 Discretization of the PDE

In order to choose an appropriate time discretization scheme for the PDE (3.8), we note that the linear differential operator (3.7) is degenerate. Therefore, PDE (3.8) can be considered as a limit case of a convection dominated PDE, especially in the direction without diffusion term. Therefore, in order to avoid spurious oscillations related to the use of standard finite differences schemes, we propose a suitable version of the method of characteristics (see [7] or [28], for example).

Note that PDE (3.8) turns out to be similar to the one arising in the pricing of Asian options with continuous arithmetic averaging. Thus, we follow the idea first proposed in [33] for this kind of problem, which consists of choosing a semi-Lagrangian method (also referred as the characteristics method) in the direction without diffusion combined with a Crank-Nicolson finite differences scheme in the direction with diffusion. This method has been also used for solving PDE models for the valuation of business companies in [22].

For solving the coupled non-linear problem (3.8)-(3.9) we apply the proposed time discretization scheme to the step of solving equation (3.8).

For the time discretization, we first consider the change of time variable $\tau = T - t$, where τ represents the time to compliance date. Therefore, equation (3.8) can be equivalently written in the domain $\widetilde{\Omega} = (0, \gamma) \times (0, 1) \times (0, 1)$ as follows

$$\frac{\mathrm{D}P}{\mathrm{D}\tau} - \mathcal{A}P = 0, \tag{3.14}$$

where the involved differential operators are given by

$$\frac{\mathrm{D}P}{\mathrm{D}\tau} = \frac{\partial P}{\partial \tau} - \hat{b}\exp(\hat{G}\hat{g} - \bar{g})\frac{\partial P}{\partial \hat{B}},$$
$$\mathcal{A}P = \frac{\hat{g}^2\sigma_g^2}{2}\frac{\partial^2 P}{\partial \hat{G}^2} + \hat{g}\alpha_g\left(f(T-\tau) - \left(\hat{G}\hat{g} - \bar{g}\right) + \frac{\beta_g\omega}{2\alpha_g}\right)\frac{\partial P}{\partial \hat{G}} + \frac{\hat{g}\beta_g}{2}\frac{\partial \theta}{\partial \hat{G}} - rP.$$

Note that $\dfrac{\mathrm{D}P}{\mathrm{D}\tau}$ represents the material derivative of P in the direction $\hat{B}$ associated to the one-dimensional velocity field

$$v = -\hat{b}\exp(\hat{G}\hat{g} - \bar{g}),$$

which does not depend on B.

Moreover, $\mathcal{A}$ denotes the second order convection-diffusion-reaction differential operator in the direction $\hat{G}$. Note that this splitting of the differential operator governing equation (3.8) is the departure point of the proposed time discretization scheme.

First, we use a characteristics scheme to discretize in time the term associated to the material derivative. This semi-Lagrangian scheme is based on a finite difference discretization of the time derivative along the characteristic lines (see [7], [28], [62], for example).

For this purpose, we introduce $N_T > 0$ and a time step $\Delta\tau = \gamma/N_T$ for considering a uniform time mesh with nodes given by $\tau^n = n\Delta\tau$, for $n = 0, 1, \ldots, N_T$. At each time step we consider the initial value ODE problem satisfied by the trajectory associated to the velocity field v through the point $(\tau^{n+1}, \hat{B})$:

$$\begin{cases} \dfrac{d\chi}{ds}(s) = -\hat{b}\exp\left(\hat{G}\hat{g} - \bar{g}\right), \\ \chi\left(\tau^{n+1}\right) = \hat{B}. \end{cases}$$

Note that the solution of this ODE problem is given by

$$\chi(s) = \hat{B} + (\tau^{n+1} - s)\hat{b}\exp\left(\hat{G}\hat{g} - \bar{g}\right).$$

In order to build the finite differences approximation of the material derivative along the characteristics, we introduce $\chi^n = \chi(\tau^n)$, which is given by

$$\chi^n\left(\hat{B}, \hat{G}\right) = \hat{B} + \Delta\tau\hat{b}\exp\left(\hat{G}\hat{g} - \bar{g}\right),$$

and represents the position at time τ^n of the point placed at $\left(\hat{B},\hat{G}\right)$ at time τ^{n+1} and moving according to the velocity field v.

Next, we introduce the approximation for the material derivative:

$$\frac{\mathrm{D}P}{\mathrm{D}\tau}\left(\tau^{n+1},\hat{B},\hat{G}\right)\approx\frac{P\left(\tau^{n+1},\hat{B},\hat{G}\right)-P\left(\tau^{n},\chi^{n}\left(\hat{B},\hat{G}\right),\hat{G}\right)}{\Delta\tau}. \tag{3.15}$$

Secondly, by using a Crank-Nicolson scheme ($\hat{\theta}=0.5$ in the so called $\hat{\theta}$-method) for the second order differential term $\mathcal{A}P$ in equation (3.14), we obtain:

$$\begin{aligned}
&\frac{P^{n+1}-P^{n}\circ\chi^{n}}{\Delta\tau}-\frac{\hat{\theta}\hat{g}^{2}\sigma_{g}^{2}}{2}\frac{\partial^{2}P^{n+1}}{\partial\hat{G}^{2}}-\frac{(1-\hat{\theta})\hat{g}^{2}\sigma_{g}^{2}}{2}\frac{\partial^{2}\left(P^{n}\circ\chi^{n}\right)}{\partial\hat{G}^{2}}\\
&-\hat{\theta}\hat{g}\alpha_{g}\left(f(T-\tau)-\left(\hat{G}\hat{g}-\bar{g}\right)+\frac{\beta_{g}\omega}{2\alpha_{g}}\right)\frac{\partial P^{n+1}}{\partial\hat{G}}\\
&-(1-\hat{\theta})\hat{g}\alpha_{g}\left(f(T-\tau)-\left(\hat{G}\hat{g}-\bar{g}\right)+\frac{\beta_{g}\omega}{2\alpha_{g}}\right)\frac{\partial\left(P^{n}\circ\chi^{n}\right)}{\partial\hat{G}}\\
&+r\hat{\theta}P^{n+1}+r(1-\hat{\theta})\left(P^{n}\circ\chi^{n}\right)=\frac{\hat{\theta}\hat{g}\beta_{g}}{2}\frac{\partial\theta^{n+1}}{\partial\hat{G}}+\frac{(1-\hat{\theta})\hat{g}\beta_{g}}{2}\frac{\partial\theta^{n}}{\partial\hat{G}},
\end{aligned} \tag{3.16}$$

At each time step, the evaluation of the term $P^n\circ\chi^n$ in (3.16) at the quadrature nodes is approximated by using a biquadratic interpolation formula from the values of P^n at the mesh nodes.

Note that at each time step, equation (3.16) is coupled with the following non-linear relation between P^{n+1} and θ^{n+1}:

$$\theta^{n+1}=m_{\lambda}^{\omega}(P^{n+1}+\lambda\theta^{n+1}). \tag{3.17}$$

3.1.3.2 Fixed point algorithm

Next, we propose a fixed point algorithm to approximate the solution of the non-linear problem (3.16)-(3.17). This fixed point algorithm mainly consists of solving equation (3.16) to obtain P^{n+1} for a previously computed value of θ^{n+1}, and next updating θ^{n+1} according to (3.17) with the more recent values of P^{n+1} and θ^{n+1}. Thus, the algorithm can be sketched as follows:

1. Let P^0 and θ^0 be initialized (for example $\theta^0=1$).

2. For $n = 0, 1, \ldots, N_T - 1$.

   (a) Let $\theta^{n+1,0} = \theta^n$.

   (b) For $k = 0, 1, 2, \ldots$

   - For a given $\theta^{n+1,k}$, we obtain $P^{n+1,k+1}$ by solving

$$
\begin{cases}
\left(1 + r\hat{\theta}\Delta\tau\right) P^{n+1,k+1} - \dfrac{\hat{\theta}\hat{g}^2\sigma_g^2\Delta\tau}{2}\dfrac{\partial^2 P^{n+1,k+1}}{\partial\hat{G}^2} \\
\quad -\hat{\theta}\hat{g}\alpha_g\Delta\tau\left(f(T-\tau^{n+1}) - (\hat{G}\hat{g} - \bar{g})\right)\dfrac{\partial P^{n+1,k+1}}{\partial\hat{G}} \\
\quad -\hat{\theta}\hat{g}\alpha_g\Delta\tau\left(\dfrac{\beta_g\omega}{2\alpha_g}\right)\dfrac{\partial P^{n+1,k+1}}{\partial\hat{G}} \\
\quad = \left[1 - r\Delta\tau(\,1 - \hat{\theta}\,)\right](P^n \circ \chi^n) \\
\quad +\dfrac{\left(1-\hat{\theta}\right)\hat{g}^2\sigma_g^2\Delta\tau}{2}\dfrac{\partial^2\left(P^n\circ\chi^n\right)}{\partial\hat{G}^2} \\
\quad +\left(1-\hat{\theta}\right)\hat{g}\alpha_g\Delta\tau\left(f(T-\tau^n)\right)\dfrac{\partial\left(P^n\circ\chi^n\right)}{\partial\hat{G}} \\
\quad -\left(1-\hat{\theta}\right)\hat{g}\alpha_g\Delta\tau(\hat{G}\hat{g}-\bar{g})\dfrac{\partial\left(P^n\circ\chi^n\right)}{\partial\hat{G}} \\
\quad +\left(1-\hat{\theta}\right)\hat{g}\alpha_g\Delta\tau\left[\dfrac{\beta_g}{\alpha_g}\left(P^n\circ\chi^n\right)\right]\dfrac{\partial\left(P^n\circ\chi^n\right)}{\partial\hat{G}} \\
\quad +\dfrac{(1-\hat{\theta})\hat{g}\beta_g\Delta\tau}{2}\dfrac{\partial\theta^n}{\partial\hat{G}} + \dfrac{\hat{\theta}\hat{g}\beta_g\Delta\tau}{2}\dfrac{\partial\theta^{n+1,k}}{\partial\hat{G}},
\end{cases}
\tag{3.18}
$$

     jointly with the boundary conditions.

   - We update $\theta^{n+1,k+1}$ by using the identity

$$\theta^{n+1,k+1} = m_\lambda^\omega\left(P^{n+1,k+1} + \lambda\theta^{n+1,k}\right).$$

   - We check the stopping test

$$\frac{||\theta^{n+1,k+1} - \theta^{n+1,k}||_\infty}{||\theta^{n+1,k+1}||_\infty} < \epsilon.$$

   (c) If the stopping test is satisfied then go to 2, otherwise go to (b).

In order to describe the solution of the fully discretized problem, let us introduce the notation $(\tau^n, \hat{B}_i, \hat{G}_j) = \left(n\Delta\tau, i\Delta\hat{B}, j\Delta\hat{G}\right)$ to represent a generic node of the uniform finite differences time-space mesh with time step $\Delta\tau$ and spatial steps $\Delta\hat{B}$ and $\Delta\hat{G}$, for indexes $n = 0, 1, \ldots, N_T$, $i = 0, 1, \ldots, N_{\hat{B}}$ and $j = 0, 1, \ldots, N_{\hat{G}}$.

At each fixed point iteration, the full discretization of problem (3.18) can be written as follows:

$$
\begin{aligned}
&\frac{P_{i,j}^{n+1,k+1} - P_{i,j}^{n} \circ \chi^n}{\Delta\tau} - \frac{\hat{\theta}\hat{g}^2\sigma_g^2}{2}\left(\frac{P_{i,j+1}^{n+1,k+1} - 2P_{i,j}^{n+1,k+1} + P_{i,j-1}^{n+1,k+1}}{\left(\Delta\hat{G}\right)^2}\right)\\
&- \frac{(1-\hat{\theta})\hat{g}^2\sigma_g^2}{2}\left(\frac{P_{\chi^n,j+1}^{n} - 2P_{\chi^n,j}^{n} + P_{\chi^n,j-1}^{n}}{\left(\Delta\hat{G}\right)^2}\right)\\
&- \hat{\theta}\hat{g}\alpha_g\left(f(T-\tau^{n+1}) - \left(\hat{G}_j\hat{g} - \bar{g}\right) + \frac{\beta_g\omega}{2\alpha_g}\right)\left(\frac{P_{i,j+1}^{n+1,k+1} - P_{i,j-1}^{n+1,k+1}}{2\Delta\hat{G}}\right)\\
&- (1-\hat{\theta})\hat{g}\alpha_g\left(f(T-\tau^{n}) - \left(\hat{G}_j\hat{g} - \bar{g}\right) + \frac{\beta_g\omega}{2\alpha_g}\right)\left(\frac{P_{\chi^n,j+1}^{n} - P_{\chi^n,j-1}^{n}}{2\Delta\hat{G}}\right)\\
&- \frac{\hat{\theta}\hat{g}\beta_g}{2}\left(\frac{\theta_{i,j+1}^{n+1,k} - \theta_{i,j-1}^{n+1,k}}{2\Delta\hat{G}}\right) - \frac{(1-\hat{\theta})\hat{g}\beta_g}{2}\left(\frac{\theta_{i,j+1}^{n} - \theta_{i,j-1}^{n}}{2\Delta\hat{G}}\right)\\
&+ r\hat{\theta}P_{i,j}^{n+1} + r(1-\hat{\theta})P_{\chi^n,j}^{n} = 0,
\end{aligned}
$$

where $\hat{\theta} = 0.5$ for the Crank-Nicolson time discretization, and

$$
\begin{aligned}
P_{r,s}^{l,m} &\approx P^m(\tau^l, \hat{B}_r, \hat{G}_s),\\
P_{\chi^l,s}^{l,m} &\approx P^m(\tau^l, \chi^l, \hat{G}_s),\\
\theta_{r,s}^{l,m} &\approx \theta^m(\tau^l, \hat{B}_r, \hat{G}_s),
\end{aligned}
$$

denote the corresponding approximations with the numerical method at the mesh nodes.

By taking into account the previous expression of the fully discretized problem, we have to solve a linear system with $(N_{\hat{B}}-1)\times(N_{\hat{G}}-1)$ unknowns at each time step. Moreover, if we order the finite differences mesh nodes in lexicographical order, the

resulting matrix is block diagonal with $N_{\hat{B}}-1$ blocks of tridiagonal matrices of order $N_{\hat{G}}-1$ each. So, by applying the classical Thomas algorithm for block tridiagonal matrices, each $N_{\hat{B}}-1$ linear system can be efficiently solved. Thus, at each time step and for each value of $i=1,\ldots,\ N_{\hat{B}}-1$, we have the following linear system:

$$C(\hat{G})P_i^{n+1}=b_i^n,$$

where $P_i^{n+1}=\left(P_{i,1}^{n+1},P_{i,2}^{n+1},\ldots,P_{i,N_{\hat{G}}-2}^{n+1},P_{i,N_{\hat{G}}-1}^{n+1}\right)$ is the approximation of the solution at the finite differences mesh nodes with coordinate $\hat{B}=\hat{B}_i$, and the matrix $C(\hat{G})$ is given by

$$C(\hat{G})=\begin{pmatrix} c_1(\hat{G}_1) & c_2(\hat{G}_1) & 0 & \cdots & 0 \\ c_3(\hat{G}_2) & c_1(\hat{G}_2) & c_2(\hat{G}_2) & \ddots & \vdots \\ 0 & \ddots & \ddots & \ddots & 0 \\ \vdots & \ddots & \ddots & c_1(\hat{G}_{N_{\hat{G}}-2}) & c_2(\hat{G}_{N_{\hat{G}}-2}) \\ 0 & \cdots & 0 & c_3(\hat{G}_{N_{\hat{G}}-1}) & c_1(\hat{G}_{N_{\hat{G}}-1}) \end{pmatrix}$$

where

$$c_1(\hat{G}_j)=1+r\hat{\theta}\Delta\tau+\frac{\hat{\theta}\hat{g}^2\sigma_g^2\Delta\tau}{\left(\Delta\hat{G}\right)^2},$$

$$c_2(\hat{G}_j)=-\frac{\hat{\theta}\hat{g}^2\sigma_g^2\Delta\tau}{2\left(\Delta\hat{G}\right)^2}-\frac{\hat{\theta}\hat{g}\alpha_g\Delta\tau\left(f\left(T-\tau^{n+1}\right)-\left(\hat{G}_j\hat{g}-\bar{g}\right)+\dfrac{\beta_g\omega}{2\alpha_g}\right)}{2\Delta\hat{G}},$$

$$c_3(\hat{G}_j)=-\frac{\hat{\theta}\hat{g}^2\sigma_g^2\Delta\tau}{2\left(\Delta\hat{G}\right)^2}+\frac{\hat{\theta}\hat{g}\alpha_g\Delta\tau\left(f\left(T-\tau^{n+1}\right)-\left(\hat{G}_j\hat{g}-\bar{g}\right)+\dfrac{\beta_g\omega}{2\alpha_g}\right)}{2\Delta\hat{G}}.$$

Moreover, for $j=1,\ldots,N_{\hat{G}}-1$, the jth component of the second member vector b_i^n

of the linear system is given by

$$
\begin{aligned}
(b_i^n)_j = & \left(\left[1 - r\Delta\tau \left(1 - \hat{\theta} \right) \right] - \frac{\sigma_g^2 \hat{g}^2 \Delta\tau \left(1 - \hat{\theta} \right)}{\left(\Delta\hat{G} \right)^2} \right) P^n_{\chi^n, j} \\
& + \left(\frac{\alpha_g \hat{g} \Delta\tau (1 - \hat{\theta}) \left[f(T - \tau^n) - \left(\hat{G}_j \hat{g} - \bar{g} \right) + \frac{\beta_g}{\alpha_g} P^n_{\chi^n, j} \right]}{2\Delta\hat{G}} \right) P^n_{\chi^n, j+1} \\
& + \left(\frac{\sigma_g^2 \hat{g}^2 \Delta\tau \left(1 - \hat{\theta} \right)}{2 \left(\Delta\hat{G} \right)^2} \right) P^n_{\chi^n, j+1} + \left(\frac{\sigma_g^2 \hat{g}^2 \Delta\tau \left(1 - \hat{\theta} \right)}{2 \left(\Delta\hat{G} \right)^2} \right) P^n_{\chi^n, j-1} \\
& - \left(\frac{\alpha_g \hat{g} \Delta\tau (1 - \hat{\theta}) \left[f(T - \tau^n) - \left(\hat{G}_j \hat{g} - \bar{g} \right) + \frac{\beta_g}{\alpha_g} P^n_{\chi^n, j} \right]}{2\Delta\hat{G}} \right) P^n_{\chi^n, j-1} \\
& + \frac{(1 - \hat{\theta}) \hat{g} \Delta\tau \beta_g}{2} \left(\frac{\theta^n_{i,j+1} - \theta^n_{i,j-1}}{2\Delta\hat{G}} \right) + \frac{\hat{\theta} \hat{g} \Delta\tau \beta_g}{2} \left(\frac{\theta^{n+1,k}_{i,j+1} - \theta^{n+1,k}_{i,j-1}}{2\Delta\hat{G}} \right).
\end{aligned}
$$

3.1.4 Second numerical method

In this second method, the resulting linear problem is discretized by using a Lagrange-Galerkin method which mainly consists of Crank-Nicolson characteristics scheme for time discretization combined with finite elements for the discretization in the accumulated green certificates and the natural logarithm of the renewable generation rate directions.

These numerical techniques, which result very efficient for convection dominated problems as the one treated in this work, were developed in [11] for Asian option pricing problems. Moreover, in [9], the authors address the numerical analysis of the Crank-Nicolson time discretization proposed here. Additionally, the fully discretized problem, combining Crank-Nicolson characteristics with Lagrange finite elements is studied in [10].

3.1.4.1 PDE formulation in a bounded domain

Taking into account the bounded spatial domain $\Omega = (0,1) \times (0,1)$, the boundary of which can be decomposed as

$$\Gamma = \bigcup_{i=1}^{2} (\Gamma_i^- \cup \Gamma_i^+)$$

where

$$\Gamma_i^- = \{(y_1, y_2) \in \Gamma |\ y_i = 0\},\ \ \Gamma_i^+ = \{(y_1, y_2) \in \Gamma |\ y_i = 1\},\ i = 1, 2.$$

Next, we can introduce the change of time variable $\tau = T - t$, where τ represents the time to compliance date t.

Then, we can formulate the PDE (3.3) in divergence form in order to obtain a PDE problem with initial condition in the new time variable, as follows: find $P : [0, \gamma] \times \Omega \to \mathbb{R}$ such that

$$\begin{aligned}
\frac{\partial P}{\partial \tau} - Div(\mathcal{A}\nabla P) + v \cdot \nabla P + lP &= \hat{h} + \frac{\beta_g \hat{g}}{2} \frac{\partial \theta}{\partial y_2} \text{ in } (0,\gamma) \times \Omega\,, && (3.19)\\
P(0,\cdot) &= \pi_T \mathbb{1}_{\{\hat{B}\hat{b} < R_T\}} \text{ in } \Omega, && (3.20)\\
\frac{\partial P}{\partial y_1} &= 0 \text{ on } (0,\gamma) \times \Gamma_1^+, && (3.21)\\
\frac{\partial P}{\partial y_2} &= 0 \text{ on } (0,\gamma) \times (\Gamma_2^- \cup \Gamma_2^+), && (3.22)
\end{aligned}$$

jointly with jump conditions (2.12) at compliance dates. Moreover, in (3.19), the diffusion matrix $\mathcal{A}$, the velocity field v, the linear term l and the second member function $\hat{h}$ have the following expressions:

$$\begin{aligned}
\mathcal{A} &= \begin{pmatrix} 0 & 0 \\ 0 & \dfrac{\hat{g}^2 \sigma_g^2}{2} \end{pmatrix},\\
v &= \begin{pmatrix} -\hat{b} \exp(y_2 \hat{g} - \bar{g}) \\ -\hat{g}\alpha_g \left(f(T-\tau) - (y_2 \hat{g} - \bar{g}) + \dfrac{\beta_g \omega}{2\alpha_g} \right) \end{pmatrix},\\
l &= r,\\
\hat{h} &= 0.
\end{aligned}$$

3.1.4.2 The Crank-Nicolson characteristics method

In order to obtain a time discretization of the problem (3.19), we propose a Crank-Nicolson characteristic method. This numerical scheme mainly consists on approximating the material derivative along the characteristics curves with a finite differences method. Moreover, in this method, the convective term is treated explicitly leading to a symmetric system of equations.

First, let us define

$$\frac{DP}{D\tau} = \frac{\partial P}{\partial \tau} + v \cdot \nabla P,$$

which represents the material derivative along the characteristic curve through $y = (y_1, y_2) = (\hat{B}, \hat{G})$ at time $\bar{s}$, $\chi(y, \bar{s}; s)$, which is the solution of the following final value ODE problem:

$$\frac{\partial}{\partial s}\chi(y, \bar{s}; s) = v(\chi(y, \bar{s}; s), s), \quad \chi(y, \bar{s}; \bar{s}) = y. \tag{3.23}$$

In order to discretize in time the material derivative, we introduce a number of time steps $N_T > 0$, a time step $\Delta\tau = \gamma/N_T$ and the time mesh points $\tau^n = n\Delta\tau$, $n = 0, \frac{1}{2}, 1, \frac{3}{2}, \ldots, N_T$.

Now, we approximate the material derivative at time $\tau^{n+\frac{1}{2}}$ by the quotient:

$$\frac{DP}{D\tau} \approx \frac{P^{n+1} - P^n \circ \chi^n}{\Delta\tau},$$

where $\chi^n(y) = \chi(y, \tau^{n+1}; \tau^n)$.

In some cases, the expressions of the characteristic curves or integral paths associated to the velocity field can be obtained analytically. For example, when the seasonality function f is equal to zero the components of $\chi^n(y)$ are given by

$$\begin{aligned} \chi_1^n(y) &= \hat{b}\exp(y_2\hat{g} - \bar{g}) + y_1, \\ \chi_2^n(y) &= -\hat{g}\alpha_g\left((y_2\hat{g} - \bar{g}) - \frac{\beta_g\omega}{2\alpha_g}\right) + y_2 \end{aligned}$$

However, sometimes it is necessary to approximate the characteristics by using numerical ODE solvers. In this work, we will implement a second order explicit

Runge-Kutta scheme for the cases in which the computation of an analytical solution of the final value problem (3.23) is not possible.

Now, let us write the Crank-Nicolson characteristics time discretization around $(\chi(y,\tau^{n+1};\tau^{n+\frac{1}{2}}),\tau^{n+\frac{1}{2}})$, $n=0$, ..., N_T-1, for the first equation of (3.19), namely:

$$\begin{aligned}\frac{P^{n+1}(y)-P^n(\chi^n(y))}{\Delta\tau}-\frac{1}{2}Div(\mathcal{A}\nabla P^{n+1})(y)-\frac{1}{2}Div(\mathcal{A}\nabla P^n)(\chi^n(y))\\ +\frac{1}{2}(l\,P^{n+1})(y)+\frac{1}{2}(l\,P^n)(\chi^n(y))=\frac{1}{2}\hat{h}^{n+1}(y)+\frac{1}{2}\hat{h}^n(\chi^n(y))\\ +\frac{1}{2}\frac{\beta_g\hat{g}}{2}\left(\frac{\partial\theta^{n+1}}{\partial y_2}(y)+\frac{\partial\theta^n}{\partial y_2}(\chi^n(y))\right).\end{aligned} \tag{3.24}$$

Moreover, at each time step, equation (3.24) is coupled with the following non-linear relation between P^{n+1} and θ^{n+1};

$$\theta^{n+1}=m^{\omega}_{1/2\omega}\left(P^{n+1}+\frac{1}{2\omega}\theta^{n+1}\right). \tag{3.25}$$

In order to approximate the solution of the non-linear problem (3.24)-(3.25) at each iteration of the characteristics method, we propose the following fixed point scheme:

1. Let $N_T>0$, $\epsilon>0$, P^0, θ^0 given.

2. For $n=0,1,2,...,N_T-1$

   A. Let $\theta^{n+1,0}=\theta^n$.

   B. For $k=0,1,2,...$

– For $\theta^{n+1,k}$ known, we obtain $P^{n+1,k+1}$ by solving the linear problem

$$\begin{aligned}\frac{P^{n+1,k+1}(y)-P^n(\chi^n(y))}{\Delta\tau}-\frac{1}{2}Div(\mathcal{A}\nabla P^{n+1,k+1})(y)\\ -\frac{1}{2}Div(\mathcal{A}\nabla P^n)(\chi^n(y))+\frac{1}{2}(l\,P^{n+1,k+1})(y)\\ +\frac{1}{2}(l\,P^n)(\chi^n(y))=\frac{1}{2}\hat{h}^{n+1}(y)+\frac{1}{2}\hat{h}^n(\chi^n(y))\\ +\frac{1}{2}\frac{\beta_g\hat{g}}{2}\left(\frac{\partial\theta^{n+1,k}}{\partial y_2}(y)+\frac{\partial\theta^n}{\partial y_2}(\chi^n(y))\right),\end{aligned} \tag{3.26}$$

jointly with the boundary conditions.

– We set

$$\theta^{n+1,k+1}=m^{\omega}_{1/2\omega}\left(P^{n+1,k+1}+\frac{1}{2\omega}\theta^{n+1,k}\right)$$

– We check the stopping test

$$\frac{||\theta^{n+1,k+1}-\theta^{n+1,k}||_\infty}{||\theta^{n+1,k+1}||_\infty}<\epsilon.$$

C. We go to 2 if the stopping condition is met, otherwise we repeat the above steps starting at B.

3.1.4.3 Spatial discretization

For the spatial discretization of the linear problem (3.26), we propose biquadratic Lagrange finite elements based on a quadrangular mesh of the spatial domain.

First, we need to obtain a variational formulation of such problem at each time step $n = 0, 1, 2, ..., N_T - 1$, and each fixed point iteration, $k = 0, 1, 2, ...$ For this purpose, we multiply (3.26) by a suitable test function, $\phi \in H^1(\Omega)$ and we integrate in Ω.

Moreover, assuming that $\chi^n \in \mathcal{C}^2(\Omega)$ and $(F_e^n)^{-1} \in \mathcal{C}^1(\Omega)$, we apply Green's

theorems, such as the classical Green formula and the following one proposed in [50]:

$$\begin{aligned}\int_\Omega Div(\mathcal{A}\nabla P^n)(\chi^n(y))\phi(y)\,dy = &\int_\Gamma (F_e^n)^{-T}(y)\vec{n}(y)\cdot(\mathcal{A}\nabla P^n)(\chi^n(y))\phi(y)\,dA \\ &- \int_\Omega (F_e^n)^{-1}(y)(\mathcal{A}\nabla P^n)(\chi^n(y))\cdot\nabla\phi(y)\,dy \\ &- \int_\Omega Div((F_e^n)^{-T}(y))\cdot(\mathcal{A}\nabla P^n)(\chi^n(y))\phi(y)\,dy,\end{aligned} \tag{3.27}$$

where $F_e^n = \nabla\chi^n$, $\vec{n}$ is a vector normal to the boundary pointing outward and dA denotes the integration measure on the boundary Γ.

Note that for the particular case in which there is no seasonality effect, i.e. $f = 0$, we can compute analytically the characteristic curve χ^n and its gradient F_e^n, thus obtaining:

$$(F_e^n)^{-1}(y) = \begin{pmatrix} \dfrac{-\hat{g}\hat{b}\Delta\tau\exp(y_2\hat{g}-\bar{g})}{-\beta_g\Delta\tau\hat{g}^2+1} & 1 \\ \dfrac{1}{-\beta_g\Delta\tau\hat{g}^2+1} & 0 \end{pmatrix}, \qquad Div((F_e^n)^{-T}(y)) = 0.$$

Taking into account the previous value of tensor $(F_e^n)^{-1}$, using appropriate Green's formulas and having in view that $\vec{n}\cdot\mathcal{A}\nabla P^{n+1} = 0$ on Γ due to the boundary conditions imposed in the problem (3.19)-(3.21), we can achieve the following variational formulation for the time discretized problem (3.26):

find $P^{n+1,k+1} \in H^1(\Omega)$ such that,

$$\begin{aligned}
&\int_\Omega P^{n+1,k+1}(y)\phi(y)\,dy + \frac{\Delta\tau}{2}\int_\Omega (\mathcal{A}\nabla P^{n+1,k+1})(y)\cdot\nabla\phi(y)\,dy \\
&+ \frac{\Delta\tau}{2}\int_\Omega lP^{n+1,k+1}(y)\phi(y)\,dy = \int_\Omega P^n(\chi^n(y))\phi(y)\,dy \\
&- \frac{\Delta\tau}{2}\int_\Omega (F_e^n)^{-1}(y)(\mathcal{A}\nabla P^n)(\chi^n(y))\cdot\nabla\phi(y)\,dy - \frac{\Delta\tau}{2}\int_\Omega lP^n(\chi^n(y))\phi(y)\,dy \\
&+ \frac{\Delta\tau}{2}\int_\Gamma (F_e^n)^{-T}(y)\vec{n}(y)\cdot(\mathcal{A}\nabla P^n)(\chi^n(y))\phi(y)\,dA \\
&+ \frac{\Delta\tau}{2}\int_\Omega \hat{h}^{n+1}(y)\phi(y)\,d\vec{(y)} + \frac{\Delta\tau}{2}\int_\Omega \hat{h}^n(\chi^n(y))\phi(y)\,d\vec{(y)} \\
&+ \frac{\Delta\tau}{2}\int_\Omega \frac{\beta_g\hat{g}}{2}\frac{\partial\theta^{n+1,k}}{\partial y_2}(y)\phi(y)\,dy + \frac{\Delta\tau}{2}\int_\Omega \frac{\beta_g\hat{g}}{2}\frac{\partial\theta^n}{\partial y_2}(\chi^n(y))\phi(y)\,dy.
\end{aligned} \tag{3.28}$$

In the general case, when it is not possible to compute the characteristics curves analytically, as it is pointed out in [9], denoting by $\mathcal{J} = \nabla v$, we can employ the following approximations:

$$\begin{aligned}
(F_e^n)^{-1}(y) &= \mathcal{I}(y) + \Delta\tau\mathcal{J}^n(\chi^n(y)) + \mathcal{O}(\Delta\tau^2), \\
Div((F_e^n)^{-T}(y)) &= \Delta\tau\nabla Div(v(\chi^n(y))) + \mathcal{O}(\Delta\tau^2).
\end{aligned}$$

In this work, having in view that $\nabla Div(v(\chi^n(y))) = 0$ and considering the previous approximation for the tensor $(F_e^n)^{-1}(y)$, the weak formulation (3.28) can be rewritten as

$$
\begin{aligned}
&\int_\Omega P^{n+1,k+1}(y)\phi(y)\,dy + \frac{\Delta\tau}{2}\int_\Omega (\mathcal{A}\nabla P^{n+1,k+1})(y)\cdot\nabla\phi(y)\,dy \\
&+\frac{\Delta\tau}{2}\int_\Omega lP^{n+1,k+1}(y)\phi(y)\,dy = \int_\Omega P^n(\chi^n(a))\phi(a)\,dy \\
&+\frac{\Delta\tau}{2}\int_\Omega (\mathcal{A}\nabla P^n)(\chi^n(a))\nabla\phi(y)\,dy - \frac{\Delta\tau}{2}\int_\Omega lP^n(\chi^n(y))\phi(y)\,dy \\
&-\frac{\Delta\tau}{2}\int_\Omega \Delta\tau\mathcal{J}^n(\chi^n(y))(\mathcal{A}\nabla P^n)(\chi^n(y))\nabla\phi(y)\,dy \\
&+\frac{\Delta\tau}{2}\int_\Gamma (\mathcal{I}(y)+\Delta\tau\mathcal{J}^n(\chi^n(y)))^T\vec{n}(y)\cdot(\mathcal{A}\nabla P^n)(\chi^n(y))\phi(y)\,dA \\
&+\frac{\Delta\tau}{2}\int_\Omega \hat{h}^{n+1}(y)\phi(y)\,d\vec{(y)} + \frac{\Delta\tau}{2}\int_\Omega \hat{h}^n(\chi^n(y))\phi(y)\,d\vec{(y)} \\
&+\frac{\Delta\tau}{2}\int_\Omega \frac{\beta_g\hat{g}}{2}\frac{\partial\theta^{n+1,k}}{\partial y_2}(y)\phi(y)\,dy + \frac{\Delta\tau}{2}\int_\Omega \frac{\beta_g\hat{g}}{2}\frac{\partial\theta^n}{\partial y_2}(\chi^n(y))\phi(y)\,dy.
\end{aligned}
\tag{3.29}
$$

Now, for a family of quadrangular meshes $\{\tau_h\}$ of the domain Ω, linked to each mesh $\{\tau_h\}$, we can introduce a family of piecewise quadratic Lagrangian finite elements, $(\mathcal{T}, \mathcal{Q}_2, \Sigma_\mathcal{T})$, with $\mathcal{Q}_2$ being the space of polynomials defined in $\mathcal{T}\in\tau_h$ with degree less or equal than two in each spatial variable, and $\Sigma_\mathcal{T}$ the subset of nodes of the element $\mathcal{T}$. More precisely, we can introduce the finite elements space

$$
\nu_h = \{\psi_h \in \mathcal{C}^0(\Omega)|\,\psi_{h\mathcal{T}} \in \mathcal{Q}_2, \quad \forall\mathcal{T}\in\tau_h\}, \tag{3.30}
$$

where $\mathcal{C}^0(\Omega)$ is the space of piecewise continuous functions on Ω.

3.2 Numerical examples

In this section we present some numerical results to illustrate the performance of the proposed numerical methods, as well as to discuss some quantitative and qualitative results for a real problem.

3.2.1 Academic test

As a sanity check of the code and numerical methods, in the first example we show an academic test with known analytical solution. For this purpose, we consider the following non homogeneous non-linear PDE:

$$\mathcal{L}_1[P] = h, \tag{3.31}$$

where the differential operator $\mathcal{L}_1$ is defined by (2.10) and h is given by

$$h(t, B, \widetilde{G}) = \exp\left((T-t)B\widetilde{G}\right) \times$$
$$\left[-B\widetilde{G} + \frac{1}{2}\sigma_g^2 t^2 B^2 - tB\alpha_g\left(f(t) + \frac{\beta_g}{\alpha_g}\exp\left((T-t)B\widetilde{G}\right) - \widetilde{G}\right) - \exp\left(\widetilde{G}\right)t\widetilde{G} - r\right],$$

so that $P(t, B, \widetilde{G}) = \exp\left((T-t)B\widetilde{G}\right)$ is the analytical solution of the PDE (3.31). Moreover, we consider a single period ($\gamma = 1$), with $T = 1$ and the final condition provided by the evaluation of the known solution at time $t = T$.

By choosing $\hat{b} = 1$ and $\bar{g} = 0.5$ (so that $\hat{g} = 1$) for the change of variables, we pose the PDE problem in the time-space bounded domain $\widetilde{\Omega} = [0,1] \times [0,1] \times [0,1]$ with Dirichlet boundary conditions on $\Gamma_1^{*,+}, \Gamma_2^{*,-}$ and $\Gamma_2^{*,+}$ that are given by the evaluation of the solution at the corresponding boundaries.

In this first academic test we do not include the seasonality effect, so that we take $f = 0$. Parameters in the PDE are collected in Table 3.1 and mostly taken from from [26].

Table 3.1: Parameters in the PDE model for the academic test

Parameter	T	γ	α_g	β_g	σ_g	r
Value	1	1	2	1.27×10^{-3}	0.1863	0.02

3.2.1.1 First numerical method

For the duality method we consider the parameter $\omega = 2$ and the stopping test $\epsilon = 10^{-5}$. In order to assess the performance of the proposed numerical methods, we

consider a constant relationship between the time and spatial steps, i.e.

$$\Delta\tau = c\Delta\hat{B} = c\Delta\hat{G}.$$

In order to study the error and order of the method, we first compute the discrete $\mathcal{L}^\infty$ relative error between the exact solution and the numerical approximation at the time step n as follows:

$$err_n^\infty(\Delta\tau) = \frac{\max_{i,j} |P(\tau^n, \hat{B}_i, \hat{G}_j) - P_{i,j}^n|}{\max_{i,j} |P(\tau^n, \hat{B}_i, \hat{G}_j)|}, \tag{3.32}$$

Next, we consider the maximum of errors defined in (3.32), i.e.,

$$Err^\infty(\Delta\tau) = \max_n(err_n^\infty(\Delta\tau)).$$

Moreover, the radius of the convergence is given by

$$R(\Delta\tau) = \frac{Err^\infty(\Delta\tau)}{Err^\infty(\Delta\tau/2)} \tag{3.33}$$

for the stepsize $\Delta\tau$, and the empirical order of convergence is given by $\log_2(R)$. Table 3.2 shows the errors, convergence ratio and empirical order of convergence with different time and spatial discretizations computed as in [33].

Table 3.2: First numerical method: Relative errors and empirical convergence order in academic test.

Time steps	**Space steps**	$\boldsymbol{Err^\infty(\Delta\tau)}$	$\boldsymbol{R(\Delta\tau)}$	**Order**
40	32	0.0108651	-	-
80	64	0.0055962	1.9415	0.9572
160	128	0.0028748	1.9466	0.9610
320	256	0.0014710	1.9543	0.9667
640	512	0.0007474	1.9681	0.9768
1280	1024	0.0003780	1.9771	0.9834
2560	2048	0.0001906	1.9832	0.9879

Thus, taking into account the relative errors and the convergence ratio in Table 3.2, we can conclude that a first order convergence is achieved. The results obtained in this test are published in [4].

3.2.1.2 Second numerical method

For the finite elements space in the proposed Lagrange-Galerkin method, we use quadrangular uniform meshes with the number of nodes and elements collected in Table 3.3.

Table 3.3: Second numerical method: Number of nodes and elements for quadrangular meshes.

	Mesh 4	**Mesh 8**	**Mesh 16**	**Mesh 32**	**Mesh 64**
Elements	16	64	256	1024	4096
Nodes	81	289	1089	4225	16641

Moreover, the seasonality function f represents the influence of weather conditions and is chosen as follows:

$$f(s) = a_1 \sin(4\pi s) + a_2 \cos(4\pi s) + a_3 \sin(2\pi s) + a_4 \cos(2\pi s), \tag{3.34}$$

where $a_i \in \mathbb{R},\ i \in \{1, 2, 3, 4\}$.

Errors in $L^\infty((0,1); L^2(\Omega))$ discrete norm between the exact and numerical solution, convergence ratio and order are presented in Tables 3.4 and 3.5.

On one hand, in Table 3.4 we are assuming that there is not seasonal effect, i. e. $f(t) = 0$. In this case, the characteristics curves can be computed analytically. On the other hand, in order to compute the errors shown in Table 3.5, we have taken into account seasonal factors modelled with the function (3.34) with the parameters provided in Table 3.6, which implies that the characteristics curves need to be approximated by using ode solvers.

Note that the length of the edges of each quadrangular element of the mesh is divided by two when refining the meshes shown in Table 3.3. Moreover, in both cases, the radius of convergence is given by

$$Ratio = \frac{Error(\widetilde{h})}{Error(\frac{\widetilde{h}}{2})}, \tag{3.35}$$

Table 3.4: Second numerical method: Relative errors and empirical convergence order for the academic test without seasonal effect.

Time steps	**Meshes**	**Error**	**Ratio**	**Order**
10	4	7.9499×10^{-3}	-	-
20	8	3.5846×10^{-3}	2.2177	1.1491
40	16	1.7029×10^{-3}	2.1049	1.0737
80	32	8.4004×10^{-4}	2.0272	1.0195
160	64	4.2651×10^{-4}	1.9696	0.9779

Table 3.5: Second numerical method: Relative errors and empirical convergence order for the academic test with seasonal effect.

Time steps	**Meshes**	**Error**	**Ratio**	**Order**
10	4	2.8348×10^{-2}	-	-
20	8	1.3784×10^{-2}	2.0565	1.0402
40	16	6.7905×10^{-3}	2.0299	1.0214
80	32	3.3786×10^{-3}	2.0098	1.0071
160	64	1.6903×10^{-3}	1.9988	0.9991

where the parameter $\widetilde{h}$ indicates that we start with a level of refinement in time and space and we divide by two both, the time and finite element mesh steps to get the results for $\frac{\widetilde{h}}{2}$. Finally, the empirical order of convergence is given by $\log_2(Ratio)$. Thus, $Ratio = 2$ corresponds to linear convergence.

In both cases, the computed errors and the convergence ratio illustrate first order convergence. Moreover, the qualitative results for both cases are very close. Nevertheless, the errors are lower when the characteristics curves can be computed analytically.

For the analytical tests developed in [10], a second-order convergence is obtained with respect to time and space. We point out that the academic tests in [10] were developed for linear PDE problems and under certain assumptions on the velocity

Table 3.6: Parameters in the seasonality function for the real test.

Parameter	a_1	a_2	a_3	a_4
Value	-0.1209	0.0900	0.2151	0.3859

field. In this work, a nonlinear PDE is solved and first order of convergence is met with both methods. Nevertheless, in the first method, more refined meshes are necessary to obtain similar results which translates into more computing time.

Concerning the fixed-point algorithm explained in Section 3.1.4.2, the convergence is attained in one or few iterations for the chosen tolerance of 10^{-5}. Moreover, we have checked empirically that the relative errors are not influenced too much by this tolerance, however the computational cost is highly incremented in both methods. Furthermore, the choice of the parameter ω was carried out empirically. Nevertheless, some strategies for the election of the parameter as the ones introduced in [53] could be taken into account in a future research.

3.2.2 Real case

In this case we analyze the evolution of the price of a real green certificate. For this purpose, we have used the real New Jersey market data presented in [26] for SREC markets, i.e., markets for solar renewable energy certificates.

In this setting, we carry out the valuation of a green certificate with maturity $T = 13$, which corresponds to the end of energy year 2013, which is May 31, 2013, as it is indicated in [26]. Moreover, we assume that energy year 2013 matches the time interval $(12, 13]$. Additionally, we consider that the certificate has 3 years of life, i.e. $\gamma = 3$. Hence, the beginning of the certificate is $t = T - \gamma = 10$ (or equivalently $\tau = \gamma = 3$), which is the end of energy year 2010, and the first compliance date is $t = 11$ (i.e. end of energy year 2011) which corresponds to $\tau = 2$.

For the PDE parameters we consider those ones in Table 3.7.

Table 3.8 shows the requirement, R_i, and the penalty, Π_i, values at the end of

Table 3.7: Parameters in the PDE model for the real test.

Parameter	T	γ	α_g	β_g	σ_g	r
Value	13	3	2	1.27×10^{-3}	0.1863	0.02

each year for $i = 1, 2, 3$.

Table 3.8: Requeriments and penalty values for each energy year in the real test.

Energy year	$\boldsymbol{R_i}$	$\boldsymbol{\Pi_i}$
2011	306000	675
2012	442000	658
2013	596000	641

3.2.2.1 First numerical method

We start by choosing $\hat{b} = 8 \times 10^5$ and $\bar{g} = \ln(8 \times 10^5)$, so that $\hat{g} = 2 \times \ln(8 \times 10^5)$. By using these values we pose the PDE problem in the bounded domain $\hat{\Omega} = (0, \gamma) \times (0, 1) \times (0, 1)$.

Concerning the discretization parameters, we consider 100 time steps per month for the time discretization, i.e. $\Delta\tau = \frac{1}{1200}$, and a uniform mesh with $\Delta\hat{B} = \Delta\hat{G} = 1/32$. Moreover, in the duality method we choose the parameter $\omega = 2$ and the value $\epsilon = 10^{-5}$ as tolerance for the convergence test in the fixed point iteration associated to the duality method to treat the nonlinearity in the convection term.

Next, we show the computed results in the variables (t, B, G) that are obtained with the model data and the parameters related to the numerical methods.

Firstly, in Figure 3.1 we show the price of the certificate eight months before maturity, that is at time $t = T-2/3$ (or at $\tau = 2/3$, equivalently). We can observe that the price of the certificate takes values between zero and the penalty amount. When the accumulated supply (B) becomes very high, the price of course becomes very low,

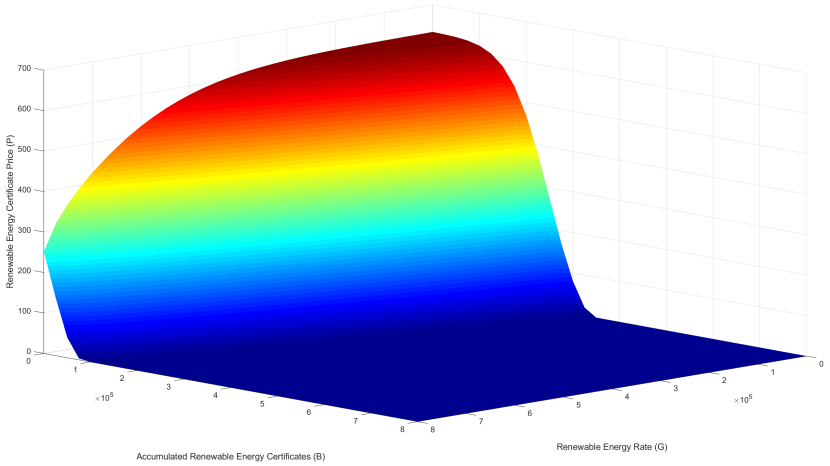

Figure 3.1: First numerical method: Renewable energy certificate price at time $t = T - 2/3$ in the real test.

and when supply is very low, the price turns out to be very high. Moreover, when the number of accumulated certificates (B) and the renewable energy rate ($G = \exp(\widetilde{G})$) tend to zero, the price approaches to penalty value π. That is, for low values of both variables, B and G, the price of the certificate is almost equal to the penalty.

Moreover, we also point out that the price of the certificate decreases when we increase the value of both state variables since, as it is indicated in [26], for high values of the variables, supply of certificates is high so the market can achieve the requirement easily and an additional certificate will not be needed for compliance. Therefore, when only B tends to zero, the price tends towards the penalty unless high values of G offset this, as it is illustrated in Figure 3.1.

When we represent the value of the certificate for a time closer to maturity, for instance at time $t = T - 1/3$ (i.e. four months before expiry date), as it is shown in Figure 3.2, we observe that low values of generation rate are associated with prices equal to the penalty amount even for values of accumulated certificates nearer to requirement since time is running out before compliance. High values of generation rate are linked to prices equal to the penalty only for lower values of banked certificates. As expected, a high current production of renewable energy compensates

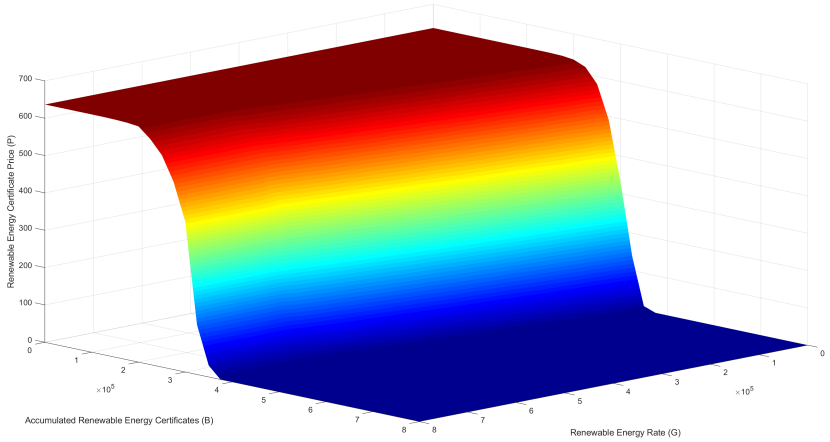

Figure 3.2: First numerical method: Renewable energy certificate price at time $t = T - 1/3$ in the real test.

for a low number of accumulated renewable energy certificates.

Finally, if we want to show the price of the certificate versus the accumulated renewable energy certificates for different times, we can create cross-sectional plots as the ones in Figure 3.3.

In order to obtain these curves we have chosen appropriate large values of renewable energy rate. At maturity, $t = T$, the price of the certificate is equal to the penalty if the requirement is not met, otherwise the price is zero. Then, as we move backwards in time we can observe that the curves move to the left and take lower values, due to the diffusion of the final value. When we arrive at a compliance date there is a jump to the right and the price increases again due to the jump condition imposed. In such figure we show the value at the first compliance date as well. Note that at maturity and compliance dates there exists a discontinuity when the number of accumulated certificates meets the requirement, because of the indicator function multiplied by the penalty, as it is pointed out in [26].

The CPU time is 223 seconds for this real case example. The CPU of the laptop we use is a Intel(R) Core(TM) i7-10750H at 2,6 GHz with 32 GB 2933 MHz DDR4 RAM. The implementation has been developed in Matlab.

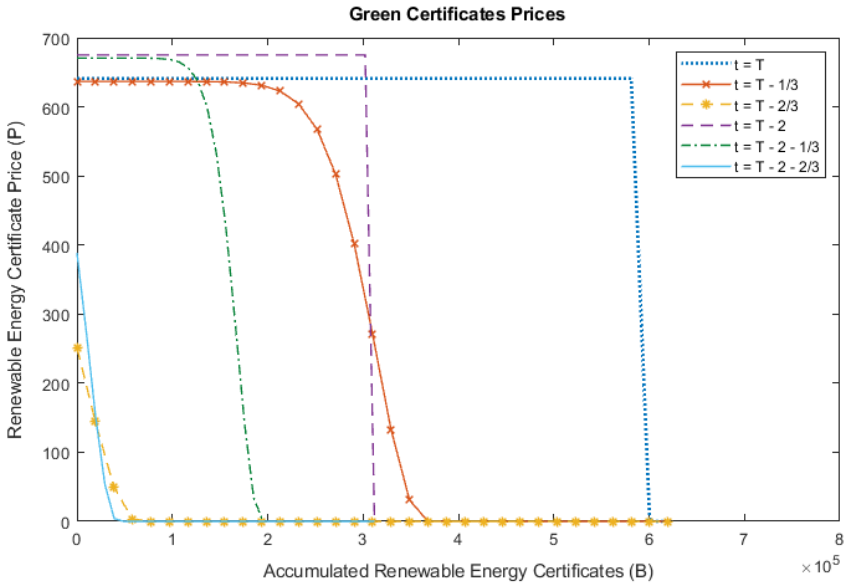

Figure 3.3: First numerical method: Price curves for different times in the real test.

3.2.2.2 Second numerical method

Regarding the parameters involved in the numerical methods, we have chosen, as in the first method, $\hat{b} = 8 \times 10^5$ and $\hat{g} = 2 \times \ln(8 \times 10^5)$. The values of the requirements at the end of each energy year and the penalties if the requirements are not met are given in Table 3.8.

Moreover, in order to solve the real case, we have employed Mesh 16 reflected in Table 3.3, which is equivalent to the one used in the first method, and for time discretization we have considered 100 time steps per month, i.e. $\Delta\tau = \frac{1}{1200}$. Finally, the parameter (ω) in the duality method is set to 2×10^{-5} and the tolerance ϵ is equal to 10^{-5}, achieving again the convergence in one or few iterations.

As with the first method, in Figure 3.4 we show the price of the certificate eight months before maturity, that is at time $t = T - 2/3$ (or $\tau = 2/3$, equivalently), and we represent the value of the certificate for a time closer to maturity, for instance at time $t = T - 1/3$, i.e. four months before expiry date, as it is shown in Figure 3.2. The results are similar to the ones obtained with the first numerical method.

Finally, we show the price of the certificate versus the accumulated renewable

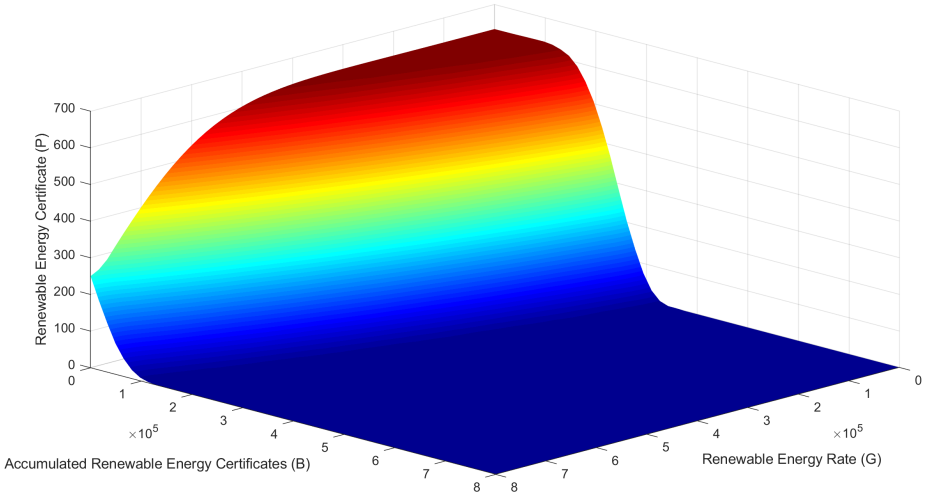

Figure 3.4: Second numerical method: Renewable energy certificate price at time $t = T - 2/3$ in the real case.

energy certificates for different times in Figure 3.6. In order to obtain these curves we have chosen appropriate large values of renewable energy rate. Again, we obtain similar results to the first numerical method, so that the comments in Section 3.2.2.1 also apply to the curves in Figure 3.6.

The CPU time is 123 seconds for this real case example, i. e., this method is faster than the first one. The CPU of the laptop we use is a Intel(R) Core(TM) i7-10750H at 2,6 GHz with 32 GB 2933 MHz DDR4 RAM. The implementation has been developed in Fortran.

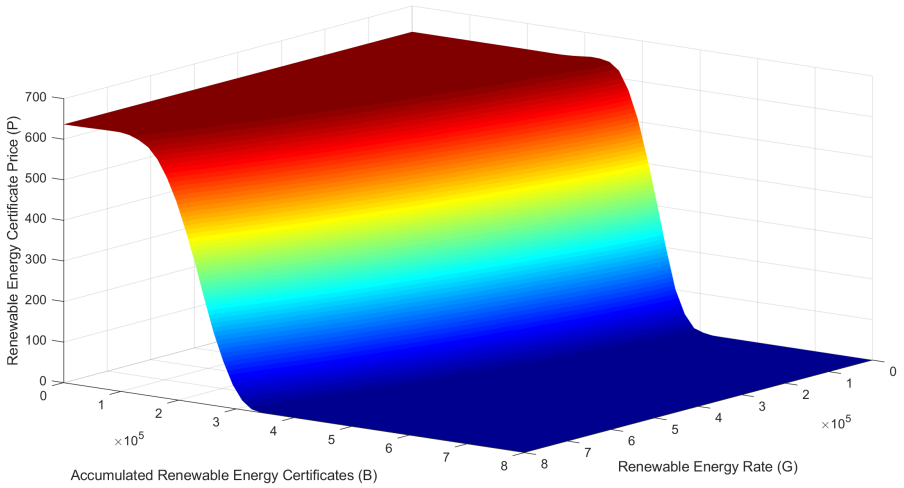

Figure 3.5: Second numerical method: Renewable energy certificate price at time $t = T - 1/3$ in the real case.

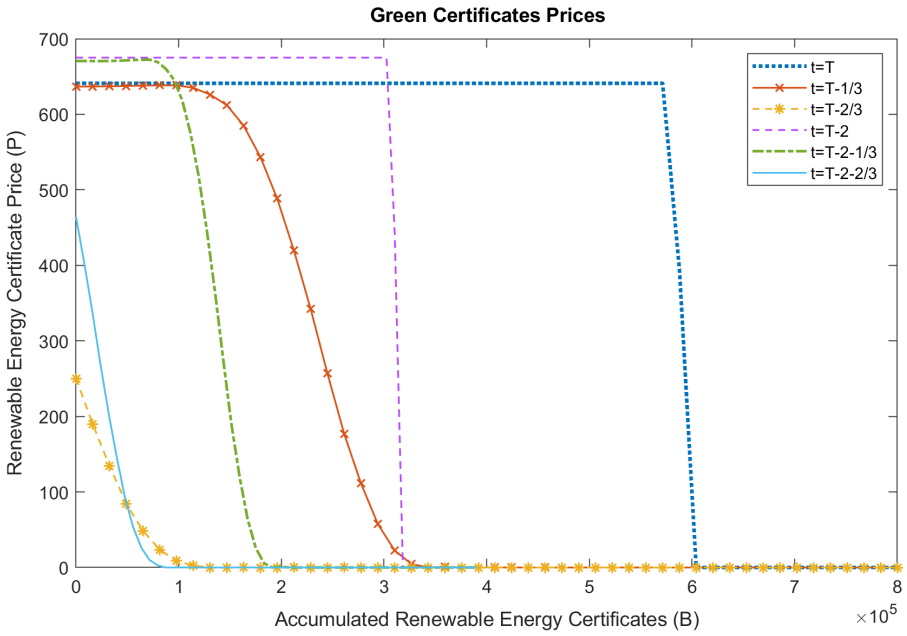

Figure 3.6: Second numerical method: Price curves for different times in the real case.

Chapter 4

Models and numerical methods for pricing of REC derivatives

4.1 Introduction

With the rapid deregulation of energy markets, more competition, increased volatility in energy prices, and much greater risks are emerging. Deregulation impacts both consumers and producers and, with this deregulation, the need for risk management and the use of derivatives for controlling exposure to energy prices is evident. In this way, investment banks and an increasing number of power marketers have the potential to make energy derivatives one of the fastest growing of all derivatives markets.

An *energy derivative* is a contract that is derived from an underlying energy-related commodity. Such a contract may be an agreement to trade a commodity at some future date or to exchange cashflows based on energy prices at future dates. A basic classification of energy derivatives is given in Figure 4.1. We distinguish between options and contracts without optionality, such as forwards, futures or swaps.

Although it is true that traded derivatives are a relatively new concept in the energy markets, the structures have been around for centuries and contracts with

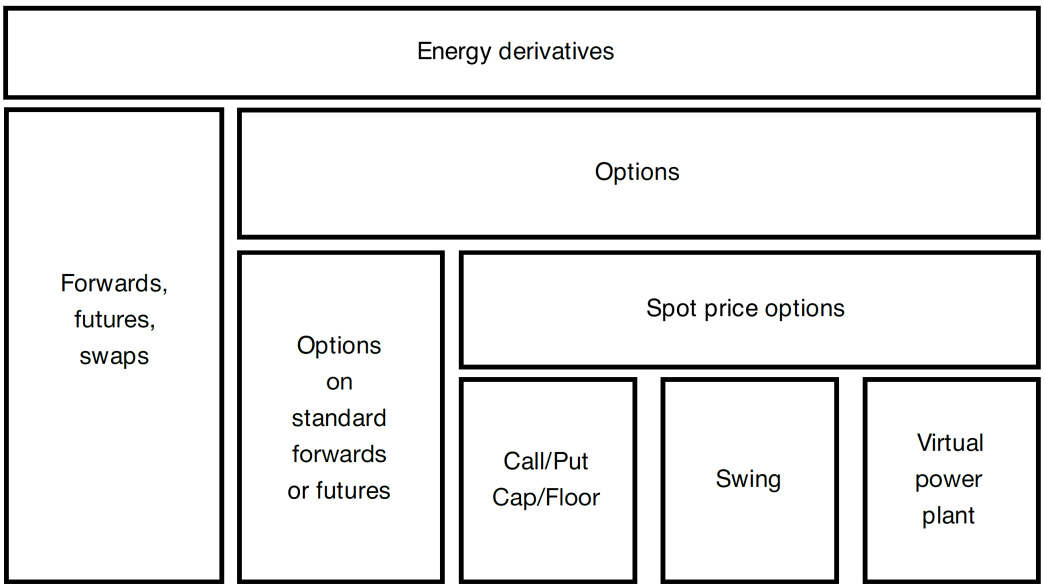

Figure 4.1: Overview of energy derivatives.

derivative characteristics have existed in energy markets for decades. There are many contracts that enable the user to manage their exposure to energy prices, with derivatives often providing the simplest and most flexible solutions for precise risk management. A derivative security can be defined as a security whose payoff depends on the value of other more basic variables.

Among the different derivatives appearing in Figure 4.1, there are options and futures. Although the model we pose, mathematically analyze and numerically solve in this chapter can be applied to a large class of REC derivatives, in the numerical examples we will focus on options and futures contracts.

Options in energy markets have a long history. Before the formation of liberalised energy markets, optionality was needed to react to fluctuations in consumption, interruptions in transmissions or power plant outages. Power plants or gas storage facilities provided flexibility that was historically used to balance the system load and is presently being used to optimise the profit against market prices. Many options on a daily or hourly basis can be seen as an abstract model of a certain type of power plant, also spoken of as a *virtual power plant*.

This chapter introduces methods to determine the *fair value* of a derivative whose underlying is a REC. The fair value of a contract is defined as the price at which a rational market participant would be indifferent whether to buy or sell the contract. When deriving fair values, we make the general assumption that the market is *arbitrage-free*, which means that making a profit without taking any risk is not possible, although there may occasionally be such *arbitrage opportunities* in real markets. If, for a given product, market prices can be determined on a regular basis one also speaks of a *mark-to-market valuation* of a product or portfolio.

4.2 Options and futures contracts

There are two basic types of options: call and put options. A *call (put) option* contract gives the option holder the right, but not the obligation, to purchase (sell) a certain commodity at a predetermined strike price. The option seller has the obligation to deliver (purchase) the commodity upon exercise by the option holder. Typically, the option seller receives an option premium at the time the contract is signed (upfront). Options can be traded as OTC products or via commodity exchanges. Exchanged-traded options often do not give the right to physical delivery of the commodity but are financially settled, with the option holder receiving a cash payment equivalent to the value of the commodity according to a published commodity index. In some cases, the option holder receives a futures contract on exercise that finally will be financially settled.

If at the option's maturity (or expiration) date T the commodity price S_T exceeds the strike price K, then the holder of a call option will exercise the option to buy the commodity for the price K. In this case his payoff (value at maturity) is $S_T - K$. In the opposite case ($S_T < K$), the holder of a call option will not exercise the option, because the value of the commodity is lower than the price K he would have to pay upon option exercise. Therefore, the payoff for the call option at maturity is

$$C_{K,S_T} = \begin{cases} S_T - K & \text{if } S_T > K, \\ 0 & \text{otherwise.} \end{cases}$$

This can be written more concisely as $C_{K,S_T} = \max(S_T - K, 0)$. Similarly, a put option is only exercised if at maturity the commodity price is below the strike price. In this case the payoff is $K - S_T$, because the option holder receives the strike price K and has to deliver the commodity, which has the lower value S_T. If $S_T > K$, then the put option will not be exercised since the commodity could be sold at the market for a higher price. The payoff for a put option at maturity is

$$P_{K,S_T} = \begin{cases} K - S_T & \text{if } S_T < K, \\ 0 & \text{otherwise.} \end{cases}$$

Or in short, $P_{K,S_T} = \max(K - S_T, 0)$. Figure 4.2 shows the financial results for the holder of a call option as a function of the underlying prices at maturity. The financial result at maturity is the option payoff minus the option premium paid. At the break-even point, the option payoff equals the option premium. The option premium is also the maximum loss for the option holder, which he incurs if he does not exercise the option, that is the option expires worthless. For the option seller, however, the maximum loss may be unlimited, for example if he has written a call option without being in possession of the commodity. Analogous to financial markets, options can be European style (i.e., they can only be exercised at the maturity date) or American style (i.e., they can be exercised at any time until maturity).

Before to define of future contracts, we need to distinguish between the futures and the forwards. Forward and futures contracts are contractual agreements to purchase or sell a certain amount of commodity on a fixed future date (delivery date) at a predetermined contract price. The contract needs to be fulfilled regardless of the commodity price development between conclusion of the contract and delivery date. In case the spot price has increased, the seller needs to sell below the prevailing spot price at delivery and therefore incurs an opportunity loss, whereas the buyer makes an (opportunity) profit. In case prices decline, the situation is reversed. The buyer of

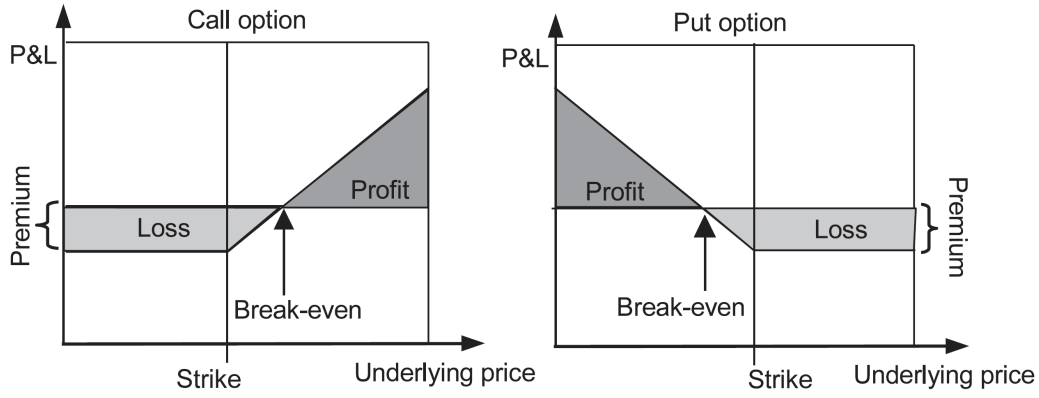

Figure 4.2: Gains and losses at maturity for an option holder.

a forward or future is said to hold a *long position* in the commodity (he profits from a price increase until delivery), the seller is said to hold a *short position* (he takes a loss from a price increase).

Although forwards and futures are similar contracts involving an agreement to buy or sell on a certain date for a certain price, important differences exist. Firstly, as we have just seen, futures are exchange standardised contracts, whereas forward contracts trade between individual institutions. Secondly, the cash flows of the two contracts occur at different times - futures are daily marked to market with cashflows passing between the long and the short position to reflect the daily futures price change, whereas forwards are settled once at maturity. Despite these differences, if future interest rates are known with certainty then futures and forwards can be treated as the same for pricing purposes.

In a futures contract both counterparties are obliged to exercise to do the trade involved in the contract. So, the seller has to sell the underlying asset and the buyer must buy it. So, in this case the holder of the futures contract has not the option to make the trade, so the value of a futures contract can be positive or negative. The final profit or loss for the buyer of a future contract (long position) at delivery date T is the value of the commodity at delivery S_T minus the contract price K (i.e., $S_T - K$),

see Figure 4.3. More precisely, the payoff of the futures is given by expression:

$$F_{K,S_T} = S_T - K.$$

Similarly, the profit or loss for the seller (short position) is $K - S_T$.

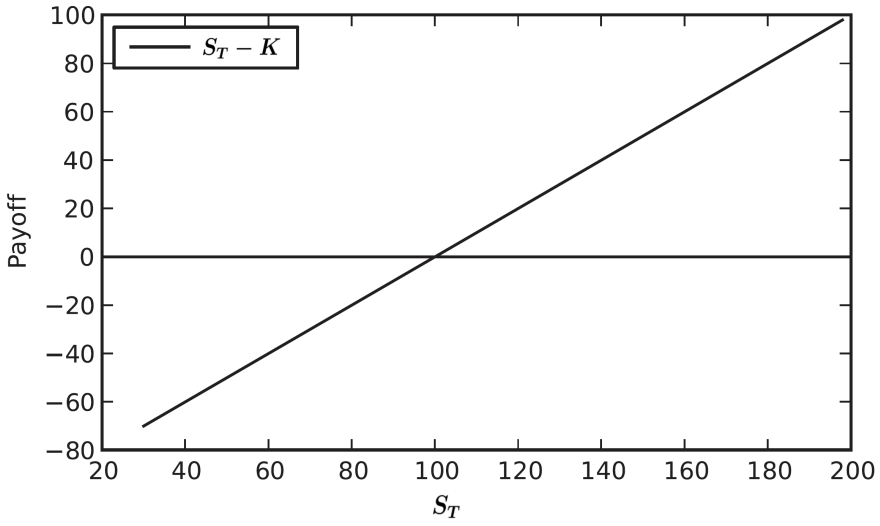

Figure 4.3: Profit or loss of a future contract.

Forward contracts are the most basic *hedging* instruments. If a producer of a commodity enters into a forward contract as a seller, he fixes his revenues and is indemnified from further price changes. On the contrary, a market participant who is dependent on the commodity for consumption may enter into a forward contract as a buyer to fix his purchasing costs for the commodity in advance.

Thus, the term "futures contract" is used for a standardised forward contract which is traded via an exchange. Often, futures contracts are financially settled, which means that only the value of the commodity at the delivery date is paid instead of a true physical delivery. Futures contracts open up the commodity market for participants who do not want to get involved in the physical handling of the commodity. Since the exchange serves as a central counterparty for futures contracts, market participants do not have to deal with multiple individual counterparties and

their associated credit risk. This also makes it easier to unwind a position entered into previously.

4.3 Mathematical model for REC derivatives

As indicated in Section 4.2, a REC derivative is a derivative contract whose underlying is a REC. We will mainly consider three cases of derivatives: a call option, a put option and a futures contract.

In order to model the price of a REC derivative, we assume the existence of a continuous, $\mathcal{F}$-adapted process V_t, which represents the price of a generic derivative with the renewable energy certificate (REC) as underlying. Moreover, we assume that the price of this derivative at time t, V_t, depends on the same two stochastic factors as the price of the REC: G_t and B_t, which are the renewable generation rate and the number of accumulated green certificates, respectively. We assume that the values of these two factors are known at the initial time $t = t_0$. The stochastic dynamics of these two factors are specified in Section 2.2.

The main objective of the model is to characterize the price of the derivative of a renewable energy certificate, V_t, at time t. In Chapter 2 and Chapter 3 we proposed the model and the numerical methods for pricing the REC in terms of a PDE problem.

In order to obtain the PDE model for the price of the derivative, we assume the existence of a function V, such that $V_t = V(t, B_t, G_t)$. Once the function V is obtained as the solution of the PDE problem, we can compute the value of V_t for given values of t, G_t and B_t.

We denote by T the maturity of the derivative, which coincides with the maturity of the certificate, and by γ the number of life years of the REC. So, we assume that the behaviour of the REC derivative is the same as the REC: its life is initialized at $t_0 = T - \gamma$ and the value of the REC derivative is unknown at $t = t_0$. moreover, we consider the single period case, so that $\gamma = 1$. Furthermore, we assume the value of

the derivative at maturity (payoff) is given by the terminal condition:

$$V_T = \zeta(K, P_T), \tag{4.1}$$

where P_T is the REC value at maturity given by the equation (2.5), $\zeta : \mathbb{R}^+ \longrightarrow \mathbb{R}^+$ is a bounded measurable function and K is the strike price of the derivative.

Note that the expression assumed in (4.1) for the payoff includes the cases of call options, put options and futures contracts. In fact, it includes a general class of derivatives where the payoff only depends on the value of the underlying REC at maturity. In this work we will only consider derivatives of European style. Therefore, exotic or American options are not included in the present framework.

Analogously to the pricing of the REC in Chapter 2, the price of the generic derivative at any time t before expiry is given by the continuous version of the uniformly integrable, non-negative martingale

$$V_t = e^{-r(T-t)}\mathbb{E}^{\mathbb{Q}}\left[\zeta(K, P_T)|\mathcal{F}_t\right],$$

where r is the constant risk free interest rate.

In order to state the FBSDE that includes the process for the price of the derivative V_t, we must complete the FBSDE (2.8) that was posed to price the REC. Note that the FBSDE (2.8) was set on the time interval $[t_0, T]$ with P_T as terminal condition of the REC.

For the pricing of a generic REC derivative, the following FBSDE is posed for $t \in [t_0, T]$:

$$\begin{cases} \widetilde{G}_t = g_0 + \displaystyle\int_{t_0}^{t} \mu_g(s, \widetilde{G}_s, P_s)\, ds + \int_{t_0}^{t} \sigma_g\, dW_s^0, \\ B_t = \displaystyle\int_{t_0}^{t} \mu_b(s, \widetilde{G}_s)\, ds, \\ P_t = \pi_T \mathbb{1}_{[0,R_T)}(B_T) - r\displaystyle\int_t^T P_s\, ds - \int_t^T e^{rs} Z_s^0\, dW_s^0, \\ V_t = \zeta(K, P_T) - r\displaystyle\int_t^T V_s\, ds - \int_t^T e^{rs} Z_s^1\, dW_s^1, \end{cases} \tag{4.2}$$

for some $\mathcal{F}_t$-adapted square integrable process Z_t^1 and Brownian motion W_t^1.

Note that there are two kinds of stochastic differential equations in (4.2) depending on the direction of time: the first two equations are forward ones while the last two are backward equations. Furthermore, the last backward equation for V_t in (4.2) is uncoupled in the sense that none of the coefficients of the forward equations for $\widetilde{G}_t$ and B_t are functions of V_t, and $\widetilde{G}_t$ and B_t are not involved in the expression of the forward equation for V_t .

The equation (4.2) can be rewritten in differential form as follows:

$$\begin{cases} d\widetilde{G}_t = \mu_g(t, \widetilde{G}_t, P_t)\, dt + \sigma_g\, dW_t^0, & \widetilde{G}_{t_0} = g_0, \\ dB_t = G_t\, dt, & B_{t_0} = 0, \\ dP_t = rP_t\, dt + Z_t^0\, dW_t^0, & P_T = \psi(B_T), \\ dV_t = rV_t\, dt + Z_t^1\, dW_t^1, & V_T = \zeta(K, P_T). \end{cases} \tag{4.3}$$

Now, assuming the existence of a solution of (4.3) and that $V_t = V(t, B_t, \widetilde{G}_t)$, where V_t is a traded asset with a drift equal to risk neutral rate under the risk neutral measure, we can use Itô's formula for a process V_t depending on the two Itô processes B_t and $\widetilde{G}$ (see [39], for example) to obtain:

$$dV_t = \left(\frac{\partial V}{\partial t} + \frac{\sigma_g^2}{2} \frac{\partial^2 V}{\partial \widetilde{G}^2} + \mu_g(t, \widetilde{G}, P) \frac{\partial V}{\partial \widetilde{G}} + \exp(\widetilde{G}) \frac{\partial V}{\partial B} \right) (t, B_t, \widetilde{G}_t)\, dt + \sigma_g \frac{\partial V}{\partial \widetilde{G}} (t, B_t, \widetilde{G}_t)\, dW_t^0.$$

Therefore, identifying the drift coefficient of the previous expression and the corresponding one of the fourth equation in (4.3), the function $V = V(t, B, \widetilde{G})$ satisfies the following linear PDE:

$$\mathcal{L}_2\,[V] = \frac{\partial V}{\partial t} + \frac{1}{2}\sigma_g^2 \frac{\partial^2 V}{\partial \widetilde{G}^2} + \mu_g(t, \widetilde{G}, P) \frac{\partial V}{\partial \widetilde{G}} + \exp(\widetilde{G}) \frac{\partial V}{\partial B} - rV = 0, \tag{4.4}$$

for a given function P, that represents the value of the REC. Note that P is the solution of the nonlinear equation posed in Chapter 2 for pricing RECs and can be obtained numerically in a previous step.

Taking into account that the value of the REC derivative at maturity is given by (4.1), the PDE (4.4) jointly with the final condition

$$V(T, B, \widetilde{G}) = \zeta(K, P(T, B, \widetilde{G})) \tag{4.5}$$

defines the final value problem modelling the price of the REC derivative. Note that the expression of $P(T, B, \widetilde{G})$ represents the value of the REC, at maturity, which is known.

4.4 Existence of a solution for the PDE pricing model of the REC derivative

In this section we address the mathematical analysis of the proposed model for pricing REC derivatives. For this purpose, we first note that the drift term involves the value of the REC and the analytical expression for this value is not known. Therefore, the mathematical analysis techniques based on the existence of sub and super solutions to obtain the existence of solution for PDE (4.4) cannot be applied.

Instead of that methodology, we will follow a probabilistic approach and we assume the required regularity on the REC price function P, so that the drift term depending on it satisfies the regularity conditions imposed on the coefficients of the PDE (4.4). We also assume that the REC price function is given, as it can be obtained as the solution of the non-linear PDE posed in Chapter 2.

Taking into account that the stochastic process for the derivative price is given by $V_t = V(t, B_t, \widetilde{G}_t)$, where the function $V = V(t, B, \widetilde{G})$ satisfies the PDE (4.4), in this section we aim to prove the existence of solution for the problem defined by the PDE (4.4) jointly with the final condition (4.5) given by the payoff of the derivative.

For this purpose, we first introduce the change of variable $G = \exp(\widetilde{G})$, so that the following equivalent PDE is obtained from (4.4):

$$\frac{\partial V}{\partial t} + G\left(\frac{1}{2}\sigma_g^2 + \mu_g(t, \log(G), P)\right)\frac{\partial V}{\partial G} + \frac{1}{2}\sigma_g^2 G^2 \frac{\partial^2 V}{\partial G^2} + G\frac{\partial V}{\partial B} - rV = 0. \qquad (4.6)$$

Note that $P = P(t, G, B)$, although its analytical expression is not available.

Next, in order to handle an easier notation in what follows, we introduce $x = (x_1, x_2)$, where

$$x_1 = G, \quad x_2 = B.$$

Thus, PDE (4.6) can be expressed as

$$\frac{\partial V}{\partial t} + x_1 \left(\frac{1}{2}\sigma_g^2 + \mu_g(t, \log(x_1), P) \right) \frac{\partial V}{\partial x_1} + \frac{1}{2}\sigma_g^2 x_1^2 \frac{\partial^2 V}{\partial x_1^2} + x_1 \frac{\partial V}{\partial x_2} - rV = 0. \tag{4.7}$$

Also, note that $P = P(t, x_1, x_2)$ in this new notation.

Next, associated to PDE (4.6), we consider the differential operator

$$\mathcal{L} = \frac{\partial}{\partial t} + x_1 \left(\frac{1}{2}\sigma_g^2 + \mu_g(t, \log(x_1), P) \right) \frac{\partial}{\partial x_1} + \frac{1}{2}\sigma_g^2 x_1^2 \frac{\partial^2}{\partial x_1^2} + x_1 \frac{\partial}{\partial x_2}, \tag{4.8}$$

it can be framed into a more general setting given by the differential operator

$$\mathcal{L} := \frac{1}{2} \sum_{i,j=1}^{p_0} a_{ij}(t,x) \partial_{x_i x_j} + \sum_{i=1}^{p_0} a_i(t,x) \partial_{x_i} + < Hx, \nabla_x >, \ t \in [0,T), \ x \in D \subseteq \mathbb{R}^d, \tag{4.9}$$

where $D = (0, +\infty) \times (0, +\infty) \subset \mathbb{R}^2$, $p_0 = 1$, $d = 2$ and H is a (2×2)-matrix with constant real entries. More precisely, we have

$$a_{11}(t,x) = \sigma_g^2 x_1^2, \quad a_1(t,x) = x_1 \left(\frac{1}{2}\sigma_g^2 + \mu_g(t, \log(x_1), P) \right), \quad H = \begin{pmatrix} 0 & 0 \\ 1 & 0 \end{pmatrix}. \tag{4.10}$$

In this case, $p_0 < d$ implies that no ellipticity condition on $\mathcal{L}$ is satisfied (i.e. the second order part is fully degenerate).

Following [43], we will first prove that the following main structural assumption on the local-generator $\mathcal{L}$ is satisfied.

Assumption 4.4.1. *The matrix H is such that the Kolmogorov operator*

$$\mathcal{K} = \frac{1}{2} \sum_{j=1}^{p_0} \partial_{x_j}^2 + < Hx, \nabla_x > + \partial_t, \quad x \in \mathbb{R}^d, \tag{4.11}$$

is hypoelliptic on $\mathbb{R} \times \mathbb{R}^d$. Equivalently, the vector fields $\partial_{x_1}, ..., \partial_{x_{p_0}}$ and $Y := < Hx, \nabla_x > + \partial_t$ satisfy the Hörmander condition

$$\operatorname{rank}(\mathfrak{L}(\partial_{x_1}, ..., \partial_{x_{p_0}}, Y)) = d,$$

at each point of $\mathbb{R} \times \mathbb{R}^d$ (see [36]). Here $\mathfrak{L}(\partial_{x_1}, ..., \partial_{x_{p_0}}, Y)$ denotes the Lie algebra generated by $\partial_{x_1}, ..., \partial_{x_{p_0}}, Y$.

In order to prove the previous Assumption , first note that in our case ($p_0 = 1,\ d = 2$), $Y = x_1\partial_{x_2} + \partial_t$ and we obtain the following Kolmogorov operator

$$\mathcal{K} = \frac{\sigma_g^2 x_1^2}{2}\partial_{x_1^2} + x_1\partial_{x_2}, \tag{4.12}$$

which is the same as in the classical Asian options pricing problem that has been analyzed in [5], for example. So, the operator fulfills the following Hörmander condition

$$[\partial_{x_1}, Y] = \partial_{x_1}Y - Y\partial_{x_1} = \partial_{x_2}.$$

Therefore, we have

$$\operatorname{rank}(\mathfrak{L}(\partial_{x_1}, Y)) = 2,$$

so that the previous Assumption 4.4 is satisfied.

As stated in [43], the following second assumption is also required.

Assumption 4.4.2. *There exist $M \in \mathbb{N}_0,\ \alpha \in (0,1]$ and $k > 0$ such that:*

(i) $a_{ij},\ a_i \in C_H^{M,\alpha}((t_0,T)\times D)$ for any $i,j = 1,...,p_0$, with all the (Lie) derivatives bounded by k;

(ii) the following coercivity condition holds on D:

$$k^{-1}|\xi|^2 \leq \sum_{i,j=1}^{p_0} a_{ij}(t,x)\xi_i\xi_j \leq k|\xi|^2, \quad t \in (t_0,T), x \in D, \xi \in \mathbb{R}^{p_0}.$$

When considering condition i) in the previous assumption, we first note that the functional coefficient a_1 depends on t and x through the function P, which represents the price of the REC and it is given by the solution of the corresponding non-linear PDE problem. As the existence and uniqueness of solution P of the non linear-problem, as well as the regularity of the solution, remains as an open problem, we shall assume the required regularity to P so that the requirements of condition i) in Assumption 4.4.2 for the coefficients a_i in (4.10) are satisfied.

Moreover, in order to satisfy the coercivity condition ii) in Assumption 4.4.2 and also condition i) we consider $D = (a, +\infty) \times (0, +\infty)$, with $a > 0$, as in the classical Asian options problem [43].

Following [43] and [52], we present some results under which the existence of solution can be proved.

For a given $T > 0$, we consider a continuous $\mathbb{R}^d$-valued strong Markov process $X = (X_t)_{t\in[t_0,T)}$ with transition probability function $p = p(t, x; T_1, d\zeta)$, defined on the filtered probability space $(\Omega, \mathcal{F}, (\mathcal{F}^t_{T_1})_{t_0\le t\le T_1<T}, (P_{t,x})_{t_0\le t\le T})$. For any bounded Borel measurable function φ, we denote by

$$E_{t,x}[\varphi(X_{T_1})] := (\boldsymbol{T}_{t,T_1}\varphi)(x) := \int_{\mathbb{R}^d} p(t, x; T_1, d\zeta)\varphi(\zeta), \quad t_0 \le t < T_1 < T,\ x \in \mathbb{R}^d,$$

the $P_{t,x}$-expectation and the semigroup associated with the transition probability function p, respectively (see Chapter 2.1 in [31]).

The following assumption will be used to give the definition of local diffusion.

Assumption 4.4.3. *Let X be a continuous $\mathbb{R}^d$-valued strong Markov process $X = (X_t)_{t\in[t_0,T)}$ with transition probability function $p = p(t, x; T_1, d\zeta)$, we assume that:*

(i) For any $t \in [t_0, T)$, $\delta > 0$ and J, compact subset of D, there exist the limits

$$\lim_{T_1-t\longrightarrow t_0^+} \int_{\{|x-\zeta|>\delta\}\cap J} \frac{p(t, x; T_1, d\zeta)}{T_1 - t} = 0, \quad \textit{uniformly w.r.t. } x \in \mathbb{R}^d,$$
$$\lim_{T_1-t\longrightarrow t_0^+} \int_{|x-\zeta|>\delta} \frac{p(t, x; T_1, d\zeta)}{T_1 - t} = 0, \quad \textit{uniformly w.r.t. } x \in J.$$

(ii) For any $t \in [t_0, T)$, $\delta > 0$, $1 \le i, j \le d$ and J, compact subset of D, there exist the limits

$$\lim_{T_1-t\longrightarrow t_0^+} \int_{|x-\zeta|<\delta} (\zeta_i - x_i)\frac{p(t, x; T_1, d\zeta)}{T_1 - t} = \begin{cases} a_i(t, x) + (Hx)_i, & \textit{if } i = 1, ..., p_0, \\ (Hx)_i, & \textit{if } i = p_0 + 1, ..., d, \end{cases}$$
$$\lim_{T_1-t\longrightarrow t_0^+} \int_{|x-\zeta|<\delta} (\zeta_i - x_i)(\zeta_j - x_j)\frac{p(t, x; T_1, d\zeta)}{T_1 - t} = \begin{cases} a_{ij}(t, x), & \textit{if } i, j = 1, ..., p_0, \\ 0, & \textit{if } i, j = p_0 + 1, ..., d, \end{cases}$$

uniformly w.r.t. $x \in J$, *for* $a_{ij}, a_i \in L^{\infty}_{loc}([t_0, T) \times D)$ *and some* H *as in Assumption 4.4, i.e.* H *takes the block form*

$$H = \begin{pmatrix} * & * & \cdots & * & * \\ H_1 & * & \cdots & * & * \\ 0 & H_2 & \cdots & * & * \\ \vdots & \vdots & \ddots & \vdots & \vdots \\ 0 & 0 & \cdots & H_r & * \end{pmatrix},$$

where H_j *is a* $(p_j \times p_{j-1})$*-matrix with full rank (equal to* p_j*) for* $j = 1, ..., r$, *the* $*$*-blocks are arbitrary,* $p_0 \geq p_1 \geq \cdots \geq 1$ *and* $p_0 + \cdots + p_r = d$.

Definition 4.4.1. *Let* $\mathcal{L}$ *an operator as in (4.9). We say that* X *is a local diffusion generated by* $\mathcal{L}$ *on* D *(an* $\mathcal{L}$*-local diffusion) if the conditions (i) and (ii) of Assumption 4.4.3 hold. In case they hold with* $D = \mathbb{R}^d$ *then we call* X *a global diffusion generated by* $\mathcal{L}$ *(an* $\mathcal{L}$*-global diffusion).*

Note that in our case, as $D \subset \mathbb{R}^2$ then X is an $\mathcal{L}$*-local diffusion.*

The main result we use in this section is the following theorem taken from [43], that states the existence of a local (on D) transition density $\Gamma(t, x; T_1, \zeta)$ for X, reveals its intrinsic regularity w.r.t. both the forward and backward variables and shows that it solves a forward and a backward Kolmogorov equation on $(t, T) \times D$ and $(t_0, T_1) \times D$, respectively.

Note that the backward Kolmogorov equation that will appear in the forthcoming theorem corresponds to the linear PDE governing the price of the derivative of the REC.

Before stating the theorem, we need to introduce the following assumption.

Assumption 4.4.4. X *is a Feller process on* D, *i.e. for any* $T_1 \in (t_0, T)$ *and bounded* $\varphi \in C(\mathbb{R}^d)$ *the function* $(t, x) \longmapsto E_{t,x}[\varphi(X_{T_1})]$ *is continuous on* $(t_0, T_1) \times D$.

Note that, since the coercivity condition in Assumption 4.4.2-(ii) only holds on D, the Feller property for the semigroup $\varphi \longmapsto E_{t,\cdot}[\varphi(X_{T_1})]$ is not ensured.

The following result summarizes some properties of the law of X.

Theorem 4.4.5. *Let X be a local diffusion on $\mathbb{R}^d$ generated by $\mathcal{L}$ on D (in the sense of Definition 4.4.1) and let Assumptions 4.4 and 4.4.2 be in force. Then:*

a) X has a local transition density Γ on D, namely a non-negative measurable function $\Gamma(t,x;T_1,y)$ defined for any $t_0 < t < T_1 < T$ and $x \in \mathbb{R}^2$, $y \in D$, such that

$$p(t,x;T_1,A) = \int_A \Gamma(t,x;T_1,y)\,dy, \quad A \in \mathcal{B}(D) \text{ (Borel subset of } D).$$

Furthermore, $\Gamma(t,x;T_1,\cdot)$ is continous on D and locally bounded uniformly w.r.t. $x \in \mathbb{R}^d$.

b) If $M \geq 2$, then for any $(t,x) \in (t_0,T) \times \mathbb{R}^2$ the function $\Gamma(t,x;\cdot,\cdot) \in C_H^{M,\alpha}((t,T) \times D)$ and solves the forward Kolmogorov equation

$$\mathcal{L}^* u = 0, \qquad \text{on } (t,T) \times D,$$

where $\mathcal{L}^*$ is the formal adjoint of $\mathcal{L}$.

c) If Assumption 4.4.4 is also in force, then for any $(T_1,y) \in (t_0,T) \times D$ the function $\Gamma(\cdot,\cdot;T_1,y) \in C_H^{M+2,\alpha}((t_0,T_1) \times D)$ and solves the backward Kolmogorov equation

$$\mathcal{L} u = 0, \qquad \text{on } (t_0,T_1) \times D.$$

Taking into account the previous arguments concerning the assumptions, we can apply the previous theorem taken from [43] (more precisely, Theorem 1.5 in [43]) to obtain the existence of a local transition density for the process $X = (G,B)$, which is the fundamental solution of (4.6).

In terms of this fundamental solution, we can obtain the existence of solution for PDE (4.6), which admits the representation:

$$V(t,x) = \int_{B_R} \Gamma(t,x;T,y)\zeta(K,y)\,dy, \tag{4.13}$$

where B_R denotes the ball centered at the origin with radius R and ζ defines the payoff of the derivative in terms of the strike price K.

Note that PDE (4.6) has not a unique solution due to the lack of boundary conditions in the mathematical analysis here considered. Nevertheless, numerical methods for solving (4.6) can be applied with appropriate boundary conditions.

Finally, as PDE (4.6) is equivalent to PDE (4.4), then we have obtained the existence of solution for the final value problem defined by the PDE (4.4) jointly with the final condition (4.5).

4.5 Numerical methods for the REC derivatives pricing models

Once we have developed the mathematical analysis methodology to obtain the existence of solution for the final value problem defined by the PDE (4.4) jointly with the final condition (4.5), since there are no analytical expressions for the solutions, we propose a set of numerical methods to approximate it.

These methods are mainly the same as those ones proposed in Chapter 3 to solve the final value problem associated to the the model for RECs pricing.

However, there is an important difference between the PDE governing RECs pricing and RECs derivatives pricing. While the numerical solution of a non-linear PDE is required in the first case, in the second one a linear PDE needs to be solved once we know the price of the REC.

Actually, for obtaining the price of a REC derivative, we first solve the nonlinear PDE to obtain the REC price and from them we can compute the price of the derivative.

In order to explain the methods for the numerical solution of the final value problem defined by (4.4)-(4.5), in this section we assume that the prices of the REC are know at the corresponding space-time mesh in each method.

As indicated in the previous section, if we assume that the RECs prices function P is given, the governing PDE for the pricing of the REC derivative is linear and we do not need to use a duality algorithm. This is the main difference with respect to

the numerical solution of the RECs pricing problem.

Next, we describe the numerical solution of (4.4)-(4.5).

4.5.1 Localization and analysis of boundary conditions

In order to apply the numerical discretization using finite differences or finite elements to the PDE problem, it is necessary to consider a bounded computational domain. Thus, we approximate the linear PDE problem (4.4) through a localization procedure, which consists in truncating the initial unbounded domain to a bounded one and introducing the appropriate conditions at the boundaries of the bounded domain. We apply an analogous procedure to the one presented in Section 3.1.2.

Let $\bar{\Omega}^* = (T-\gamma, T) \times (0, +\infty) \times \mathbb{R}$ be the initial unbounded domain. Moreover, let $\bar{\Omega} = (T-\gamma, T) \times (0, \hat{b}) \times (-\bar{g}, \bar{g})$ be the truncated bounded domain where $\hat{b}$ and $\bar{g}$ are large enough real numbers, which are influenced by the requirement of the payoff function. Now, we introduce the changes of variables:

$$\hat{B} = \frac{B}{\hat{b}}, \qquad \hat{G} = \frac{\widetilde{G} + \bar{g}}{\hat{g}},$$

with $\hat{g} = 2\bar{g}$, so that the truncated domain $\Omega^* = (T-\gamma, T) \times (0,1) \times (0,1)$ in the new variables $(t, \hat{B}, \hat{G})$ is considered.

In order to establish the boundaries of the truncated domain which require boundary conditions to be imposed, we follow the results in [51] and introduce the notation $y = (y_0, y_1, y_2)$, with

$$y_0 = t, \quad y_1 = \hat{B}, \quad y_2 = \hat{G}, \tag{4.14}$$

so that equation (3.7) can be equivalently written as

$$\sum_{i,j=0}^{2} a_{ij} \frac{\partial^2 V}{\partial y_i y_j} + \sum_{j=0}^{2} a_j \frac{\partial V}{\partial y_j} + b_0 V = 0, \quad \text{in } \Omega^*, \tag{4.15}$$

where

$$
\begin{aligned}
A = (a_{ij}) &= \begin{pmatrix} 0 & 0 & 0 \\ 0 & 0 & 0 \\ 0 & 0 & \dfrac{\hat{g}^2\sigma_g^2}{2} \end{pmatrix}, \\
\vec{a} = (a_j) &= \begin{pmatrix} 1 \\ \hat{b}\exp(y_2\hat{g} - \bar{g}) \\ \hat{g}\alpha_g \left(f(y_0) - (y_2\hat{g} - \bar{g}) + \dfrac{\beta_g}{\alpha_g} P(y) \right) \end{pmatrix}, \quad b_0 = -r,
\end{aligned}
\tag{4.16}
$$

and we use the notation

$$
\begin{aligned}
&\Omega^* = \prod_{i=0}^{2} \left(\underline{y}_i, \overline{y}_i \right), \quad \Gamma^* = \partial\Omega^*, \\
&\Gamma_i^{*,-} = \left\{ y \in \Gamma^* / y_i = \underline{y}_i \right\}, \quad \Gamma_i^{*,+} = \left\{ y \in \Gamma^* / y_i = \overline{y}_i \right\}, \quad i = 0, 1, 2.
\end{aligned}
$$

Next, we denote by $\vec{n} = (n_0, n_1, n_2)$ the normal vector to Γ^* pointing inwards Ω^*. Let us define the following subsets of Γ^*:

$$
\begin{aligned}
\Sigma^0 &= \left\{ y \in \Gamma^* / \sum_{i,j=0}^{2} a_{ij} n_i n_j = 0 \right\}, \quad \Sigma^1 = \Gamma^* - \Sigma^0, \\
\Sigma^2 &= \left\{ y \in \Sigma^0 / \sum_{i=0}^{2} \left(a_i - \sum_{j=0}^{2} \frac{\partial a_{ij}}{\partial y_j} \right) n_i < 0 \right\}.
\end{aligned}
$$

Following [51], we need to impose boundary conditions at $\Sigma^1 \cup \Sigma^2$. Thus, for (4.14), we conclude:

$$
\Sigma^0 = \Gamma_0^{*,-} \cup \Gamma_0^{*,+} \cup \Gamma_1^{*,-} \cup \Gamma_1^{*,+}, \quad \Sigma^1 = \Gamma_2^{*,-} \cup \Gamma_2^{*,+}, \quad \Sigma^2 = \Gamma_0^{*,+} \cup \Gamma_1^{*,+},
$$

so that

$$
\Sigma^1 \cup \Sigma^2 = \Gamma_0^{*,+} \cup \Gamma_1^{*,+} \cup \Gamma_2^{*,-} \cup \Gamma_2^{*,+}.
$$

Hence, as in the case of RECs, we impose the following homogeneous Neumann boundary conditions at the spatial boundaries that require boundary conditions:

$$
\begin{aligned}
&\frac{\partial V}{\partial y_1} = 0, \text{ on } \Gamma_1^{*,+}, \\
&\frac{\partial V}{\partial y_2} = 0, \text{ on } \Gamma_2^{*,-} \cup \Gamma_2^{*,+},
\end{aligned}
\tag{4.17}
$$

jointly with the final condition

$$V(T, y_1, y_2) = \zeta(K, P(T, y_1, y_2)). \tag{4.18}$$

at the boundary $y_0 = T$, corresponding to (4.5) in the new notation.

4.5.2 First numerical method

As in the first method for the numerical solution of the REC pricing model, we use a characteristics scheme to discretize the material derivative operator in one of the spatial directions combined with the use of a second order implicit finite differences scheme in the other spatial direction that also includes a second order derivatives term.

4.5.2.1 Discretization of the PDE

Analogously to the results presented in Section 3.1.3.1, for the time discretization, we first consider the change of time variable $\tau = T - t$, where τ represents the time to maturity. So, the equation (4.4) can be equivalently written as follows:

$$\frac{\mathrm{D}V}{\mathrm{D}\tau} - \mathcal{A}V = 0, \tag{4.19}$$

where the involved differential operators are given by

$$\frac{\mathrm{D}V}{\mathrm{D}\tau} = \frac{\partial V}{\partial \tau} - \hat{b}\exp(\hat{G}\hat{g} - \bar{g})\frac{\partial V}{\partial \hat{B}},$$
$$\mathcal{A}V = \frac{\hat{g}^2\sigma_g^2}{2}\frac{\partial^2 V}{\partial \hat{G}^2} + \hat{g}\alpha_g\left(f(T-\tau) - \left(\hat{G}\hat{g} - \bar{g}\right) + \frac{\beta_g}{\alpha_g}P(T-\tau, \hat{B}, \hat{G})\right)\frac{\partial V}{\partial \hat{G}} - rV.$$

Note that $\dfrac{\mathrm{D}V}{\mathrm{D}\tau}$ represents the material derivative of V in the direction $\hat{B}$ associated to the one-dimensional velocity field $v = -\hat{b}\exp(\hat{G}\hat{g} - \bar{g})$, which does not depend on B. Moreover, $\mathcal{A}$ denotes the second order convection-diffusion-reaction differential operator in the direction $\hat{G}$.

First, we use a characteristics scheme to discretize in time the term associated to the material derivative as in the case of REC in Section 3.1.3.1. For this purpose,

at each time step $\Delta\tau = \gamma/N_T$, for $N_T > 0, n = 0, 1, ..., N_T$. At each time step we consider the ODE problem satisfied by the trajectory associated to the velocity field v through the point $(\tau^{n+1}, \hat{B})$:

$$\begin{cases} \dfrac{d\chi}{ds}(s) = -\hat{b}\exp\left(\hat{G}\hat{g} - \bar{g}\right), \\ \chi\left(\tau^{n+1}\right) = \hat{B}. \end{cases}$$

Note that the solution of this ODE problem is given by

$$\chi(s) = \hat{B} + (\tau^{n+1} - s)\hat{b}\exp\left(\hat{G}\hat{g} - \bar{g}\right).$$

In order to build the finite differences approximation of the material derivative along the characteristics, we introduce $\chi^n = \chi(\tau^n)$, which is given by

$$\chi^n\left(\hat{B}, \hat{G}\right) = \hat{B} + \Delta\tau\hat{b}\exp\left(\hat{G}\hat{g} - \bar{g}\right),$$

and represents the position at time τ^n of the point placed at $\left(\hat{B}, \hat{G}\right)$ at time τ^{n+1} and moving according to the velocity field v.

Next, we introduce the approximation for the material derivative:

$$\frac{\mathrm{D}V}{\mathrm{D}\tau}\left(\tau^{n+1}, \hat{B}, \hat{G}\right) \approx \frac{V\left(\tau^{n+1}, \hat{B}, \hat{G}\right) - V\left(\tau^n, \chi^n\left(\hat{B}, \hat{G}\right), \hat{G}\right)}{\Delta\tau}. \tag{4.20}$$

Secondly, by using a Crank-Nicolson scheme ($\hat{\theta} = 0.5$ in the so called $\hat{\theta}$-method) for the second order differential term $\mathcal{A}v$ in equation (4.19), we obtain:

$$\begin{aligned} &\frac{V^{n+1} - V^n \circ \chi^n}{\Delta\tau} - \frac{\hat{\theta}\hat{g}^2\sigma_g^2}{2}\frac{\partial^2 V^{n+1}}{\partial\hat{G}^2} - \frac{(1-\hat{\theta})\hat{g}^2\sigma_g^2}{2}\frac{\partial^2\left(V^n \circ \chi^n\right)}{\partial\hat{G}^2} \\ &- \hat{\theta}\hat{g}\alpha_g\left(f(T-\tau) - \left(\hat{G}\hat{g} - \bar{g}\right) + \frac{\beta_g}{\alpha_g}P^{n+1}\right)\frac{\partial V^{n+1}}{\partial\hat{G}} \\ &- (1-\hat{\theta})\hat{g}\alpha_g\left(f(T-\tau) - \left(\hat{G}\hat{g} - \bar{g}\right) + \frac{\beta_g}{\alpha_g}(P^n \circ \chi^n)\right)\frac{\partial\left(V^n \circ \chi^n\right)}{\partial\hat{G}} \\ &+ r\hat{\theta}V^{n+1} + r(1-\hat{\theta})\left(V^n \circ \chi^n\right) = 0, \end{aligned} \tag{4.21}$$

At each time step, the evaluation of the term $V^n \circ \chi^n$ in (4.21) at the quadrature nodes is approximated by using a biquadratic interpolation formula from the values

of V^n at the mesh nodes. The same procedure is applied for the computation of the values $P^n \circ \chi^n$.

Also, it is important to point out that at each time step we first advance one step in the solution of the nonlinear PDE that provides the price of the REC at time t^{n+1}, P^{n+1}, and next we advance one step in the solution of the linear PDE for the price of the derivative at time t^{n+1} to obtain V^{n+1}.

As in the REC case, in order to describe the solution of the fully discretized problem, let us introduce the notation $(\tau^n, \hat{B}_i, \hat{G}_j) = \left(n\Delta\tau, i\Delta\hat{B}, j\Delta\hat{G}\right)$ to represent a generic node of the uniform finite differences time-space mesh with time step $\Delta\tau$ and spatial steps $\Delta\hat{B}$ and $\Delta\hat{G}$, for indexes $n = 0, 1, \ldots, N_T$, $i = 0, 1, \ldots, N_{\hat{B}}$ and $j = 0, 1, \ldots, N_{\hat{G}}$.

The full discretization of problem (4.21) can be written as follows:

$$
\begin{aligned}
&\frac{V_{i,j}^{n+1} - V_{i,j}^{n} \circ \chi^n}{\Delta\tau} - \frac{\hat{\theta}\hat{g}^2\sigma_g^2}{2}\left(\frac{V_{i,j+1}^{n+1} - 2V_{i,j}^{n+1} + V_{i,j-1}^{n+1}}{\left(\Delta\hat{G}\right)^2}\right) \\
&- \frac{(1-\hat{\theta})\hat{g}^2\sigma_g^2}{2}\left(\frac{V_{\chi^n,j+1}^{n} - 2V_{\chi^n,j}^{n} + V_{\chi^n,j-1}^{n}}{\left(\Delta\hat{G}\right)^2}\right) \\
&- \hat{\theta}\hat{g}\alpha_g\left(f(T-\tau^{n+1}) - \left(\hat{G}_j\hat{g} - \bar{g}\right) + \frac{\beta_g}{\alpha_g}P_{i,j}^{n+1}\right)\left(\frac{V_{i,j+1}^{n+1} - V_{i,j-1}^{n+1}}{2\Delta\hat{G}}\right) \\
&- (1-\hat{\theta})\hat{g}\alpha_g\left(f(T-\tau^{n}) - \left(\hat{G}_j\hat{g} - \bar{g}\right) + \frac{\beta_g}{\alpha_g}(P_{\chi^n,j}\right)\left(\frac{V_{\chi^n,j+1}^{n} - V_{\chi^n,j-1}^{n}}{2\Delta\hat{G}}\right) \\
&+ r\hat{\theta}V_{i,j}^{n+1} + r(1-\hat{\theta})V_{\chi^n,j}^{n} = 0,
\end{aligned}
$$

where $\hat{\theta} = 0.5$ for the Crank-Nicolson time discretization, and $V_{r,s}^{l} \approx V(\tau^l, \hat{B}_r, \hat{G}_s)$ and $V_{\chi^l,s}^{l} \approx V(\tau^l, \chi^l, \hat{G}_s)$ denote the corresponding approximations with the proposed numerical method at the mesh nodes. Moreover, $P_{r,s}^{l} \approx P(\tau^l, \hat{B}_r, \hat{G}_s)$ and $P_{\chi^l,s}^{l} \approx P(\tau^l, \chi^l, \hat{G}_s)$ denote the corresponding approximations at the mesh nodes of the REC price obtained with the numerical method proposed for solving the nonlinear PDE problem defined by equation (4.4).

By taking into account the previous expression of the fully discretized problem,

we have to solve a linear system with $(N_{\hat{B}}-1)\times(N_{\hat{G}}-1)$ unknowns at each time step. Moreover, if we order the finite differences mesh nodes in lexicographical order, the resulting matrix is block diagonal with $N_{\hat{B}}-1$ blocks of tridiagonal matrices of order $N_{\hat{G}}-1$ each. So, by applying the classical Thomas algorithm for tridiagonal matrices, each $N_{\hat{B}}-1$ linear system can be efficiently solved.

Thus, at each time step and for each value of $i=1,\ldots,N_{\hat{B}}-1$, we have the following linear system:

$$\bar{C}(\hat{G})V_i^{n+1}=\bar{b}_i^n,$$

where $V_i^{n+1}=\left(V_{i,1}^{n+1},V_{i,2}^{n+1},\ldots,V_{i,N_{\hat{G}}-2}^{n+1},V_{i,N_{\hat{G}}-1}^{n+1}\right)$ is the approximation of the solution at the finite differences mesh nodes with coordinate $\hat{B}=\hat{B}_i$, and the matrix $\bar{C}(\hat{G})$ is given by

$$\bar{C}(\hat{G})=\begin{pmatrix}
\bar{c}_1(\hat{G}_1) & \bar{c}_2(\hat{G}_1) & 0 & \cdots & 0\\
\bar{c}_3(\hat{G}_2) & \bar{c}_1(\hat{G}_2) & \bar{c}_2(\hat{G}_2) & \ddots & \vdots\\
0 & \ddots & \ddots & \ddots & 0\\
\vdots & \ddots & \ddots & \bar{c}_1(\hat{G}_{N_{\hat{G}}-2}) & \bar{c}_2(\hat{G}_{N_{\hat{G}}-2})\\
0 & \cdots & 0 & \bar{c}_3(\hat{G}_{N_{\hat{G}}-1}) & \bar{c}_1(\hat{G}_{N_{\hat{G}}-1})
\end{pmatrix}$$

where

$$\bar{c}_1(\hat{G}_j)=1+r\hat{\theta}\Delta\tau+\frac{\hat{\theta}\hat{g}^2\sigma_g^2\Delta\tau}{\left(\Delta\hat{G}\right)^2},$$

$$\bar{c}_2(\hat{G}_j)=-\frac{\hat{\theta}\hat{g}^2\sigma_g^2\Delta\tau}{2\left(\Delta\hat{G}\right)^2}-\frac{\hat{\theta}\hat{g}\alpha_g\Delta\tau\left(f\left(T-\tau^{n+1}\right)-\left(\hat{G}_j\hat{g}-\bar{g}\right)+\dfrac{\beta_g}{\alpha_g}P_{i,j}^{n+1}\right)}{2\Delta\hat{G}},$$

$$\bar{c}_3(\hat{G}_j)=-\frac{\hat{\theta}\hat{g}^2\sigma_g^2\Delta\tau}{2\left(\Delta\hat{G}\right)^2}+\frac{\hat{\theta}\hat{g}\alpha_g\Delta\tau\left(f\left(T-\tau^{n+1}\right)-\left(\hat{G}_j\hat{g}-\bar{g}\right)+\dfrac{\beta_g}{\alpha_g}P_{i,j}^{n+1}\right)}{2\Delta\hat{G}}.$$

Moreover, for $j=1,\ldots,N_{\hat{G}}-1$, the jth component of the second member vector $\bar{b}_i^n$

of the linear system is given by

$$
\begin{aligned}
(\bar{b}_i^n)_j = & \left(\left[1 - r\Delta\tau \left(1 - \hat{\theta} \right) \right] - \frac{\sigma_g^2 \hat{g}^2 \Delta\tau \left(1 - \hat{\theta} \right)}{\left(\Delta\hat{G} \right)^2} \right) V^n_{\chi^n,j} \\
& + \left(\frac{\alpha_g \hat{g} \Delta\tau (1 - \hat{\theta}) \left[f(T - \tau^n) - \left(\hat{G}_j \hat{g} - \bar{g} \right) + \frac{\beta_g}{\alpha_g} P^n_{\chi^n,j} \right]}{2\Delta\hat{G}} \right) V^n_{\chi^n,j+1} \\
& + \left(\frac{\sigma_g^2 \hat{g}^2 \Delta\tau \left(1 - \hat{\theta} \right)}{2 \left(\Delta\hat{G} \right)^2} \right) V^n_{\chi^n,j+1} + \left(\frac{\sigma_g^2 \hat{g}^2 \Delta\tau \left(1 - \hat{\theta} \right)}{2 \left(\Delta\hat{G} \right)^2} \right) V^n_{\chi^n,j-1} \\
& - \left(\frac{\alpha_g \hat{g} \Delta\tau (1 - \hat{\theta}) \left[f(T - \tau^n) - \left(\hat{G}_j \hat{g} - \bar{g} \right) + \frac{\beta_g}{\alpha_g} P^n_{\chi^n,j} \right]}{2\Delta\hat{G}} \right) V^n_{\chi^n,j-1}.
\end{aligned}
$$

4.5.3 Second numerical method

In this second method, the derivatives valuation problem is discretized by using a Lagrange-Galerkin method, which mainly consists of applying a Crank-Nicolson characteristics scheme for time discretization combined with finite elements for the discretization in the accumulated green certificates and the natural logarithm of the renewable generation rate directions. Thus, the method is analogous to the one used in Section 3.1.4, whitout the presence of a nonlinear term.

4.5.3.1 PDE formulation in a bounded domain

As in the case of the valuation of a REC, we consider the bounded spatial domain $\Omega = (0,1) \times (0,1)$, whose boundary $\Gamma = \bigcup_{i=1}^{2} (\Gamma_i^- \cup \Gamma_i^+)$ can be decomposed as

$$
\Gamma_i^- = \{(y_1, y_2) \in \Gamma |\ y_i = 0\},\ \ \Gamma_i^+ = \{(y_1, y_2) \in \Gamma |\ y_i = 1\},\ i = 1, 2,
$$

we formulate the PDE (4.4) in divergence form after making the change of time variable $\tau = T - t$, where τ represents the time to maturity, in order to obtain a PDE

problem with initial condition: find $V : [0,\gamma] \times \Omega \to \mathbb{R}$ such that

$$\begin{aligned}
\frac{\partial V}{\partial \tau} - Div(\mathcal{A}\nabla V) + v_P \cdot \nabla V + lV &= \hat{h} \text{ in } (0,\gamma) \times \Omega\,, && (4.22)\\
V(0,\cdot) &= \zeta(K, P_T) \text{ in } \Omega, && (4.23)\\
\frac{\partial V}{\partial y_1} &= 0 \text{ on } (0,\gamma) \times \Gamma_1^+, && (4.24)\\
\frac{\partial V}{\partial y_2} &= 0 \text{ on } (0,\gamma) \times (\Gamma_2^- \cup \Gamma_2^+), && (4.25)
\end{aligned}$$

Moreover, in (4.22), the diffusion matrix $\mathcal{A}$, the velocity field v_P, the linear term l and the second member function $\hat{h}$ have the following expressions:

$$\begin{aligned}
\mathcal{A} &= \begin{pmatrix} 0 & 0 \\ 0 & \dfrac{\hat{g}^2\sigma_g^2}{2} \end{pmatrix},\\
v_P &= \begin{pmatrix} -\hat{b}\exp(y_2\hat{g} - \bar{g}) \\ -\hat{g}\alpha_g \left(f(T-\tau) - (y_2\hat{g} - \bar{g}) + \dfrac{\beta_g}{\alpha_g} P(\tau, y_1, y_2) \right) \end{pmatrix},\\
l &= r,\\
\hat{h} &= 0.
\end{aligned}$$

Note that the velocity field depends on the value of the REC P, which in turn can be computed in terms of (τ, y_1, y_2) in a previous step.

4.5.3.2 The Crank-Nicolson characteristics method

In order to obtain a time discretization of the problem (4.22), we propose a Crank-Nicolson characteristics method. As in the numerical solution of the RECs pricing problem, this numerical scheme mainly consists on approximating the material derivative along the characteristics curves with an upwinded finite differences method, which leads to a symmetric system of equations.

First, let us define

$$\frac{DV}{D\tau} = \frac{\partial V}{\partial \tau} + v_P \cdot \nabla V,$$

which represents the material derivative along the characteristic curve through $y = (y_1, y_2) = (\hat{B}, \hat{G})$ at time $\bar{s}$. If we denote the characteristics curve associated to the velocity field v_P by $\chi(y, \bar{s}; s)$, then it can be characterized as the solution of the following final value ODE problem:

$$\frac{\partial}{\partial s}\chi(y, \bar{s}; s) = v_P(s, \chi(y, \bar{s}; s)), \quad \chi(y, \bar{s}; \bar{s}) = y. \tag{4.26}$$

Note that we only know the approximations of function P at the mesh points of a finite element mesh for the different time steps used in the time discretization, so that we only know the value of the velocity field v_P at those mesh point in space and time. Therefore, we cannot compute analytically the expression of the characteristics curves (even for the case $f = 0$) and we need to approximate them by means of a numerical method.

In order to discretize in time the material derivative, we introduce a number of time steps $N_T > 0$, a time step $\Delta\tau = \gamma/N_T$ and the time mesh points $\tau^n = n\Delta\tau$, $n = 0, \frac{1}{2}, 1, \frac{3}{2}, \ldots, N_T$.

Now, we approximate the material derivative at time $\tau^{n+\frac{1}{2}}$ by the finite differences quotient:

$$\frac{DV}{D\tau} \approx \frac{V^{n+1} - V^n \circ \chi^n}{\Delta\tau},$$

where $\chi^n(y) = \chi(y, \tau^{n+1}; \tau^n)$.

In order to obtain χ^n, since the characteristic curves cannot be obtained analytically, we consider one step of the first order explicit Euler scheme to approximate the solution of the final value problem (4.26), that is:

$$\chi^n(y) \approx y - \Delta t \; v_P^{n+1}(y). \tag{4.27}$$

Now, let us write the Crank-Nicolson characteristics time discretization around $(\chi(y, \tau^{n+1}; \tau^{n+\frac{1}{2}}), \tau^{n+\frac{1}{2}})$, $n = 0$, ..., $N_T - 1$, for the first equation of (4.22), namely:

$$\frac{V^{n+1}(y) - V^n(\chi^n(y))}{\Delta\tau} - \frac{1}{2}Div(\mathcal{A}\nabla V^{n+1})(y) - \frac{1}{2}Div(\mathcal{A}\nabla V^n)(\chi^n(y)) + \frac{1}{2}(l\,V^{n+1})(y) + \frac{1}{2}(l\,V^n)(\chi^n(y)) = \frac{1}{2}\hat{h}^{n+1}(y) + \frac{1}{2}\hat{h}^n(\chi^n(y)). \tag{4.28}$$

4.5.3.3 Spatial discretization

For the spatial discretization of the problem (4.28), as in the case of the REC pricing problem, we propose biquadratic Lagrange finite elements. Thus, first, we need to obtain a variational formulation of such problem at each time step $n = 0, 1, 2, ..., N_T - 1$, and each fixed point iteration, $k = 0, 1, 2, ...$ For this purpose, we multiply (4.28) by a suitable test function, $\phi \in H^1(\Omega)$ and we integrate in Ω.

Moreover, assuming that $\chi^n \in \mathcal{C}^2(\Omega)$ and $(F_e^n)^{-1} \in \mathcal{C}^1(\Omega)$, as in the REC valuation problem, we apply Green's theorems, such as the classical Green formula and the following one proposed in [50]:

$$\begin{aligned}\int_\Omega Div(\mathcal{A}\nabla V^n)(\chi^n(y))\phi(y)\,dy = &\int_\Gamma (F_e^n)^{-T}(y)\vec{n}(y)\cdot(\mathcal{A}\nabla V^n)(\chi^n(y))\phi(y)\,dA \\ &- \int_\Omega (F_e^n)^{-1}(y)(\mathcal{A}\nabla V^n)(\chi^n(y))\cdot\nabla\phi(y)\,dy \\ &- \int_\Omega Div((F_e^n)^{-T}(y))\cdot(\mathcal{A}\nabla V^n)(\chi^n(y))\phi(y)\,dy,\end{aligned} \tag{4.29}$$

where $F_e^n = \nabla\chi^n$, $\vec{n}$ is a vector normal to the boundary pointing outward and dA denotes the integration measure on the boundary Γ.

In this case, in order to achieve the variational formulation of the problem, since it is not possible to compute the characteristics curves analytically. Thus, as it is pointed out in [9], denoting by $\mathcal{J} = \nabla v_P$, we can employ the following approximations:

$$\begin{aligned}(F_e^n)^{-1}(y) &= \mathcal{I}(y) + \Delta\tau\mathcal{J}^n(\chi^n(y)) + \mathcal{O}(\Delta\tau^2), \\ Div((F_e^n)^{-T}(y)) &= \Delta\tau\nabla Div(v_P(\chi^n(y))) + \mathcal{O}(\Delta\tau^2).\end{aligned}$$

In this work, having in view that $\nabla Div(v_P(\chi^n(y))) = 0$ and considering the previous approximation for the tensor $(F_e^n)^{-1}(y)$, the weak formulation can be written as

$$\begin{aligned}
&\int_\Omega V^{n+1}(y)\phi(y)\,dy + \frac{\Delta\tau}{2}\int_\Omega (\mathcal{A}\nabla V^{n+1})(y)\cdot\nabla\phi(y)\,dy \\
&+\frac{\Delta\tau}{2}\int_\Omega lV^{n+1}(y)\phi(y)\,dy = \int_\Omega V^n(\chi^n(a))\phi(a)\,dy \\
&+\frac{\Delta\tau}{2}\int_\Omega (\mathcal{A}\nabla V^n)(\chi^n(a))\nabla\phi(y)\,dy - \frac{\Delta\tau}{2}\int_\Omega lV^n(\chi^n(y))\phi(y)\,dy \\
&-\frac{\Delta\tau}{2}\int_\Omega \Delta\tau\mathcal{J}^n(\chi^n(y))(\mathcal{A}\nabla V^n)(\chi^n(y))\nabla\phi(y)\,dy \\
&+\frac{\Delta\tau}{2}\int_\Gamma (\mathcal{I}(y)+\Delta\tau\mathcal{J}^n(\chi^n(y)))^T\vec{n}(y)\cdot(\mathcal{A}\nabla V^n)(\chi^n(y))\phi(y)\,dA \\
&+\frac{\Delta\tau}{2}\int_\Omega \hat{h}^{n+1}(y)\phi(y)\,d\vec{(y)} + \frac{\Delta\tau}{2}\int_\Omega \hat{h}^n(\chi^n(y))\phi(y)\,d\vec{(y)}.
\end{aligned} \tag{4.30}$$

Now, for a family of quadrangular meshes $\{\tau_h\}$ of the domain Ω, linked to each mesh $\{\tau_h\}$, we can introduce a family of piecewise quadratic Lagrangian finite elements, $(\mathcal{T}, \mathcal{Q}_2, \Sigma_\mathcal{T})$, with $\mathcal{Q}_2$ being the space of polynomials defined in $\mathcal{T} \in \tau_h$ with degree less or equal than two in each spatial variable, and $\Sigma_\mathcal{T}$ the subset of nodes of the element $\mathcal{T}$. More precisely, we can introduce the finite elements space

$$\nu_h = \{\psi_h \in \mathcal{C}^0(\Omega) |\, \psi_{h_\mathcal{T}} \in \mathcal{Q}_2, \quad \forall \mathcal{T} \in \tau_h\}, \tag{4.31}$$

where $\mathcal{C}^0(\Omega)$ is the space of piecewise continuous functions on Ω.

4.6 Numerical examples

In this section, we present some results obtained with the previous methods to obtain the price of some derivatives contracts whose underlying is a REC. More precisely, we consider the cases of European vanilla call and put options on RECs, as well as a

futures contracts on the same underlying. Note that these three derivatives are the most basic ones.

4.6.1 REC call option

As previously indicated, the first example corresponds to a European vanilla call option on a REC, the price of which at time t is given by $V_t^C = V^C(t, B_t, \widetilde{G}_t)$ and its payoff at maturity V_T^C is given by

$$V_T^C = (P_T - K)^+,$$

where $K \geq 0$ is the strike price.

For $t \in [T-\gamma, T]$, the discounted call price is a martingale under the measure $\mathbb{Q}$. Therefore, the call option price at time t is given as the discounted conditional expectation of its terminal condition under this measure, i.e.,

$$V_t^C = e^{-r(T-t)}\mathbb{E}^{\mathbb{Q}}\left[(P_T - K)^+ | \mathcal{F}_t\right], \qquad t \in [T-\gamma, T].$$

Thus, the discounted call price can be represented as an Itô integral with respect to the Brownian motion W_t^1.

Note that the PDE problem (4.4) is linear because

$$\mu_g(t, \widetilde{G}, P) = \alpha_g \left(f(t) + \frac{\beta_g}{\alpha_g} P - \widetilde{G} \right)$$

and the value function of the REC, P, is assumed to be given, as it has been previously obtained by solving a nonlinear PDE.

More precisely, the formulation of the call option pricing problem is now:

$$\mathcal{L}_2\left[V^C\right] = \frac{\partial V^C}{\partial t} + \frac{1}{2}\sigma_g^2 \frac{\partial^2 V^C}{\partial \widetilde{G}} + \alpha_g \left(f(t) + \frac{\beta_g}{\alpha_g} P - \widetilde{G} \right) \frac{\partial V^C}{\partial \widetilde{G}} + \exp(\widetilde{G}) \frac{\partial V^C}{\partial B} - r V^C = 0, \tag{4.32}$$

jointly with the final condition

$$V^C(T, B, \widetilde{G}) = (P(T, B, \widetilde{G}) - K)^+. \tag{4.33}$$

In this setting, we carry out the valuation of a European call option with maturity $T = 13$, which corresponds to the end of energy year 2013, which is May 31, 2013 as in the previous numerical examples presented in Section 3.2.2 for RECs pricing. Moreover, for simplicity we assume that the life of the option pricing contract, γ, is one year and also that the REC corresponds to the case of a single compliance period.

Note that we could also address the pricing of the call option on a REC with multiple compliance periods. In that case, the duration of the option contract would start at the beginning of the RECs duration period or before, with a payoff also defined by condition (4.33). This comment also applies to the other derivatives we are pricing in this Section.

For the parameters α_g, β_g, σ_g and r appearing in the PDE, we consider those ones in Table 3.7 and we will consider the strike price $K = \pi_T/2$, where the penalty π_T is the value of the REC at maturity.

4.6.1.1 First numerical method

As in the REC pricing problem, the underlying variables in the PDE are the accumulated renewable energy certificates (B) and the renewable energy rate (G), therefore we choose the same computational bounded domain as in the RECs pricing problem.

More precisely, we choose $\hat{b} = 8 \times 10^5$ and $\bar{g} = \ln(8 \times 10^5)$, so that $\hat{g} = 2 \times \ln(8 \times 10^5)$. By using these values we pose the PDE problem in the bounded domain $\hat{\Omega} = (0, \gamma) \times (0, 1) \times (0, 1)$.

Concerning the discretization parameters, after solving the problem with different time steps and uniform spatial meshes, we show the results corresponding to the consideration of 100 time steps per month for the time discretization, i.e. $\Delta\tau = \frac{1}{1200}$, and a uniform mesh with $\Delta\hat{B} = \Delta\hat{G} = 1/32$.

Next, we first present the computed results in the variables (t, B, G) that are obtained with the model data and the parameters related to the numerical methods.

Firstly, in Figure 4.4 we show the price surface of the REC call option four months

before maturity, that is at time $t = T - 1/3$ (or at $\tau = 1/3$, equivalently). Thus, the price is represented with respect to the underlying variables in the PDE as in the case of the RECs pricing problem. Note that results are qualitative very similar to the RECs price, as roughly in a call option the holder of the option is betting on an increase of the underlying asset (in this case, the REC). So the higher values of the call option price are obtained in the region with higher values of the REC price, while the option price tends to zero in the region with lower values of the REC.

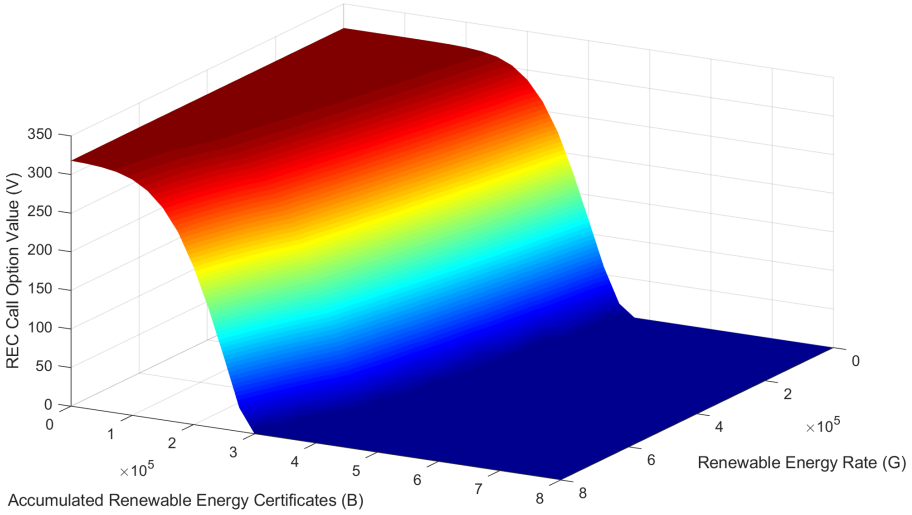

Figure 4.4: First numerical method: REC option call price surface at $t = T - 1/3$.

Next, as usually in many representations of derivatives prices, we will show the value of the derivative with respect to the underlying asset. For this purpose, we have chosen to represent parameterized curves in the plane defined by the REC price (P) and the derivative price (V^C) at a fixed time t. More precisely, we fix a value of the variable G equal to one of the mesh values, namely $G = G_j$. We also fix a time t^n included in the time discretization mesh. Thus, we consider the points $(P(t^n, B_i, G_j), V^C(t^n, B_i, G_j))$ in that plane.

Following the previous methodology, for a fixed value of G equal to 200000 and a couple of time values, we show some curves to illustrate the REC call option price

versus the price of the certificate for different times. More precisely, in Figure 4.5 we show the curve at time $T - 1/3$, while in Figure 4.6 we consider time $T - 2/3$.

Note that results are shown for all obtained values of the REC, however we are mainly interested in the option prices associated to REC values near the strike price.

Although the qualitative results in Figure 4.5 and Figure 4.6 clearly correspond to a call option, we note that some differences are observed with respect to results observed in the case of a more classical call option on an underlying asset which follows a stochastic dynamics driven by a geometric Brownian motion (Black-Scholes assumption). Actually, certain differences are expected, as the underlying REC price does not follow such a dynamics. Indeed, the stochastic dynamics of the REC price depends on the dynamics of its corresponding underlying factors.

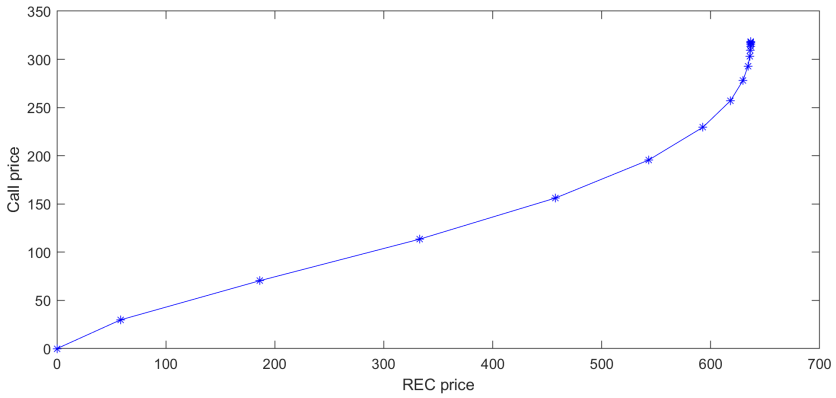

Figure 4.5: First numerical method: REC call option price versus REC price at time $t = T - 1/3$.

The total CPU time to obtain the price of the option at time $t = T - 1/3$ (i.e., $\tau = 1/3$) is 38 seconds. It is important to point out that to obtain the option prices, at each time step of any of the proposed numerical methods, we previously compute the price of the REC by advancing one time step in the numerical solution of the nonlinear PDE governing the REC pricing problem. Thus, the previously indicated computational time corresponds to the one required to obtain not only the option price but also the renewable energy certificate price (REC).

Note that in the REC pricing problem we indicated the computational times

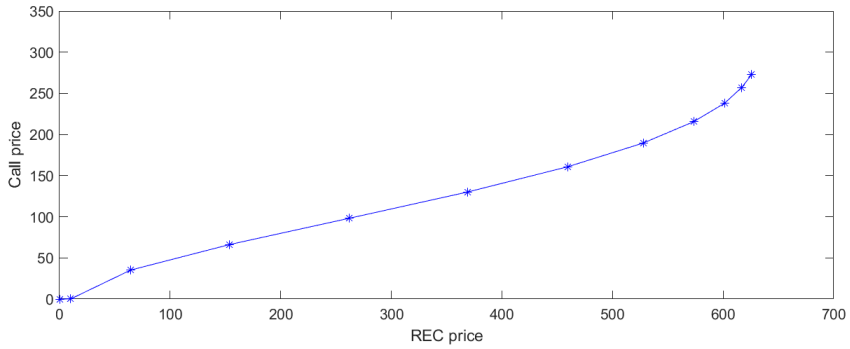

Figure 4.6: First numerical method: REC call option price versus REC price at time $t = T - 2/3$.

required to obtain the REC price at time $T - 2 - 2/3$ (i.e., $\tau = 8/3$), which requires the use of eight times the number of time steps used for the REC options pricing problem, as the time step is the same in both cases. Furthermore, the number of iterations in the duality algorithm for the nonlinear problem is not the same inside each time iteration. These two facts explain the comparison of the computational times indicated in this section and the analogous one devoted to the numerical solution of the REC pricing problem.

Concerning the technical characteristics of the computer, the CPU of the laptop we use for the computation is an Intel(R) Core(TM) i7-10750H at 2,6 GHz with 32 GB 2933 MHz DDR4 RAM. The implementation has been developed in Matlab.

4.6.1.2 Second numerical method

In order to solve the problem with the proposed Lagrange-Galerkin method, we have considered the same computational domain as in the first numerical methods, so that we have chosen $\hat{b} = 8 \times 10^5$ and $\hat{g} = 2 \times \ln(8 \times 10^5)$.

As in the numerical solution of the REC pricing problem with this second numerical method, we present the results that correspond to the use of the Mesh 16 that appears in Table 3.3, which is equivalent to the one used in the first method. For the time discretization, we have considered 100 time steps per month, i.e. $\Delta\tau = \frac{1}{1200}$.

For the certificate pricing, the values of the requirements at the end of each energy

year and the penalties if the requirements are not met are given in Table 3.8.

As with the previous method, in Figure 4.7 we show the price surface of the REC call option (in terms of the underlying factors B and G) four months before the maturity date of the option, that is at time $t = T - 1/3$ (or at $\tau = 1/3$, equivalently). Note by comparison with the ones presented in Figure 4.4, the results are very similar to those ones obtained with the alternative first numerical method.

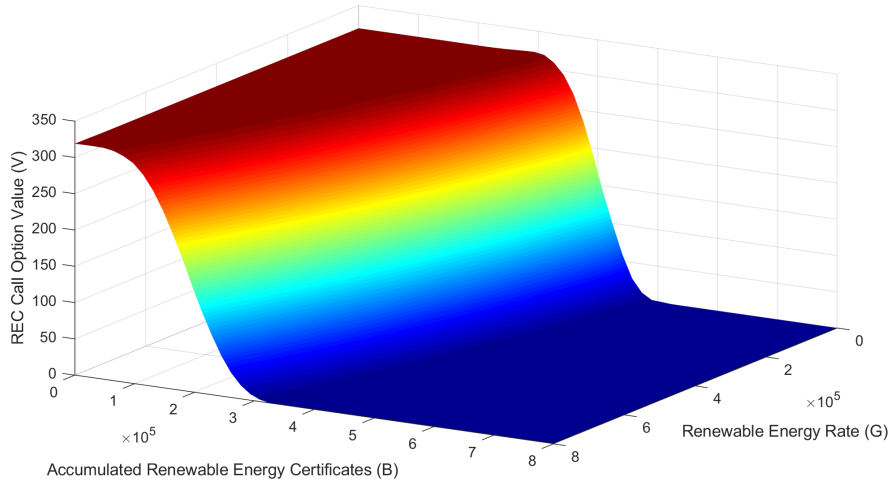

Figure 4.7: Second numerical method: REC call option price surface at $t = T - 1/3$.

Next, as in the first numerical method, for a fixed value of G equal to 200000, we make a representation of the price of the option versus the price of the REC for the same two different times. Thus, in Figure 4.8 we exhibit the curve at time $t = T - 1/3$ and in Figure 4.9 at time $t = T - 2/3$. Again, we point out that the results are shown for all obtained values of the REC, however we are mainly interested in the option prices associated to REC values near the strike price. Comparing the results in Figure 4.8 and Figure 4.9 with the correponding ones of the first numerical method in Figure 4.5 and Figure 4.6, we observe some small differences and we conjecture that results obtained with the second numerical method seem more in agreement with the expected behaviour of the call option.

In this second numerical method, the total CPU time to obtain the price of the

option at time $t = T - 1/3$ is 27 seconds. Again, we point out that the previously indicated computational time actually corresponds to the one required to obtain not only the option price but also the renewable energy certificate price (REC). Note that the chosen discretization parameters for this second numerical method are selected so that the computational time can be compared with the first method, in view of the characteristics of the time and space meshes that have been used for the first method in the previous section.

So, the second numerical method results to be quicker to obtain the results.

Again, we recall that the CPU of the laptop is a Intel(R) Core(TM) i7-10750H at 2,6 GHz with 32 GB 2933 MHz DDR4 RAM. The implementation has been developed in Fortran.

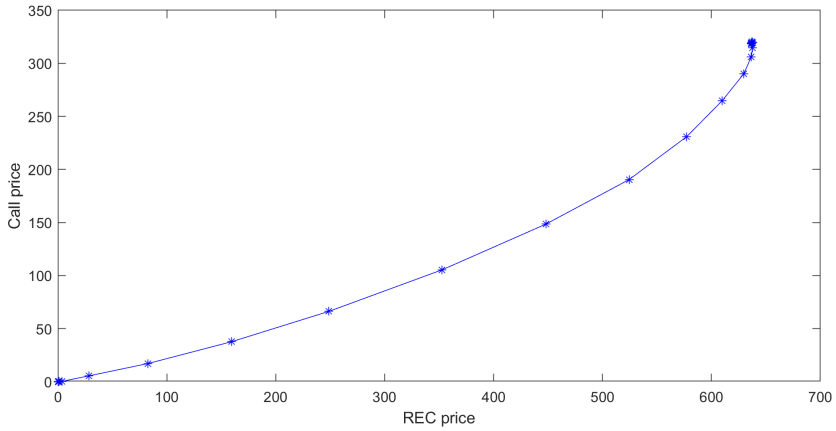

Figure 4.8: Second numerical method: REC call option price versus REC price at time $t = T - 1/3$.

4.6.2 REC put option

In this example, we consider a European vanilla put option, the price of which is denoted by V_t^P at time t. Moreover, the payoff of the put option at maturity date T, is given by

$$V_T^P = (K - P_T)^+,$$

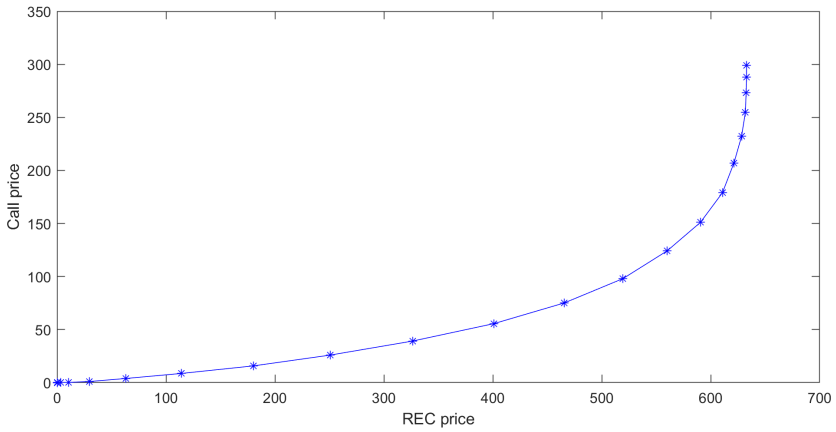

Figure 4.9: Second numerical method: REC call option price versus REC price at time $t = T - 2/3$.

where $K \geq 0$ represents the strike.

For $t \in [T-\gamma, T]$, the discounted put option price is a martingale under the measure $\mathbb{Q}$, therefore it is given as the discounted conditional expectation of its terminal value under this measure, i.e.,

$$V_t^P = e^{-r(T-t)}\mathbb{E}^{\mathbb{Q}}\left[(K - P_T)^+ | \mathcal{F}_t\right], \qquad t \in [T-\gamma, T].$$

As in the case of the call option, the discounted put option price can be represented as an Itô integral with respect to the Brownian motion W_t^1.

Assuming that $V_t^P = V^P(t, B_t, \widetilde{G}_t)$, the function V^P satisfies the linear PDE (4.4), so formulation of the put option pricing problem consists in the PDE:

$$\mathcal{L}_2\left[V^P\right] = \frac{\partial V^P}{\partial t} + \frac{1}{2}\sigma_g^2 \frac{\partial^2 V^P}{\partial \widetilde{G}} + \alpha_g\left(f(t) + \frac{\beta_g}{\alpha_g}P - \widetilde{G}\right)\frac{\partial V^P}{\partial \widetilde{G}} + \exp(\widetilde{G})\frac{\partial V^P}{\partial B} - rV^P = 0,$$

jointly with the final condition

$$V^P(T, B, \widetilde{G}) = (K - P(T, B, \widetilde{G}))^+.$$

In this setting, we carry out the valuation of a European put option with maturity $T = 13$, as in the case of the European call option. Again, for the PDE parameters α_g, β_g, σ_g and r, we consider those ones in Table 3.7 and we will consider the strike price $K = \pi_T/2$, where the penalty π_T is the value of the REC at maturity.

4.6.2.1 First numerical method

As in the case of call option, we have applied the first numerical method for solving the PDE problem that models the put option pricing problem. More precisely, we have applied the same numerical parameters as in the call option case.

First, we show the computed results in the variables (t, B, G) that are obtained with the model data and the parameters related to the numerical methods. Thus, in Figure 4.10 we show the price surface of the REC call option four months before maturity, that is at time $t = T - 1/3$ (or at $\tau = 1/3$, equivalently). Note that results are qualitatively the expected ones. In a put option the holder of the option is betting on an future decrease of the underlying asset (in this case, the REC). So the higher values of the put option price are obtained in the region with lower values of the REC price, while the option price is higher in the region with lower values of the REC.

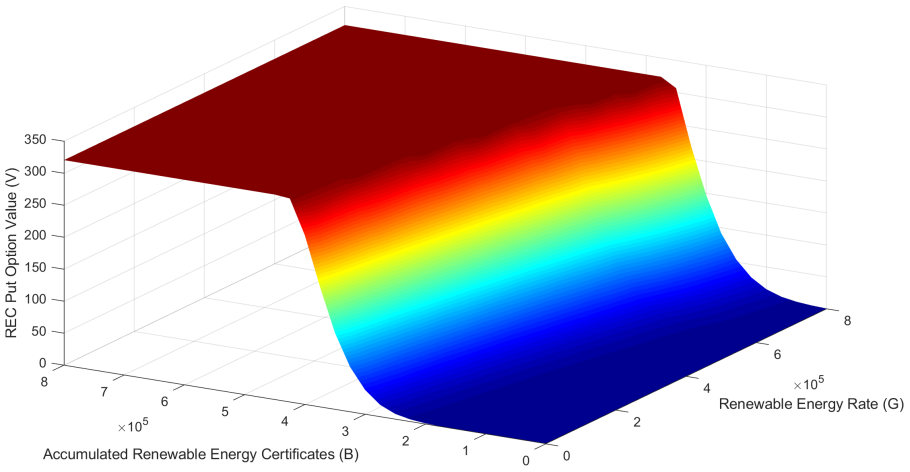

Figure 4.10: First numerical method: REC put option price surface at $t = T - 1/3$.

Furthermore, as previously explained in the case of the call option, for a fixed value of G equal to 200000 (that corresponds to a particular value of $\widetilde{G}_j$ included in the chosen mesh), we show some parameterized curves illustrating the price of the put option versus the REC price, at different times included in the mesh for time

discretization. More precisely, in Figure 4.11, we show the obtained curve at time $t = T - 1/3$ and in Figure 4.12 at time $t = T - 2/3$.

As in the case of call options, we note that some differences are observed in Figure 4.11 and in Figure 4.12 with respect to results usually obtained in the case of a more classical put option on an underlying asset which follows a stochastic dynamics driven by a geometric Brownian motion (Black-Scholes assumption). Actually, certain differences are expected, as the underlying REC price does not follow such a dynamics. Indeed, the stochastic dynamics of the REC price depends on the dynamics of its corresponding underlying factors. Furthermore, in the case of the put option presented in this section, also the convexity of the curves changes with respect to the previously mentioned classical case.

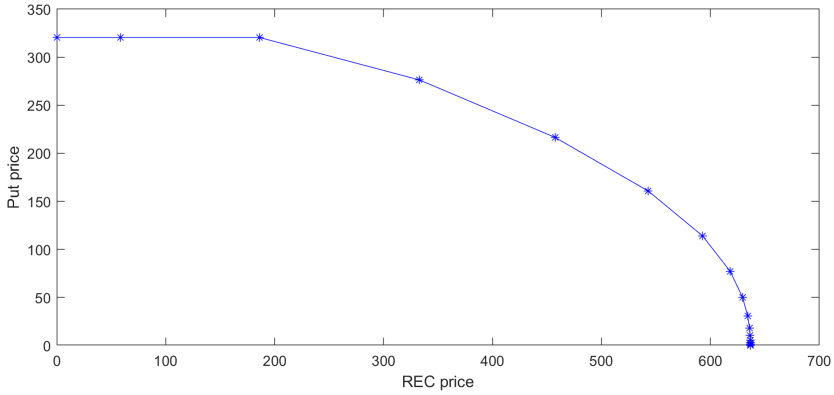

Figure 4.11: First numerical method: REC put option price versus REC price at time $t = T - 1/3$.

As the presented results correspond to the same data and numerical parameters chosen for the first numerical method in the call option pricing problem of previous section, the computational time of achieving the price of the REC put option is the same as in the previous call option case.

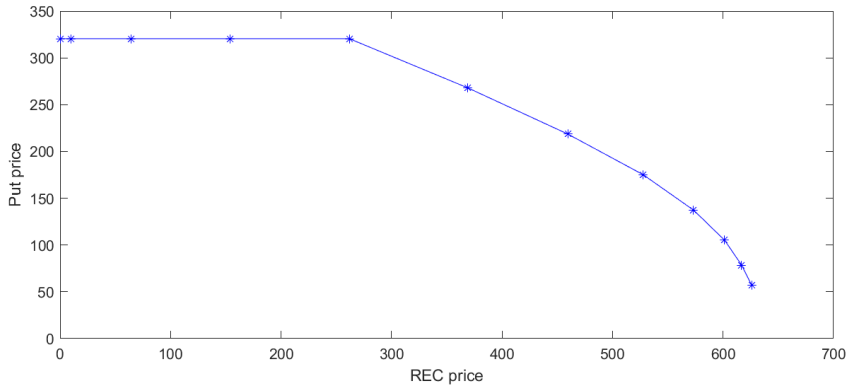

Figure 4.12: First numerical method: REC put option price versus REC price at time $t = T - 2/3$.

4.6.2.2 Second numerical method

In order to solve the put option pricing problem with the second numerical method (i.e., Lagrange-Galerkin method), we have considered $\hat{b} = 8 \times 10^5$ and $\hat{g} = 2 \times \ln(8 \times 10^5)$, so that the computational domain is the same as in the first nummerical method.

As in the call option and REC pricing problems, we present the numerical results corresponding to the spatial mesh Mesh 16, the data of which appear in Table 3.3. Note that Mesh 16 is equivalent to the one used in the first method. Moreover, for the time discretization we have considered 100 time steps per month, i.e. $\Delta\tau = \frac{1}{1200}$.

As with the first method, in Figure 4.13 we show the price surface of the REC put option four months before maturity, that is at time $t = T - 1/3$ (or at $\tau = 1/3$, equivalently). Note that the results are very similar to those ones obtained when using the first numerical method.

Next, following the same methodology as in previous cases and numerical methods, for a fixed value of G equal to 200000, we show the price of the option versus the price of the REC for the same two different times. More precisely, in Figure 4.14, we exhibit the curve at time $t = T - 1/3$ and in Figure 4.15 at $t = T - 2/3$.

Again, we point out that the results are shown for all obtained values of the REC, however we are mainly interested in the option prices associated to REC values

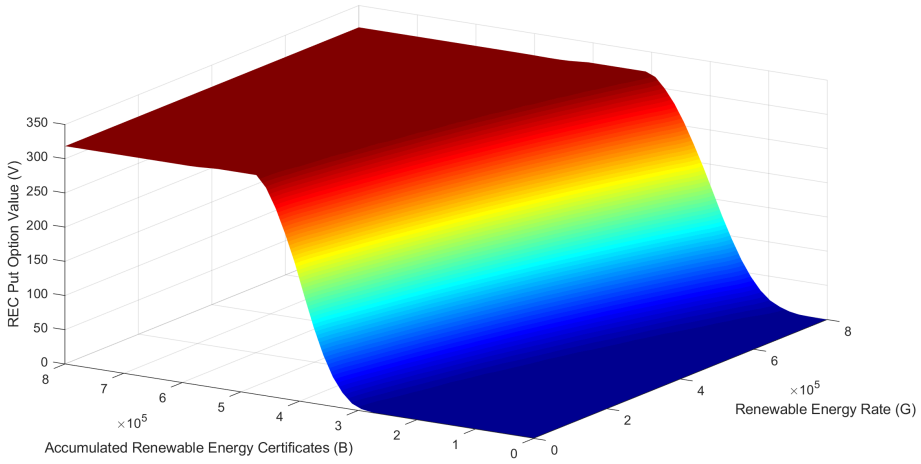

Figure 4.13: Second numerical method: REC put option price surface at $t = T - 1/3$.

near the strike price. Comparing the results in Figure 4.14 and Figure 4.15 with the corresponding ones of the first numerical method in Figure 4.11 and Figure 4.12, we observe some differences and we conjecture that results obtained with the second numerical method seem more in agreement with the expected behaviour of the call option. Note that in the first numerical method the price exhibits a larger flat behaviour in the region with lower prices of the REC, while in the second numerical method the slope is large near the larger values of the REC.

By considering the same arguments as in the first numerical method, in the second numerical method the total CPU time to obtain the price of the put option is the same as in the call option pricing problem with the second method.

4.6.3 REC futures contract

As previously indicated, the last example we consider is a futures contract on the REC, the price of which at time t is given by $V_t^F = V^F(t, B_t, G_t)$. In the futures contract, as both counterparties have the obligation to make the transaction, the

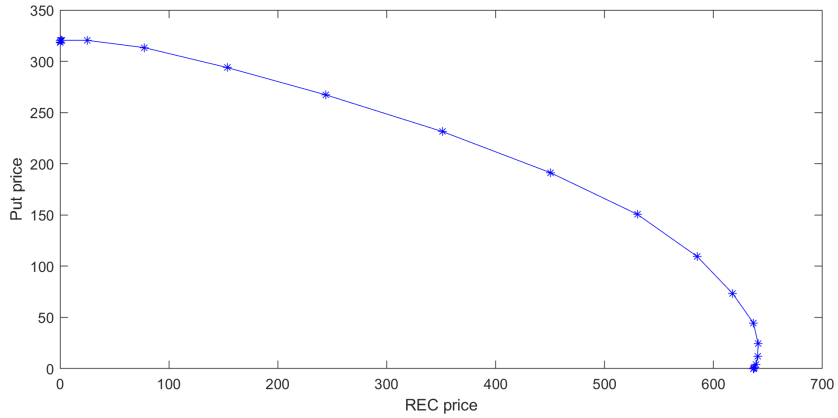

Figure 4.14: Second numerical method: REC put option price versus REC price at time $t = T - 1/3$.

payoff at maturity date T is given by

$$V_T^F = P_T - K,$$

where $K \geq 0$ is the strike price of the futures contract.

As in the case of any derivative on the REC, for $t \in [T-\gamma, T]$, the discounted futures contract price is a martingale under the measure $\mathbb{Q}$. Therefore, the futures contract price can be obtained as the discounted conditional expectation of its payoff under this measure, i.e.,

$$V_t^F = e^{-r(T-t)}\mathbb{E}^{\mathbb{Q}}\left[P_T - K|\mathcal{F}_t\right], \qquad t \in [T-\gamma, T].$$

The discounted future contract price can be represented as an Itô integral with respect to the Brownian motion W_t^1.

Moreover, the PDE (4.4) governing the price of the futures contract is linear because

$$\mu_g(t, \widetilde{G}, P) = \alpha_g \left(f(t) + \frac{\beta_g}{\alpha_g} P - \widetilde{G} \right)$$

and the value of the REC, P, is assumed to be given, as it can be previously obtained by solving a nonlinear PDE,

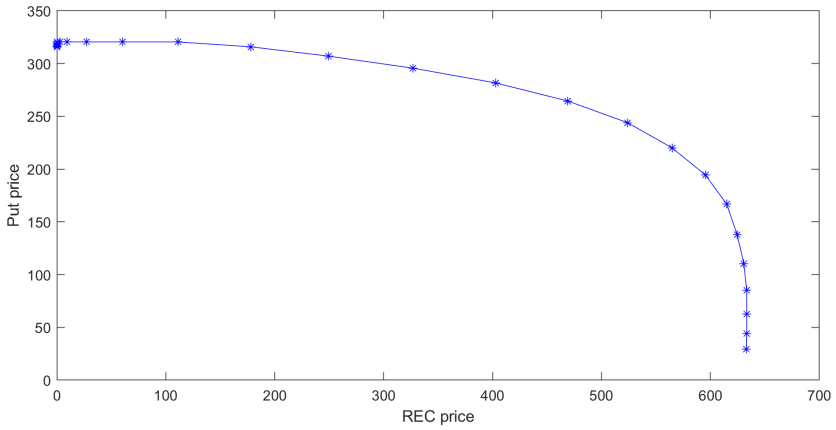

Figure 4.15: Second numerical method: REC put option price versus REC price at time $t = T - 2/3$.

More precisely, the formulation of the futures contract pricing problem is defined by the linear PDE:

$$\mathcal{L}_2\left[V^F\right] = \frac{\partial V^F}{\partial t} + \frac{1}{2}\sigma_g^2 \frac{\partial^2 V^F}{\partial \widetilde{G}} + \alpha_g \left(f(t) + \frac{\beta_g}{\alpha_g} P_t - \widetilde{G} \right) \frac{\partial V^F}{\partial \widetilde{G}} + \exp(\widetilde{G}) \frac{\partial V^F}{\partial B} - r V^F = 0,$$

jointly with the final condition

$$V^F(T, B, \widetilde{G}) = P(T, B, \widetilde{G}) - K.$$

Analogously to the previously described derivatives pricing problems, we address the valuation of a futures contract with maturity $T = 13$ and the parameter $\gamma = 1$, which implies that the duration of the contract is from $T - 1$ to T. Also we assume a single compliance date for the underlying REC. Again, for the PDE parameters α_g, β_g, σ_g and r, we consider those ones in Table 3.7 and we consider the strike price $K = \pi_T/2$, where the penalty π_T is the value of the REC at maturity.

4.6.3.1 First numerical method

As in the REC and options cases, we choose $\hat{b} = 8 \times 10^5$ and $\bar{g} = \ln(8 \times 10^5)$, so that $\hat{g} = 2 \times \ln(8 \times 10^5)$. By using these values, we pose the PDE problem in the computational bounded domain $\hat{\Omega} = (0, \gamma) \times (0, 1) \times (0, 1)$.

Concerning the discretization parameters, we show the results that correspond to 100 time steps per month for the time discretization, i.e. $\Delta\tau = \frac{1}{1200}$, and a uniform mesh with $\Delta\hat{B} = \Delta\hat{G} = 1/32$.

As in previous cases, we first show the computed futures contract prices with respect to the variables (t, B, G) that are obtained with the model data and the parameters related to the numerical methods.

Thus, in Figure 4.16 we exhibit the price surface of the REC futures contract four months before maturity, that is at time $t = T - 1/3$ (or at $\tau = 1/3$, equivalently).

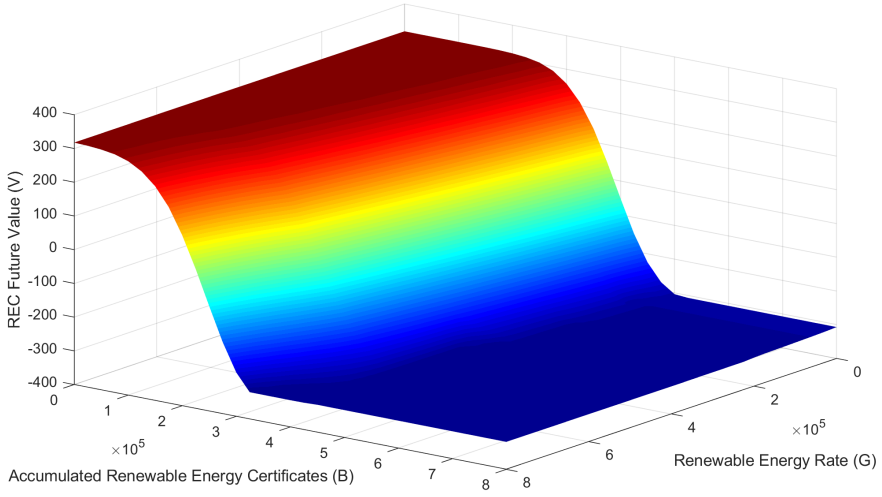

Figure 4.16: First numerical method: REC future contract price surface at $t = T - 1/3$.

Additionally, as in the case of the options, for a fixed value of G equal to 200000, we represent the price of the futures contract versus the price of the REC for two different times. More precisely, in Figure 4.17 we show the curve at time $t = T - 1/3$, while in Figure 4.18 we consider the time $t = T - 2/3$.

Unlike in the case of options, it is well-known that prices of futures contracts become negative mainly when the the prices of the underlying asset, the REC in this case, are below the strike price of the contract. This is observed in all figures in this section, where the expected behaviour for the price is obtained.

Moreover, concerning Figure 4.17 and Figure 4.18, note that we present the values of the futures contract for all the REC prices that correspond to $G = 200000$, although we are mainly interested in having accurate prices for the values of the REC near the strike price of the futures contract, because usually the value of the REC will move around this strike value. So, the prices for extreme values of the REC are not so interesting from the financial point of view.

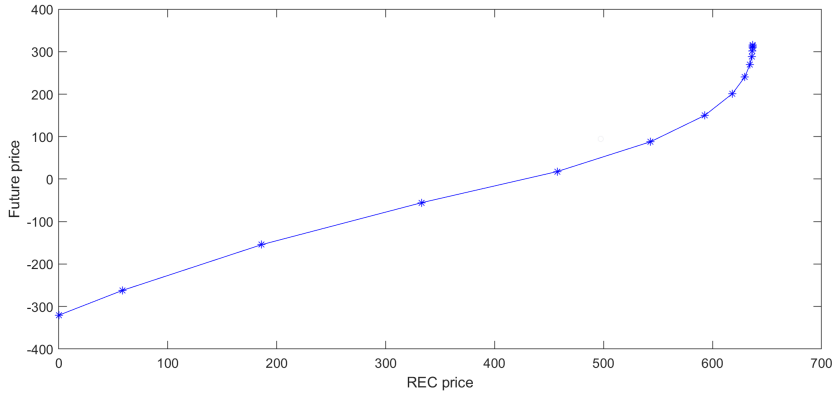

Figure 4.17: First numerical method: REC future contract price versus REC price at time $t = T - 1/3$.

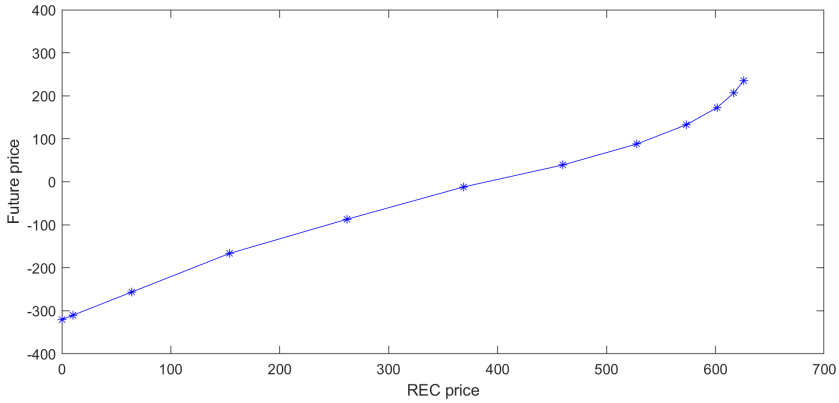

Figure 4.18: First numerical method: REC future contract price versus REC price at time $t = T - 2/3$.

The CPU time to obtain the price of the futures contract at time $t = T - 1/3$ is 38 seconds, the same as the ones for REC call and put options. Note that the only

difference in the linear PDE problem from one derivative to another is the expression of the final condition due to the change of the payoff. As in the previously presented option pricing examples, in order to obtain the price of the futures contract, at each time step of the numerical method we first compute the price of the REC and then we update the futures contract price at the same time step.

4.6.3.2 Second numerical method

Regarding the parameters involved in the numerical methods, as in the first method, we have chosen $\hat{b} = 8 \times 10^5$ and $\hat{g} = 2 \times \ln(8 \times 10^5)$.

As all the previous examples of pricing problems, in order to obtain the price of the futures with the proposed Lagrange-Galerkin method, we present the numerical results corresponding to the spatial mesh Mesh 16, the data of which appear in Table 3.3. In this way, we use a spatial mesh which is equivalent to the spatial discretization that we use in the first method. Moreover, for the time discretization we have considered 100 time steps per month, i.e. $\Delta\tau = \frac{1}{1200}$.

Analogously to the first numerical method, in Figure 4.19 we show the price surface of the REC futures contract four months before maturity, that is at time $t = T - 1/3$ (or at $\tau = 1/3$, equivalently).

All figures show the expected behaviour of the prices of the futures contract on the REC. Moreover, if we compare the results obtained when using the second numerical method that appear in the figures with the analogous ones exhibited in the figures of the previous section provided by the first numerical method, we observe that they are very close each other, specially in the region of financial interest.

Furthermore, for a fixed value of G equal to 200000, we display the prices of the futures contract versus the REC prices for the same two times used in the first numerical method. More precisely, in Figure 4.20 we show the computed curve at time $t = T - 1/3$, while in Figure 4.21 we show the analogous curve at time $t = T - 2/3$.

The CPU time to obtain the price of the futures contract at time $t = T - 1/3$ with this second numerical method is 27 seconds. As expected the computational time is

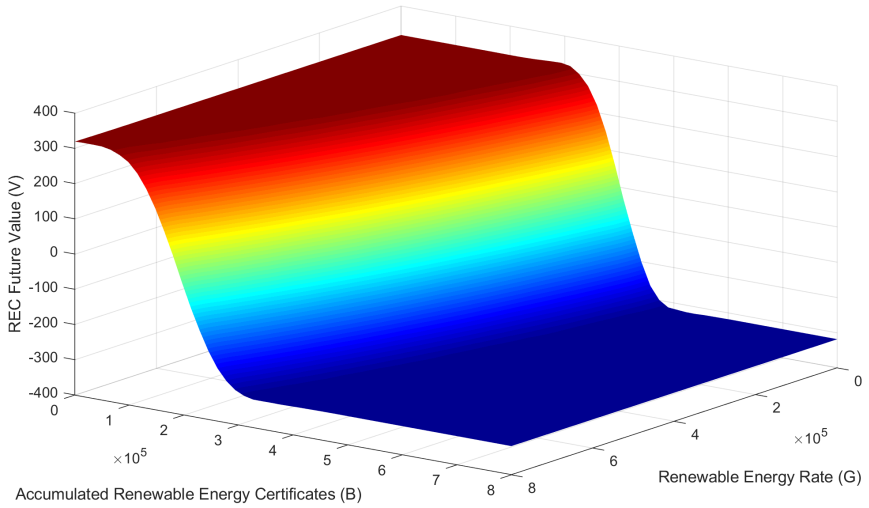

Figure 4.19: Second numerical method: REC future contract price surface at $t = T - 1/3$.

the same as the one for the computation of the REC call and put options prices at the same time $t = T - 1/3$.

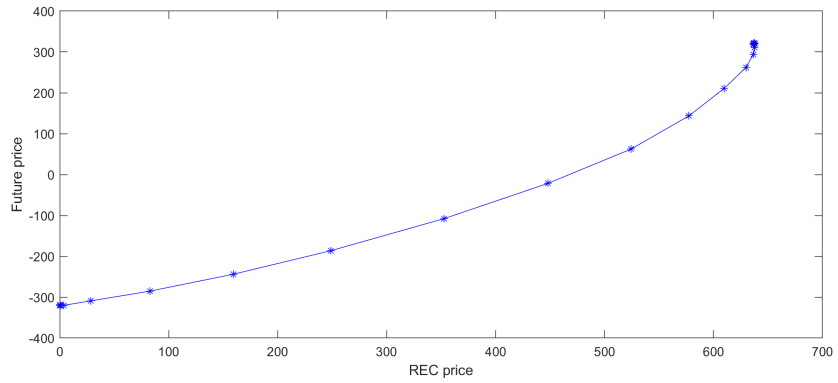

Figure 4.20: Second numerical method: REC future contract price versus REC price at time $t = T - 1/3$.

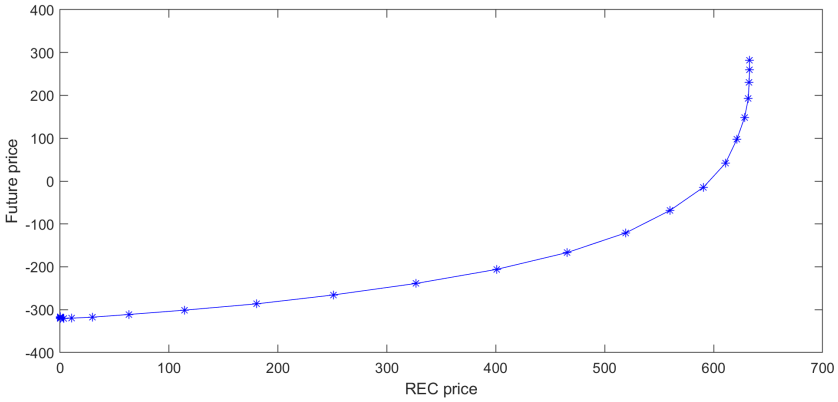

Figure 4.21: Second numerical method: REC future contract price versus REC price at time $t = T - 2/3$.

Conclusions

The objective of this research work has been the contribution to the modelling, mathematical analysis and numerical solution of pricing problems related to renewable energy certificates (RECs) and some financial derivatives on them.

After the comprehensive study of these specific financial products, which are traded in energy markets, the proposed mathematical models for their valuation are posed in terms of partial differential equations (PDEs), either nonlinear or linear. Also mathematical tools from the domain of stochastic calculus and forward and backward stochastic differential equations are required to build the models. Thus, the statement of the models is one of the achievements of this work.

Once the PDE models are posed for the different financial products, in some cases the mathematical analysis allows to obtain the existence of solution for the PDE problem. More precisely, in the case of European style derivatives on RECs, the model can be formulated in terms of a final value problem associated to a linear Kolmogorov PDE, with one of the coefficients depending on the value of the REC which is assumed to be a given function with appropriate properties to obtain the existence of solution. For this purpose, mainly a probabilistic approach based on previous results in the literature has to be used, because alternative approaches based on sub and supersolutions would require the analytical expression of the coefficients, that is not available due to their dependence on the value of the REC. Therefore, the existence of solution for the derivatives pricing model is another relevant achievement of this work. On the other hand, the existence of solution for the nonlinear PDE problem that models the pricing of the REC is an open problem, that can be addressed

in a future research.

Another relevant point in this thesis concerns to the effective numerical solution of the different pricing problems. In the pricing of RECs, the main difficulty comes from the nonlinear convection term due to the dependence of the drift term on the unknown of the problem. Concerning this issue, one of the main novelties of the thesis is the original treatment of this nonlinear term in a implicit form. More precisely, an appropriate maximal monotone operator is introduced to formulate the nonlinear problem. In this way, the nonlinear convection term can be treated by means of a duality algorithm proposed by Bermúdez and Moreno, which is based on the Yosida approximation of maximal monotone operators. After a linearization procedure based on this duality method, the resulting linear PDE is degenerate due to the lack of diffusion term in one of the spatial directions. Understanding this degeneration as a limit case of convection dominating diffusion case, we propose two alternative numerical methods for the full discretization of the nonlinear problem. The first one is based on a semi-Lagrangian (also known as characteristics) scheme in the direction without diffusion, combined with suitable finite differences schemes for the spatial discretization. The second numerical combines a characteristics-Crank Nicolson scheme for time discretization with a finite elements method for spatial discretization. Both methods have already been proposed in the literature for other related problems arising in quantitative finance. Numerical results obtained in an academic problem with analytical solution, that has been used as sanity check, illustrate the performance of the sets of methods. Next, the consideration of a real REC pricing problem is addressed, so that comparison of methods as well as the performance of the methods and models can be validated. Therefore, the numerical solution of a nonlinear PDE model for the pricing of REC with appropriate numerical methods is an important achievement of this thesis.

Next, taking into account that the model for pricing European derivatives on RECs is based on a linear PDE after previously computing the values of RECs, some parts of the numerical methodology used for RECs pricing is applied to the pricing of

REC derivatives. More precisely, examples concerning to European vanilla call and put options, as well as a futures contract are considered. Therefore, the numerical solution of the pricing problems for this derivatives is another achievement of this work.

The work developed in this thesis also opens the possibility of future work on different lines. For example, as we mentioned before, the mathematical analysis for the existence and uniqueness of solution of the nonlinear PDE problem for pricing RECS seems one interesting challenge. Related to this future target, also the existence and uniqueness of solution of the associated FBSDE would require attention, the difference with respect to to the analogous FBSDE appearing in emission markets being the fully coupling of the three SDEs involved in the case of RECs, which makes the problem much more difficult. Other lines of interesting future research are related to the consideration of more complex derivatives on RECs. For example, the consideration of American options on RECs or other more complex (exotic) derivatives traded on the markets could be addressed on the basis of the research and achievements developed in the present thesis work.

Resumen extenso

En esta tesis se estudia la valoración de unos productos financieros específicos que se negocian en los mercados de energía. En concreto, en primer lugar se aborda el modelado matemático, el análisis y la resolución numérica del problema de valoración de certificados de energía renovable. A continuación, se estudian los productos financieros derivados que tiene a los certificados de energía renovable como activo subyacente. Entre ellos, nos centraremos en algunos ejemplos de valoración de opciones europeas y contratos de futuros.

Con objeto de contextualizar el problema de valoración de derivados financieros cuyos subyacentes son los certificados de energía renovable, en la memoria realizamos una breve revisión de diferentes mercados de energía. Dentro de los mercados energéticos, destaca el mercado de la electricidad. Los precios de la electricidad se determinan mediante el principio de la oferta y la demanda. Esta ausencia de regularización afecta a los precios incrementando su volatilidad e introduciendo incertidumbre. Debido a ello, las empresas participantes en este tipo de mercados necesitan productos financieros que les protejan frente a los precios altos de la electricidad, pero también que les den la posibilidad de obtener beneficios cuando los precios sean bajos. Asimismo, deben protegerlos frente a posibles escenarios de alta volatilidad. En la literatura, se han estudiado diferentes productos con estos objetivos. Uno ejemplo de esos productos son las *opciones swing*, que han sido estudiadas y valoradas en [15] utilizando dos factores estocásticos.

Con el objetivo marcado de intentar lograr cero emisiones, se han establecido diferentes mecanismos para reducir las mismas. Mediante el protocolo de Kyoto en el

año 1997, se establecieron los tres primeros mecanismos. En Europa se implementó el denominado sistema "cap-and-trade", mediante el cual se establece un límite de emisiones de CO_2 durante un periodo de cumplimiento determinado. Cada compañía recibe al inicio de dicho periodo una cantidad de certificados de emisiones, que se determina en relación a dicho límite, equivalente cada uno de ellos a una tonelada de CO_2 emitida. Estos certificados pueden ser utilizados para compensar las emisiones al final del periodo. Durante el período de cumplimiento, los derechos de emisión se negocian activamente y esto conduce a la formación del precio del certificado.

Debido a la relación existente entre la producción de electricidad y las emisiones de CO_2, el uso de ciertas energías renovables para la producción de electricidad está siendo fuertemente considerada por los responsables políticos. Sin embargo, en ocasiones, algunas energías renovables aún no son competitivas. Para favorecer el desarrollo y uso de este tipo de renovables, se han desarrollado instrumentos o mecanismos que favorecen la generación de electricidad mediante un tipo concreto de renovable. Por ejemplo, en el mercado de energía solar de New Jersey se comercializan los certificados de energía renovable conocidos como SRECs (por sus siglas en inglés, Solar Renewable Energy Certificate), que han sido estudiados en [26].

De manera general, los certificados de energía renovable están siendo utilizados para establecer políticas de protección del medio ambiente fomentando el desarrollo de la energía sostenible. Entre sus beneficios destacan los siguientes:

- Ayudan a luchar contra el cambio climático y a reducir el coste de las energías renovables.
- Son un instrumento para que las empresas puedan demostrar su liderazgo en el desarrollo sostenible y en la reducción de la huella de carbono.
- Ayudan a cumplir con los objetivos establecidos en los reglamentos ambientales por parte de las entidades gubernamentales.
- Suponen una fuente de ingresos añadida a la venta de la electricidad para los productores de energía renovable.

- Generan oportunidades para que las empresas amplíen su cartera de productos de energía verde en zonas donde aún no se han realizado inversiones en fuentes de energía renovable.

Teniendo en cuenta lo anterior, este tipo de certificados constituyen una herramienta clave para garantizar que se produce la mayor cantidad de energía mediante renovables, por lo que su presencia en los últimos años ha ido en aumento. Cada REC (por sus siglas en inglés, Renewable Energy Certificate), corresponde a un volumen específico de electricidad, equivalente a 1 MWh generado con una fuente renovable y vertida a la red eléctrica. Cuando una compañía eléctrica genera una cantidad de energía, recibe a cambio certificados que puede sacar al mercado o transferir a otros organismos e instituciones.

Muchos países requieren que las empresas de energía compren o generen energía renovable, como por ejemplo solar o eólica. Para ello, se establece un estándar de cartera renovable (RPS) (Renewable Portfolio Standard en inglés) en el que se requiere que cierta cantidad de energía renovable sea creada cada año. De este modo, se impulsan los intercambios de certificados de energía renovable (REC). Por ejemplo, una compañía eléctrica puede comprar estos certificados al propietario para cumplir con el requisito de energía renovable que le impone el estado.

Estos certificados se pueden vender, intercambiar o canjear, y el propietario del REC puede afirmar que ha comprado energía renovable. Si bien los programas convencionales de comercio de emisiones de carbono utilizan sanciones e incentivos para alcanzar los objetivos de emisiones establecidos, los REC simplemente incentivan la energía renovable sin emisiones de carbono, al proporcionar un subsidio a la producción de electricidad a partir de fuentes renovables.

En los primeros capítulos de la tesis, se estudia la valoración de RECs. De manera análoga a los modelos planteados para la valoración de instrumentos financieros en los mercados de emisiones en [20] y [37], planteamos el valor de dicho REC como la solución de un sistema acoplado de ecuaciones diferenciales estocásticas hacia adelante y hacia atras ("forward-backward" en inglés y con siglas FBSDE). Concretamente, se

considera que un REC depende de dos factores: la tasa de generación de renovables y el número de certificados acumulados, asumiendo que la dinámica de estos factores es estocástica. Así, se plantea una ecuación diferencial estocástica hacia adelante para la evolución de la tasa de generación de renovables, y una ecuación diferencial estocástica hacia atrás para la evolución del número de certificados acumulados. En particular, la tasa de generación está gobernada por un proceso Ornstein-Uhlenbeck (OU) y está influenciada por las condiciones climatológicas.

Los certificados de energía renovable tienen unos años de vida, entendidos éstos como el número de años desde la emisión de los certificados, durante los cuales el REC es válido para alcanzar uno o varios requerimientos. Así, estudiamos certificados de un único periodo o de varios periodos de cumplimiento. Al llegar a la fecha de cumplimiento, si dicho requerimiento no es alcanzado deberá pagarse una multa o penalización establecida en la emisión de dicho REC.

Asumiendo la existencia de solución de la FBSDE y aplicando el lema de Itô, deducimos la siguiente ecuación en derivadas parciales (EDP) no lineal para obtener el valor del REC:

$$\mathcal{L}_1[P] = \frac{\partial P}{\partial t} + \frac{1}{2}\sigma_g^2 \frac{\partial^2 P}{\partial \widetilde{G}^2} + \alpha_g \left(f(t) + \frac{\beta_g}{\alpha_g} P - \widetilde{G} \right) \frac{\partial P}{\partial \widetilde{G}} + \exp(\widetilde{G}) \frac{\partial P}{\partial B} - rP = 0,$$

que, junto con el valor del REC en su fecha de vencimiento, define el problema de valor final que debemos resolver.

En cuanto a la solución numérica del problema de valor final asociado a dicha EDP no lineal, nos encontramos ante varias dificultades para las que proponemos las metodologías adecuadas. En primer lugar, dado que el planteamiento del problema se hace sobre un dominio no acotado en las variables espaciales, se realiza un truncamiento del dominio y se proponen las condiciones de contorno más apropiadas desde el punto de vista financiero y matemático para resolver el problema en dicho dominio, como en [40]. La segunda dificultad surge de la presencia del término convectivo no lineal de la EDP. Una novedad de esta tesis es tratar esta no linealidad mediante el algoritmo de dualidad de Bermúdez-Moreno propuesto en [8]. Mediante este algoritmo, basado en la aproximación de un operador maximal

monótono adecuado, obtenemos un problema linealizado tras aplicar un algorimo de punto fijo, que discretizamos mediante dos métodos numéricos diferentes. Por un lado, se propone un esquema semi-Lagrangiano en tiempo en una de las direcciones, combinado con métodos de diferencias finitas. Por otro lado, se considera un método de Lagrange-Galerkin, basado en un esquema de características Crank-Nicolson en tiempo combinado con elementos finitos en las variables espaciales. El sistema de ecuaciones lineales que se obtiene en cada paso de tiempo e iteración de punto fijo, se ha resuelto mediante el clásico algoritmo de Thomas para matrices tridiagonales por bloques. Tras el análisis realizado a los ejemplos numéricos que presentamos, los conjuntos de métodos numéricos resultan adecuados para la valoración de RECs.

Una vez que obtenemos el valor del certificado, planteamos un modelo para la valoración de derivados finacieros cuyo subyacente es un REC. De manera general, un derivado financiero es un contrato cuyo valor depende de uno o más activos, denominados activos subyacentes. Normalmente, el activo subyacente es una acción (o capital), un tipo de intercambio de divisas, el precio de mercado de las materias primas (como el petróleo o el trigo), un crédito/bono (tipo de interés) u otra variable. Un derivado se negocia entre dos partes, a las que se hace referencia como contrapartes. Estas contrapartes están sujetas a un conjunto de términos y condiciones previamente acordados en el contrato de derivados, que determinan sus derechos y obligaciones. El precio del derivado es la prima que el comprador del derivado debe pagar para obtener los derechos garantizados por el contrato. En general, las dos principales razones para utilizar derivados financieros son la cobertura del riesgo y la especulación.

Existen varios tipos de derivados dependiendo del tipo de flujos de pago del contrato entre las contrapartes. Los tipos más comunes de derivados son las opciones, futuros/forwards y swaps. Teniendo en cuenta que en esta tesis se considera la valoración de opciones y futuros, se presentan brevemente dichos derivados. En particular, una opción es un contrato que otorga el derecho (pero no la obligación) a su tenedor de comprar (*call*) o vender (*put*) alguna cantidad del activo subyacente en una fecha futura, por un precio acordado. Dependiendo del momento en que se

ejerza el derecho a comprar o vender, las opciones se denominan opciones europeas o americanas. Una opción se denomina *europea* si el derecho a comprar o vender puede ser ejercido solamente en la fecha de vencimiento, y se conoce como *americana* si puede ejercerse en cualquier instante anterior al vencimiento. Cuando la función de pago a vencimiento de una opción, call o put, depende del valor de los activos subyacentes a vencimiento, se dice que es una opción de tipo vainilla. Existen otros tipos de opciones, normalmente conocidos como *exóticas*, cuya estructura es más compleja que las vainilla.

Además de las opciones, existen otros derivados, como por ejemplo los *contratos a plazo* o *contratos forward*. Un *contrato a plazo* es un acuerdo entre dos partes mediante el cual se obliga a las partes contratantes a comprar o vender un activo específico por un precio específico, conocido como *precio a plazo* o *precio forward*, en una fecha específica en el futuro, la fecha de vencimiento. Este contrato tiene similitudes con los contratos de opciones considerando el precio forward como el precio de ejercicio. Sin embargo, los contratos a plazo son diferentes de los contratos de opciones en que el dinero no cambia de manos hasta la fecha de vencimiento. Otra diferencia con las opciones es que su precio se estable de antemano. Un *contrato de futuros* es en esencia un contrato a plazo, pero con algunas diferencias. Mientras que un contrato a plazo puede establecerse entre dos partes, en los futuros generalmente se negocia un intercambio que especificará ciertas características estándar del contrato, como la fecha de vencimiento y el precio del contrato. A pesar de estas diferencias, se puede demostrar que bajo algunos supuestos no demasiado restrictivos, el precio de futuros es casi el mismo que el precio a plazo. Cuando las tasas de interés son predecibles, los dos coinciden exactamente.

Tanto en el problema de la valoración de las opciones europeas como en el caso de los contratos de futuros, y en el de un derivado general sobre certificados de energías renovables, suponemos que el precio del producto derivado depende de los mismos factores estocásticos que el precio del REC. No obstante, al asumir que el precio del REC es conocido a la hora de valorar el derivado, la metodología desarrollada da

lugar a una ecuación en derivadas parciales lineal. Para el problema de valor final asociado a la EDP lineal que modela la valoración de un derivado sobre un REC, se ha realizado el análisis matemático del modelo estudiando la existencia de solución. Una vez probada la existencia de solución para el modelo basado en la EDP lineal, se proponen los dos métodos numéricos utilizados en la discretización del problema lineal que surge en cada etapa del punto fijo de la resolución numérica del problema de EDP no lineal de valoración del REC. A continuación, se plantean los casos de las opciones europeas y contratos de futuros, como ejemplos de valoración de derivados. Una vez aplicados los métodos numéricos propuestos a dichos casos, los resultados obtenidos muestran el comportamiento esperado, tanto para el valor de la opciones como para el contrato de futuros.

El esquema de esta memoria es la siguiente:

En el Capítulo 1, se presentan unas ideas básicas sobre los mercados de energía para poner en contexto la relevancia que están adquiriendo este tipo de mercados, así como los productos financieros relacionados con ellos, en la actualidad. Así, se describen las características principales del mercado eléctrico y de emisiones, y la relación de éstos con la aparición de los mercados de energía renovable junto con sus características.

En el Capítulo 2, se plantea el modelo para valorar certificados de energía renovable (REC). Para ello, al inicio del capítulo, se presenta un sistema de ecuaciones diferenciales estocásticas de tipo forward-backward (FBSDE) con los dos factores estocásticos que gobierna la dinámica del precio del REC. A continuación, se obtiene la ecuación en derivadas parciales (EDP) no lineal correspondiente. La existencia de solución del problema asociado a la EDP no lineal es un problema abierto.

El Capítulo 3 describe los métodos numéricos utilizados para la resolución del problema de valor final asociado a la EDP no lineal planteado en el Capítulo 2. Este capítulo comienza con el tratamiento del término convectivo no lineal de la EDP obtenida en el Capítulo, mediante un algoritmo de dualidad de tipo Bermúdez-Moreno. Como el problema se plantea inicialmente sobre un dominio no

acotado, es necesario truncarlo a un dominio acotado para abordar la resolución numérica. A continuación, se proponen y describen dos métodos numéricos para la resolución del problema de EDP lineal obtenido tras la aplicación de una técnica de punto fijo para el problema no lineal resultante del método de dualidad. El capítulo termina con dos ejemplos, utilizando y comparando los métodos numéricos propuestos en un test académico con solución analítica y en un caso real.

En el Capítulo 4 establecemos el modelo matemático que gobierna la valoración de derivados financieros cuyo subyacente es un REC y proponemos los métodos numéricos para la resolución del modelo. El esquema de la primera parte del capítulo es similar al del Capítulo 2. La principal novedad respecto a éste es que se analiza la existencia de solución del problema de valor final asociado a una EDP lineal que se plantea para la valoración de un derivado sobre un REC. En la segunda parte del capítulo, se plantean y describen las técnicas numéricas apropiados para obtener una solución numérica de dicho problema. Las técnicas numéricas utilizadas son similares a la introducidas en el Capítulo 3. Por último, presentamos los modelos numéricos y algunos resultados obtenidos en la valoración de opciones europeas y contratos de futuros.

Los métodos y algoritmos propuestos se han implementado en Matlab y Fortran. Los distintos tests realizados muestran el acertado ajuste de ambos métodos en la valoración del precio de los certificados de energía renovable, así como de las opciones europeas y contratos de futuros basados en dichos certificados.

Resumo extenso

Nesta tese estúdase a valoración duns derivados financeiros concretos que se negocian nos mercados de enerxía. De xeito preciso, en primeiro lugar abórdase a modelaxe matemática, a análise e a resolución numérica do problema de valoración de certificados de enerxía renovable. A continuación, estúdanse os productos financeiros derivados que teñen aos certificados de enerxía renovable coma activo subxacente. Entre eles, centrarémonos nalgúns exemplos de valoración de opcións europeas e contratos de futuros.

Co obxecto de contextualizar o problema de valoración de derivados financeiros que teñen coma subxacentes os certificados de enerxía renovable, na memoria realizamos unha pequena revisión de diferentes mercados de enerxía. Dentro dos mercados enerxéticos, destaca o mercado da electricidade. Os prezos da electricidade son determinados baixo o principio da oferta e a demanda. Esta falla de regularización atinxe aos prezos acrecentando a súa volatilidade e introducindo incerteza. Debido a elo, as empresas participantes neste tipo de mercados necesitan produtos financeiros que lles protexan frente aos prezos altos da electricidade pero tamén que lles den a posibilidade de obter beneficios cando os prezos sexan baixos. Na literatura, lévanse estudados ata agora diferentes produtos con estes obxectivos. Un exemplo deses produtos son as *opcións swing*, que foron estudadas e valoradas en [15] empregando dous factores estocásticos.

Co marcado obxectivo de procurar acadar cero emisións, establecéronse diferentes mecanismos para reducir as mesmas. Mediante o protocolo de Kyoto no ano 1997, establecéronse os tres primeiros mecanismos. En Europa implementouse o

denominado sistema "cap-and-trade", mediante o cal establécese un límite de emisións de CO_2 durante un periodo de cumprimento determinado. Cada compañía recibe ao inicio de dito periodo unha cantidade de certificados de emisións, que se determina en relación a dito límite, equivalente cada un deles a unha tonelada de CO_2 emitida. Estos certificados poden ser empregados para compensar as emisións ao final do periodo. Durante o periodo de cumprimento, os dereitos de emisión negócianse activamente e esto conduce á formación do prezo do certificado.

Debido á relación existente entre a produción de electricidade e as emisións de CO_2, o emprego de certas renovables para a produción da electricidade está sendo fortemente considerada polos responsables políticos. Porén, en ocasións, algunhas renovables aínda non son competitivas. Para favorecer o desenvolvemento e emprego deste tipo de renovables, desenvolvéronse instrumentos que benefician a xeración de electricidade mediante un tipo específico de renovable. Por exemplo, no mercado de enerxía solar de New Jersey comercialízanse os certificados de enerxía renovable coñecidos como SRECs (polas súas siglas en inglés, Solar Renewable Energy Certificate), que foron estudados en [26].

De maneira xeral, os certificados de enerxía renovable están a ser empregados para establecer políticas de protección do medio ambiente favorecendo o desenvolvemento da enerxía sostible. Entre os seus beneficios destacan os seguintes:

- Axudan a loitar contra o cambio climático e a reducir o coste das enerxías renovables.

- Son unha ferramenta para que as empresas poidan demostrar o seu liderado no desenvolvemento sostible e na redución da pegada de carbono.

- Axudan a cumprir cos obxectivos establecidos nos reglamentos ambientais por parte das entidades gubernamentais.

- Supoñen unha fonte de ingresos engadida á venda da electricidade para os produtores de enerxía renovable.

- Xeran oportunidades para que as empresas amplíen a súa carteira de produtos de enerxía verde en zonas onde aínda non se realizaron inversións en fontes de enerxía renovable.

Tendo en conta o anterior, este tipo de certificados constitúen unha ferramenta chave para garantir que se produce a maior cantidade de enerxía mediante renovable, polo que a súa presenza nos últimos anos foise incrementando. Cada REC (polas súas siglas en inglés, Renewable Energy Certificate), corresponde a un volume específico de electricidade, equivalente a 1 MWh xerado cunha fonte renovable e vertida á rede eléctrica. Cando unha compañía eléctrica xera unha cantidade de enerxía, recibe a cambio certificados que poden sacar ao mercado ou transferir a outros organismos e institucións.

Moitos países requiren que as empresas de enerxía merquen ou xeren enerxía renovable, como por exemplo solar ou eólica. Para elo, establécese un estándar de carteira renovable (RPS) (Renewabel Portfolio Standard en inglés) no que se require que certa cantidade de enerxía renovable sexa creada cada ano. Deste xeito, impúlsanse os intercambios de certificados de enerxía renovable. Por exemplo, unha compañía eléctrica pode mercar estos certificados ao dono para cumprir co requisito de enerxía renovable que lle impón o estado.

Estos certificados pódense vender, intercambiar ou trocar, e o dono do REC pode afirmar que mercou enerxía renovable. Se ben os programas convencionais de comercio de emisións de carbono empregan sancións e incentivos para acadar os obxectivos de emisións establecidos, os REC simplemente incentivan a enerxía renovable sen emisións de carbono, ao proporcionar un subsidio á produción de electricidade a partir de fontes renovables.

Nos primeiros capítulos da tese, estúdase a valoración de RECs. De xeito análogo aos modelos formulados para a valoración de instrumentos financeiros nos mercados de emisións en [20] e [37], formulamos o valor de dito REC coma a solución dun sistema acoplado de ecuacións diferenciais estocásticas hacia adiante e hacia atrás ("forward-backward" en inglés e con siglas FBSDE). Concretamente, considérase que

un REC depende de dous factores: a taxa de xeración de renovables e o número de certificados acumulados, asumindo que a dinámica destes factores é estocástica. Así, formúlase unha ecuación diferencial estocástica hacia adiante para a evolución da taxa de xeración de renovables, e unha ecuación diferencial estocástica hacia atrás para a evolución do número de certificados acumulados. En concreto, a taxa de xeración está gobernada por un proceso Ornstein-Uhlenbeck (OU) e está influenciada polas condicións climatolóxicas.

Estos certificados de enerxía renovable teñen uns anos de vida, entendidos éstos coma o número de anos dende a emisión dos certificados, durante os cales o REC é válido para acadar un ou varios requerimentos. Así, estudamos certificados dun único periodo ou de varios periodos de cumprimento. Ao chegar á data de cumprimento, se dito requerimento non é acadado deberá pagarse unha multa ou penalización establecida na emisión de dito REC.

Asumindo a existencia de solución da FBSDE e aplicando o lema de Itô, deducimos a seguinte ecuación en derivadas parciais (EDP) non lineal para obter o valor do REC:

$$\mathcal{L}_1[P] = \frac{\partial P}{\partial t} + \frac{1}{2}\sigma_g^2 \frac{\partial^2 P}{\partial \widetilde{G}^2} + \alpha_g \left(f(t) + \frac{\beta_g}{\alpha_g} P - \widetilde{G} \right) \frac{\partial P}{\partial \widetilde{G}} + \exp(\widetilde{G}) \frac{\partial P}{\partial B} - rP = 0,$$

que, xunto co valor do REC na súa data de vencemento, define o problema de valor final que temos que resolver.

En canto á solución numérica do problema de valor final asociado a dita EDP non lineal, atopámonos ante diferentes dificultades para as que propoñemos as metodoloxías axeitadas. En primeiro lugar, dado que a formulación do problema faise sobre un dominio non acotado nas variables espaciais, realízase un truncamento do dominio e propóñense as condicións de contorno máis axeitadas dende o punto de vista financeiro e matemático para resolver o problema en dito dominio, coma en [40]. A segunda dificultade xurde da presenza do término convectivo non lineal da EDP. A novidade desta tese é tratar esta non linealidade mediante o algoritmo de dualidade de Bermúdez-Moreno proposto en [8]. Mediante este algoritmo, baseado na aproximación dun operador maximal monótono axeitado, obtemos un problema linealizado tras empregar un algoritmo de punto fixo, que discretizamos mediante dous métodos

numéricos diferentes. Por un lado, propónse un esquema semi-Lagrange en tempo nunha das direccións, conxugado con métodos de diferenzas finitas. Por outro lado, considérase un método de Lagrange-Galerkin, baseado nun esquema de características Crank-Nicolson en tempo conxugado con elementos finitos nas variables espaciais. O sistema de ecuacións lineais que se obtén en cada paso de tempo e iteración de punto fixo, resólvese mediante o clásico algoritmo de Thomas para matrices tridiagonais por bloques. Tras a análise realizada aos exemplos numéricos que amosamos, os conxuntos de métodos númericos resultan axeitados para a valoración de RECs.

Unha vez que obtemos o valor do certificado, formulamos o modelo para a valoración de derivados financeiros que teñen coma subxacente un REC. Normalmente, un derivado financeiro é un contrato que ten un valor que depende dun ou máis activos denominados activos subxacentes. Polo xeral, o activo subxacente é unha acción (ou capital), un tipo de intercambio de divisas, o prezo de mercado das materias primas (como o petróleo ou o trigo), un crédito/bono (tipo de xuro) ou outra variable. Un derivado negóciase entre dúas partes, ás que se fai referencia coma contrapartes. Estas contrapartes están suxeitas a un conxunto de términos e condicións previamente acordados no contrato de derivados, que determinan os seus dereitos e obligacións. O prezo do derivado é a prima que o comprador do derivado debe pagar para obter os dereitos garantizados polo contrato. En xeral, as dúas principais razóns para utilizar derivados financeiros son a cobertura do risco e a especulación.

Existen varios tipos de derivados dependendo do tipo de fluxos de pago do contrato entre as contrapartes. Os tipos mais comúns de derivados son as opcións, futuros/forwards e swaps. Tendo en conta que nesta tese considérase a valoración de opcións e futuros, preséntanse brevemente ditos derivados. En concreto, unha opción é un contrato que outorga o dereito (pero non a obriga) ao seu posuidor de mercar (*call*) ou vender (*put*) algunha cantidade do activo subxacente nunha data futura, por un prezo acordado. Dependendo do momento no que se exerza o dereito de mercar ou vender, as opcións denomínanse opcións europeas ou americanas. Unha opción

denomínase *europea* se o dereito a mercar ou vender pode ser exercido soamente na data de vencemento, e se coñece coma *americana* se pode exercerse en calquera instante anterior ao vencemento. Cando a función de pago a vencemento dunha opción, call ou put, depende do valor dos activos subxacentes a vencemento, dícese que é unha opción tipo vainilla. Existen outros tipos de opcións, normalmente coñecidos como *exóticas*, que teñen unha estructura máis complexa que as vainilla.

Amais das opcións, existen outros derivados como por exemplo os *contratos a prazo* ou *contratos forward*. Un *contrato a prazo* é un acordo entre dúas partes mediante o cal obrígase ás partes contratantes a mercar ou vender un activo específico por un prezo específico, coñecido como *prezo a prazo* ou *prezo forward*, nuna data concreta no futuro, a data de vencemento. Este contrato ten similitudes cos contratos de opcións considerando o prezo forward como o prezo de exercicio. Porén, os contratos a prazo son diferentes dos contratos de opcións no que o diñeiro non cambia de mans ata a data de vencemento. Outra diferenza coas opcións é que o seu prezo establécese de antemán. Un *contrato de futuros* é en esencia un contrato a prazo, pero con algunhas diferenzas. Namentres un contrato a prazo pode establecerse entre dúas partes, nos futuros xeralmente negóciase un intercambio que especificará certas características estándar do contrato, como a data de vencemento e o prezo do contrato. Malia estas diferenzas, pódese demostrar que baixo algúns supostos non demasiado restritivos, o prezo de futuros é case o mesmo que o prezo a prazo. Cando as taxas de xuro son previsibles, os dous concordan exactamente.

Tanto no problema da valoración do prezo das opcións europeas coma no caso dos contratos de futuros, e no dun derivado xeral sobre certificados de enerxías renovables, supoñemos que o prezo do produto derivado depende dos mesmos factores estocásticos que o prezo do REC. Non obstante, ao asumir que o prezo do REC é coñecido á hora de valorar o derivado, a metodoloxía desenvolvida da lugar a unha ecuación en derivadas parciais lineal. Para o problema de valor final asociado á EDP lineal que modela a valoración dun derivado sobre un REC, realizouse a análise matemática do modelo estudando a súa existencia de solución. Unha vez probada a existencia de

solución para o modelo baseado na EDP lineal, propóñense os dous métodos numéricos empregados na discretización do problema lineal que xurde en cada etapa do punto fixo da resolución numérica do problema de EDP non lineal de valoraión do REC. A continuación, formúlanse os casos das opcións europeas e contratos de futuros, coma exemplos de valoración de derivados. Unha vez empregados os métodos numéricos propostos a ditos casos, os resultados obtidos mostran o comportamento esperado, tanto para o valor das opcións coma para o contrato de futuros.

O esquema desta memoria é o siguiente:

No Capítulo 1, preséntanse unhas ideas elementais sobre os mercados de enerxía para pór en contexto a relevancia que están adquirindo este tipo de mercados, así coma os produtos financeiros relacionados con eles, na actualidade. Así, descríbense as características principais do mercado eléctrico e de emisións, e a relación destes coa aparición dos mercados de enerxía renovable xunto coas súas características.

No Capítulo 2, formúlase o modelo para valorar certificados de enerxía renovable (REC). Para elo, ao inicio do capítulo, preséntase un sistema de ecuacións diferenciais estocásticas de tipo forward-backward (FBSDE) cos dous factores estocásticos que goberna a dinámica do prezo do REC. A continuación, obtense a ecuación en derivadas parciais (EDP) non lineal correspondente. A existencia de solución do problema asociado á EDP non lineal é un problema aberto.

O Capítulo 3 describe os métodos numéricos empregados para a resolución do problema de valor final asociado á EDP non lineal formulado no Capítulo 2. Este capítulo comeza co tratamento do término convectivo non lineal da EDP obtida no Capítulo 2, mediante un algoritmo de dualidade de tipo Bermúdez-Moreno. Coma o problema formúlase inicialmente sobre un dominio non acotado, é preciso truncalo a un dominio acotado para abordar a súa resolución numérica. A continuación, propóñense e descríbense dous métodos numéricos para a resolución do problema de EDP lineal obtido tras a aplicación dunha técnica de punto fixo para o problema non lineal resultante do método de dualidade. O capítulo finaliza con dous exemplos, empregando e comparando os métodos numéricos propostos nun test académico con

solución analítica e un caso real.

No Capítulo 4 establecemos o modelo matemático que goberna a valoración de derivados financeiros que teñen coma subxacente un REC e propoñemos os métodos numéricos para a resolución do modelo. O esquema da primeira parte do capítulo é semellante ao do Capítulo 2. A principal novidade respecto a éste é que se analiza a existencia de solución do problema de valor final asociado a unha EDP lineal que se formula para a valoración dun derivado sobre un REC. Na segunda parte do capítulo, formúlanse e descríbense as técnicas numéricas axeitadas para obter unha solución numérica de dito problema. As técnicas numéricas empregadas son semellantes ás introducidas no Capítulo 3. Por último, presentamos os modelos numéricos e algúns resultados obtidos na valoración de opcións europeas e contratos de futuros.

Os métodos e algoritmos propostos implementáronse en Matlab e Fortran. Os distintos tests realizados mostran o axeitado axuste de ámbolos dous métodos na valoración do prezo dos certificados de enerxía renovable, así coma das opcións europeas e contratos de futuros baseados en ditos certificados.

Bibliography

[1] I. Arregui, J. J. Cendán, C. Parés, C. Vázquez, Numerical simulation of a 1-d elastohydrodynamic problem in magnetic storage devices, ESAIM Mathematical Modelling and Numerical Analysis, 42 (2008), 645-665.

[2] I. Arregui, J. J. Cendán, C. Vázquez, A duality method for the compressible Reynolds equation. Application to the simulation of read-write processes in magnetic reading devices, Journal of Computational and Applied Mathematics, 175 (2005), 31-40.

[3] I. Arregui, J. J. Cendán, C. Vázquez, Adaptative numerical methods for an hydrodynamic problem arising in magnetic reading devices, Mathematics and Computers in Simulation, 99 (2014), 190-202.

[4] M. A. Baamonde-Seoane, M. C. Calvo-Garrido, M. Coulon, C. Vázquez, Numerical solution of a nonlinear PDE model for pricing Renewable Energy Certificates (RECs), Applied Mathematics and Computation, 404 (2021), 126199.

[5] E. Barucci, S. Polidoro, V. Vespri, Some results on partial differential equations and asian options, Mathematical Models and Methods in Applied Sciences, 11 (03) (2011).

[6] F. E. Benth, M. Eriksson, S. Westgaard, Optimal management of green certificates in the Swedish-Norwegian market, Journal of Energy Markets, 10 (2017), 1-39.

[7] M. Bercovier, O. Pironneau, and V. Sastri, Finite elements and characteristics for some parabolic-hyperbolic problems, Applied Mathematical Modelling, 7 (1983), pp. 89-96.

[8] A. Bermúdez, C. Moreno, Duality methods for solving variational inequalities, Computers & Mathematics with Applications, 7 (1981), 43-58.

[9] A. Bermúdez, M. R. Nogueiras and C. Vázquez, Numerical analysis of convection-diffusion-reaction problems with higher order characteristics finite elements. Part I: Time discretization, SIAM Journal on Numerical Analysis, 44 (2006), 1829–1853.

[10] A. Bermúdez, M. R. Nogueiras and C. Vázquez, Numerical analysis of convection-diffusion-reaction problems with higher order characteristics finite elements. Part II: Fully discretized scheme and quadrature formulas, SIAM Journal on Numerical Analysis, 44 (2006), 1854–1876.

[11] A. Bermúdez, M.R. Nogueiras, C. Vázquez, Numerical solution of variational inequalities for pricing Asian options with high order Lagrange-Galerkin methods, Applied Numerical Mathematics, 56 (2006), 1256-1270.

[12] F. Black, M. Scholes, The pricing of options and corporate liabilities, Journal of Political Economy,81 (1973), 637-654.

[13] H. Brézis, Analyse Fonctionelle, Masson, Paris, 1983.

[14] M. Burguer, B. Graeber, G. Schindlmayr, Managing Energy Risk: An Integrated View on Power and Other Energy Markets, Wiley Finance (2007), Chichester.

[15] M. C. Calvo-Garrido, M. Ehrhardt, C. Vázquez, Pricing swing options in electricity markets with two stochastic factors using a partial differential equation approach, The Journal of Computational Finance, 20 (2017), 81-107.

[16] M. C. Calvo-Garrido, M. Ehrhardt, C. Vázquez, Jump-diffusion models with two stochastic factors for pricing swing options in electricity markets with partial-integro differential equations, Applied Numerical Mathematics, 139 (2019), 77-92.

[17] R. Carmona, F. Fehr, J. Hinz, Optimal stochastic control and carbon price formation, SIAM Journal on Control and Optimization 48 (4) (2009), 2168-2190.

[18] R. Carmona, F. Fehr, J. Hinz, A. Porchet, Market designs for emissions trading schemes, SIAM Rev. 52(3) (2010), 403-452.

[19] R. Carmona, J. Hinz, Risk-neutral models for emission allowance prices and option valuation, Management Science, 57 (2011), 1453-1468.

[20] R. Carmona, F. Delarue, G-E. Espinosa, N. Touzi, Singular Forward-Backward Stochastic Differential Equations and Emissions Derivatives, The Annals of Applied Probability, 23 (3) (2013), 1086-1128.

[21] A. Cartea, M. G. Figueroa, Pricing in Electricity Markets: A mean reverting jump diffusion model with seasonality, Applied Mathematical Finance, 12 (4) (2005), 313-335.

[22] D. Castillo, A. M. Ferreiro, J. A. García-Rodríguez, C. Vázquez, Numerical methods to solve PDE models for pricing business companies in different regimes and implementation in GPUs, Applied Mathematics and Computation, 219 (2013), 11233-11257.

[23] Y. Chen, B. F. Hobbs, S. Leyffer, T. S. Munson, Leader-follower equilibria for electric power and NOx allowance markets, Computational Management Science 3 (4) (2006), 307-330.

[24] M. Chesney, L. Taschini, The endogenous price dynamics of emission allowances and an application to CO_2 option pricing, Applied Mathematical Finance, 19 (5) (2012), 447-475.

[25] M. Coulon, Modelling Price Dynamics Through Fundamental Relationships in Electricity and Other Energy Markets, Mansfield College (2009), University of Oxford.

[26] M. Coulon, J. Khazaei, W. B. Powell, SMART-SREC: A stochastic model of the New Jersey solar renewable energy certificate market, Journal of environmental Economics and Management, 73 (2015), 13-31.

[27] K. M. Currier, A regulatory adjustment process for the determination of the optimal percentage requirement in an electricity market with Tradable Green Certificates, Energy Policy, 62 (2013), 1053-1057.

[28] J. Douglas, Jr., and T. F. Russell, Numerical methods for convection-dominated diffusion problems based on combining the method of characteristics with finite element or finite difference procedures, SIAM Journal on Numerical Analysis, 19 (1982), pp. 871-885.

[29] F. Dong, L. Shi, X. Ding, Y. Li, Y. Shi, Study on China's renewable energy policy reform and improved design of renewable portfolio standard, Energies, 12 (11) (2019), 2147.

[30] A. Eydeland, K. Wolyniec, Energy and Power Risk Management: New Developments in Modeling, Pricing and Hedging, Wiley Finance (2003), New York.

[31] A. Friedman, Stochastic differential equations and applications, Vol. 1, Academic Press [Harcourt Brace Jovanovich, Publishers], New York-London, 1975, Probability and Mathematical Statistics, Vol. 28.

[32] M. Ghaffari, A. Hafezalkotob, A. Makui, Analysis of implementation of Tradable Green Certificates system in a competitive electricity market: a game theory approach, Journal of Industrial Engineering International, 12 (2016), 185–197.

[33] Y. d'Halluin, P. A. Forsyth, G. Labahn, A semi-Lagrangian approach for American Asian options under jump-diffusion, SIAM J. Sci. Comput. 27 (2005), 315-345.

[34] B. M. Hambly, S. Howison, T. Kluge, Modelling spikes and pricing swing options in electricity markets, Quant. Finance 9 (2009) 937–949.

[35] J. M. Harrison, S. R. Pliska, Martingales and stochastic integrals in the theory of continuous trading, Stochastic Process, Appl., 11 (1981), 215-260.

[36] L. Hörmander, Hypoelliptic second order differential equations, Acta Math., 119 (1964), 147-171.

[37] S. Howison, D. Schwarz, Risk-neutral pricing of financial instruments in emission markets: a structural approach, SIAM Review, 57 (2015), 95-127.

[38] M. Hustveit, J. S. Frogner, S-E. Fleten, Tradable green certificates for renewable support: The role of expectations and uncertainty, Energy, 141 (2017), 1717-1727.

[39] K. Itô, On stochastic differential equations, Memoirs of the American Mathematical Society, 4 (1951), 1–51.

[40] N. Kangro, R. Nicolaides, Far field boundary conditions for Black-Scholes equation, SIAM J. Numer. Anal. 38 (2000), 1357-1368.

[41] J. Khazaei, M. Coulon, W. B. Powell, ADAPT: A Price-Stabilizing Compliance Policy for Renewable Energy Certificates: The Case of SREC Markets, Operations Research, Vol. 65 (6) (2017), 1429-1445.

[42] C. R. Knittel and M. R. Roberts. An empirical examination of deregulated electricity prices, Energy Economics 27 (5) (2005), 791-817.

[43] A. Lanconelli, S. Pagliarani, A. Pascucci, Local densities for a class of degenerate diffusions, Ann. Inst. H. Poincaré Probab. Statist., 56 (2), 1440-1464 (2020).

[44] J. J. Lucia, E. S. Schwartz, Electricity prices and power derivatives: evidence from the nordic power exchange, Review of Derivatives Research, 5 (2002), 5-50.

[45] J. Ma, Z. Wu, D. Zhang, J. Zhang, On well-posedness of forward-backward SDEs — a unified approach, The Annals of Applied Probability, 25 (4) (2015), 2168-2214

[46] J. Ma, H. Yin, J. Zhang, On non-markovian forward-backward SDEs and backward stochastic PDEs, Working paper (2012).

[47] J. Ma, J. Yong, Forward-Backward Stochastic Differential Equations and their Applications, Springer (1999).

[48] R. C. Merton, Theory of rational option pricing, The Bell Journal of Economics and Management Science, 4 (1973), 141-183.

[49] D. W. Montgomery, Markets in licenses and efficient pollution control programs, J. Econom. Theory, 5 (1972), 395-418.

[50] M. R. Nogueiras, Numerical analysis of second order Lagrange-Galerkin schemes. Application to option pricing problems, PhD. Thesis, University of Santiago de Compostela (2005).

[51] O. A. Oleinik, E. V. Radkevic, Second Order Equations with Nonnegative Characteristic Form, A.M.S. And Plenum Press, 1973.

[52] S. Pagliarani, A. Pascucci, The exact Taylor formula of the implied volatility, Finance and Stochastics 21 (2017), 661-718.

[53] C. Parés, J. Macías, M. Castro, Duality methods with an automatic choice of parameters, Numerische Mathematik, 89 (2001), 161-189.

[54] D. Pilipović, Energy Risk, Valuing and Managing Energy Derivatives, Mc Graw-Hill, 1998.

[55] E. S. Schwartz, The Stochastic Behaviour of Commodity Prices: Implications for Valuation and Hedging, The Journal of Finance 3 (1997), 923-973.

[56] D. Schwartz, Price Modelling and Asset Valuation in Carbon Emission and Electricity Markets, Ph.D. Thesis, University of Oxford, Oxford, UK, 2012.

[57] A. Shrivats, S. Jaimungal, Optimal Generation and Trading in Solar Renewable Energy Certificate (SREC) Markets, Applied Mathematical Finance, 27 (1-2) (2020), 99-131.

[58] J. Seifert, M. Uhrig-Homburg, M. Wagner, Dynamic behavior of CO_2 spot prices, Journal of Environmental Economics and Management, 56 (2008), 180-194.

[59] M. Tanaka, Y. Chen, Market power in emissions trading: Strategically manipulating permit price through fringe firms, Applied Energy 96 (2012), 203-211.

[60] T. H. Tietenberg, Emissions Trading: Principles and Practice, RFF Press, Washington DC, 2006.

[61] T. Tietenberg, Environmental and Natural Resource Economics, sixth ed, Munich et al.: Addison Wesley, Boston (2003).

[62] C. Vázquez, An upwind numerical approach for an American and European option pricing model, Appl. Math. Comput., 97 (1998), 273-286.

[63] A. Verbruggen, Tradable Green Certificates in Flanders (Belgium), Energy Policy, 32(2) (2004), 165–176.

[64] P. Wilmott, J. Dewynne, S. Howison, Option pricing. Mathematical Models and Computation, Oxford Financial press, Oxford, 1993.

[65] X. Ye, Z. Li, C. Wang, X. Lei, W. Yuan and Z. Shi, Green Power Certificates in China: A Study on Pricing and Transaction Decisions, Chinese Automation Congress (CAC), Hangzhou, China, 2019, 5605-5608.

[66] BP web page: https://www.bp.com/.

[67] European Commission web page: https://ec.europa.eu/.

[68] International Energy Agency (IEA) web page: https://www.iea.org/.

[69] United Nation Climate Change (UNCC) web page: https://unfccc.int/.